ELECTROPHYSIOLOGICAL AND MOTORIC EFFECTS OF GALVANIC VESTIBULAR STIMULATION IN NORMAL AND PARKINSON'S DISEASE SUBJECTS

by

DIANA JEAN-YOUNG KIM

B.Sc., McGill University, 2008

A THESIS SUBMITTED IN PARTIAL FULFILLMENT OF
THE REQUIREMENTS FOR THE DEGREE OF
MASTER OF SCIENCE

in

The Faculty of Graduate Studies

(Neuroscience)

THE UNIVERSITY OF BRITISH COLUMBIA

(Vancouver)

May 2013

ABSTRACT

How vestibular input influences dynamical functional brain networks and sensorimotor processing is an unaddressed area of interest. Previous accounts have suggested that noisy galvanic vestibular stimulation is able to not only improve visuospatial processing in stroke patients, but also ameliorates some of the motor symptoms in Parkinson's disease. However, the mechanisms through which these purported benefits are obtained are currently poorly understood. In Parkinson's disease, patients suffer from symptoms of bradykinesia, or slowness of movement, as well as tremor, rigidity, postural instability and cognitive impairment. A proposed mechanism for bradykinesia is that in Parkinson's disease cortical-basal ganglia-thalamocortical networks are "stuck" in a fixed state, resulting in poorly modulated, exaggerated oscillations resonating in the beta range (13-30 Hz). This thesis addresses a number of questions: What is the effect of external vestibular sensory input on widespread, systems-level oscillatory rhythms? When the brain is in a diseased state, as in Parkinson's disease, can vestibular input modulate the abnormal dynamics of cortical-basal ganglia networks? Furthermore, is noisy galvanic vestibular stimulation consequently able to affect functional networks and information processing in the brain? Specifically, we investigated whether noisy galvanic vestibular stimulation was able to modulate synchrony of EEG oscillations in normal individuals and Parkinson's disease subjects. Upon identifying significant neuromodulatory effects of noisy galvanic vestibular stimulation across broadband rhythms in the resting-state EEG activity, we speculated that information processing may be similarly affected in task-related networks in Parkinson's disease. Subsequently, we investigated whether the same noisy vestibular stimulus would be able to improve motor performance in Parkinson's disease subjects. We found that their dynamics of

motor tracking movements were improved in a visuomotor task by stimulation. We speculate that noisy vestibular stimulation is able to reinstate the abnormal dynamics of functional networks in disease conditions. Therefore, this thesis provides a foundation for assessing the potential utility of galvanic vestibular stimulation as a novel, non-invasive, neuromodulatory therapeutic for Parkinson's disease.

PREFACE

Chapter 2 of this thesis was conducted under the supervision of Dr. Martin McKeown in collaboration Dr. Z. Jane Wang (Electrical and Computer Engineering, UBC). My role and contributions involved analyzing the data, drafting the manuscript and revising it in collaboration with Dr. Martin McKeown. Vignan Yogendrakumar and Dr. Edna Ty set up the experiment, recruited subjects and collected data. Joyce Chiang was involved in data analysis.

Chapter 3 of this thesis was conducted under the supervision of Dr. Martin McKeown in collaboration Dr. Z. Jane Wang (Electrical and Computer Engineering, UBC). My role and contributions involved analyzing the data and drafting the manuscript with Dr. Martin McKeown. Vignan Yogendrakumar and Dr. Edna Ty set up the experiment, recruited subjects and collected data. Joyce Chiang was involved in data analysis.

Chapter 4 of this thesis was conducted under the supervision of Dr. Martin McKeown in collaboration Dr. Meeko Oishi (Electrical and Computer Engineering, University of New Mexico). My role and contributions involved designing and implementing the experiment, collecting the data, recruiting subjects and drafting the manuscript with Dr. Martin McKeown. Ahmad Ashoori analyzed the data in collaboration with Dr. Martin McKeown and Dr. Meeko Oishi. Dr. Edna Ty led subject recruitment and assisted with data collection.

A version of Chapter 2 has been re-submitted with revisions for publication: Kim DJ, Yogendrakumar V, Chiang J, Ty E, Wang ZJ, McKeown MJ. Noisy galvanic vestibular stimulation modulates the amplitude of EEG synchrony patterns.

All work conducted in this thesis was approved by the UBC Clinical Research Ethics Board under the project title: Galvanic Vestibular Stimulation for improving motor performance in Parkinson's disease. The Ethics Board certificate number is H09-02016.

TABLE OF CONTENTS

LIST OF TABLES

LIST OF FIGURES

LIST OF ABBREVIATIONS

BG	basal ganglia
cTBS	continuous Theta Burst Stimulation
CVS	Caloric Vestibular Stimulation
DBS	deep brain stimulation
DLPFC/DMPFC	dorsolateral/dorsomedial prefrontal cortex
EEG	electroencephalography
fMRI	functional magnetic resonance imaging
GABA	gamma-aminobutyric acid
GPi/GPe	internal/external globus pallidus
GVS	Galvanic Vestibular Stimulation
ICA	Independent Component Analysis
iTBS	intermittent Theta Burst Stimulation
L-dopa	levodopa
LASSO	Least Absolute Shrinkage Selection Operator
LDS	linear dynamical system
LFP	local field potential
LTP/LTD	long-term potential/depression
M1	primary motor cortex
MEP	motor-evoked potentials
MPTP	1-methyl-4-phenyl-1,2,3,6-tetrahydropyridine
MSN	medium spiny neuron
NMDA	N-methyl-D-aspartate

PD	Parkinson’s disease
PPN	pedunculopontine nuclei
RBD	REM sleep behavioural disorder
REM	rapid eye-movement sleep
rTMS	repetitive Transcranial Magnetic Stimulation
SMA	supplementary motor area
SNc	substantia nigra pars compacta
STN	subthalamic nucleus
tDCS	transcranial Direct Current Stimulation
TMS	Transcranial Magnetic Stimulation
UPDRS	Unified Parkinson’s Disease Rating Scale
VA/VL	ventroanterior/ventrolateral
VOR	vestibulo-ocular reflex

ACKNOWLEDGEMENTS

There is no possibility that the work described in this thesis would have been accomplished without the help and support of many individuals.

I would like to thank my supervisor, Dr. Martin McKeown, for giving me the initial opportunity to do my Master's degree under his mentorship and for presenting me with subsequent opportunities to grow from. I am especially grateful for your sympathy during challenging personal times and patience throughout this period of learning.

My gratitude extends to my Supervisory Committee – Drs. Silke Cresswell, Jane Wang and Lara Boyd – for their input, comments and encouragement.

Thank you as well to our collaborators Dr. Jane Wang and Dr. Meeko Oishi and their graduate students Ahmad Ashoori and Joyce Chiang for their involvement and contributions to the project.

Throughout the span of three years, I have had the pleasure of working with and getting to know numerous individuals. Notably, thank you Dr. Edna Ty for your immense help with both experiments and subject recruitment. There is no way I would have possibly known how to navigate myself through this type of research had you not shared your insight. My deepest thanks go to all past and present labmates, undergraduate/summer students and engineering students with whom I have collaborated. You have all helped me in many different capacities, which I have always appreciated.

To all the research subjects, thank you all for your enthusiasm and interest in participating in research.

Lastly, a huge thank you goes to my family and friends for their moral support and encouragement.

DEDICATION

To my dad – for your unselfish love and support throughout the years.

CHAPTER 1: Introduction

1.1. General Introduction

In the Introduction section of this thesis, we provide an overview of Parkinson's disease and abnormal mechanisms involving neuronal oscillations. We also briefly outline common non-invasive brain stimulation techniques used to modulate functional networks and their present therapeutic applications towards treating neurological and psychiatric disorders. Galvanic vestibular stimulation (GVS) is one novel, non-invasive brain stimulation approach involving transcutaneous stimulation of vestibular afferents and vestibular networks. Since previous findings have suggested that GVS improves motor performance, this thesis explores the potential therapeutic utility of galvanic vestibular stimulation in Parkinson's disease via neuromodulatory mechanisms.

For the purposes of the work accomplished in this thesis – unless otherwise stated – EEG bands mentioned throughout are defined by the following frequency ranges: theta (4-7.5 Hz), alpha (8-12 Hz), beta (13-30 Hz), gamma (31-50 Hz).

1.2. Parkinson's Disease

Parkinson's disease (PD) is a debilitating, progressive neurodegenerative disorder affecting approximately 1 of 100 persons above the age of 60 years [1]. With increasing age, this prevalence rate in industrialized countries escalates to as high as 4% [2,3], and from disease diagnosis until death, PD insidiously progresses for a mean duration of 15 years [4]. Therefore, due to growing elderly populations, PD poses a significant load on patients, families, health care systems and societies [1,5]. Although it is the second most common

neurodegenerative disorder after Alzheimer's disease, PD is a complex disease whose underlying pathophysiological mechanisms are not fully established.

1.2.1. Pathogenesis of Parkinson's Disease

By classical "textbook" definition, PD is clinically defined by the syndrome of parkinsonism comprised of cardinal motor features: akinesia/bradykinesia (absence/slowness of movement), rigidity, tremor at rest and postural instability [6,7]. Pathologically, the disease is defined by the unexplained degeneration of basal ganglia nuclei – specifically, substantia nigra pars compacta (SNc) neurons projecting to the motor portion of the striatum (the putamen) [4,8,9]. Since one function of the basal ganglia circuitry involves movement execution and control, damaged SNc projections to the striatum accounts for subsequent striatal dopamine depletion and parkinsonism symptoms [10,11]. With levodopa (L-dopa) medication, a dopamine precursor replacement, motor symptoms are effectively managed [12]. Nigrostriatal dopaminergic cell loss and motor impairment are therefore essential features of the disease.

One hypothesis to explain neuronal death in PD is centred on the widespread progression of Lewy bodies, or intraneuronal misfolded protein aggregates comprised of α-synuclein [6,13,14]. Intrastriatal injections of synthetic misfolded α-synuclein proteins in wild-type mice have been demonstrated to sufficiently induce both death of SNc dopaminergic neurons and accompanying motor deficits [15]. However, it remains controversial whether Lewy bodies are causative. For example, parkinsonism can develop without the presence of Lewy bodies as in some instances when drug-induced or genetically driven [16,17]. Furthermore, Lewy bodies have been found postmortem in some individuals

without parkinsonism [8]. Lewy bodies may alternatively be a marker of pathological cell death in brain areas affected in PD [8].

In essence, the etiology of dopaminergic degeneration in PD still unknown. Adding to the complexity is the fact that the disease is multifactorial with aging, environmental and genetic risk factors interacting to contribute to disease pathogenesis [4,18]. Aging and certain environmental toxins, such as 1-methyl-4-phenyl-1,2,3,6-tetrahydropyridine (MPTP) and the herbicide paraquat, increase the risk of developing PD and have been linked with nigrostriatal cell death [4,16,19]. With respect to genetics, there is a high degree of genetic heterogeneity in PD. While 6 genes (SNCA, LRRK2, Parkin, PINK1, DJ-1, ATP13A2) have conclusively been determined to cause inheritable, monogenic PD, there are a multitude of genetic susceptibility factors linked with PD [4,20]. Additionally, multiple intracellular molecular pathways have been implicated to explain the selective death of dopaminergic cells in PD: mitochondrial dysfunction, oxidative stress, inflammation and impaired proteosomal and lysosomal degradation pathways [4,18,19]. How all these environmental, genetic and molecular factors interact to impact the aging brain and the underlying pathological cause of PD remains unestablished [19].

1.2.2. Non-Motor Symptoms and Non-Dopaminergic Systems in Parkinson's Disease

Other areas asides from the nigrostriatal system are also affected in PD, such as the hypothalamus, thalamic nuclei, neocortex and enteric nervous system [6,8]. Non-dopaminergic neuronal death also occurs in the noradrenergic neurons of the locus coeruleus, cholinergic cells of the nucleus basalis of Meynert and serotonergic projections from the raphe nuclei [4]. While dopaminergic nigrostriatal degeneration is a key characteristic of the

disease, other regions and non-dopaminergic neurons are also significantly affected, making PD a multisystem neurodegenerative disorder [6]

As a consequence, in addition to motor deficits, PD is characterized by numerous and equally insidious non-motor symptoms. Anosmia, autonomic dysfunction, constipation, sleep disorders, cognitive impairment and psychiatric disturbances contribute to the broad spectrum of clinical manifestations in PD [6,7,21]. Some of these deficits, such as impaired executive function, depression and apathy (reduced motivation) may be attributed to the fact that the basal ganglia mediates other functions aside from motor control: associative and limbic loops in the basal ganglia add to the complexity of normal basal ganglia functions [22]. As a result, PD is clinically manifested with a spectrum of motor, sensory, cognitive and autonomic deficits.

1.2.3. Pathophysiology of Parkinson's Disease: The Basal Ganglia "Rate Model"

The connections of the basal ganglia have important functions in action/motor planning, sequencing and execution [23]. At the crux of the classical model, basal ganglia output consists of GABAergic projections from the internal globus pallidus (GPi) to premotor neurons in the thalamus (Figure 1.1) [11]. Ultimately, the "direct" pathway disinhibits basal ganglia output to promote movement facilitation whereas the "indirect" pathway increases basal ganglia output to suppress movement via polysynaptic inhibitory projections [11]. It is important to note that additional anatomical projections from the cortex to subthalamic nucleus (STN) in the hyperdirect pathway may also increase basal ganglia output, thereby circumventing the supposed slower processing within the striatum and external globus pallidus (GPe) (Figure 1.1) [11]. The parallel direct and indirect pathways are respectively modulated by dopaminergic projections from the SNc to separate populations of

striatal medium spiny neurons (MSNs) expressing either excitatory D1 or inhibitory D2 receptors [11]. Using optogenetic control of neuronal activity in rodent models, Kravitz et al. (2010) confirmed that D1-mediated activation of the direct pathway reduced freezing and increased locomotion while activation of the D2-mediated indirect pathway increased freezing, increased bradykinesia and reduced locomotion. Therefore, parallel bi-directional pathways with antagonistic effects target motor cortical networks in order to regulate normal motor behaviour [10,11].

In PD, nigrostriatal denervation of the striatum has profound effects on basal ganglia circuitry. Resulting striatal dopamine depletion ranges from 44% to 98% [24], disrupting the functional connectivity of the basal ganglia. Animal models of PD in primates have demonstrated that dopamine depletion results in a subsequent functional imbalance between activity in the direct and indirect pathways with the former and latter pathways being under- and overactive, respectively [11]. Specifically, activity in the STN and GPi are excessively active while decreased in the GPe, essentially elevating GPi neuronal firing and basal ganglia output (Figure 1.1) [11,25]. In support of this, dopamine-depleted primates treated with MPTP experience parkinsonism motor symptoms, which are reversed by STN lesions (Figure 1.1) [26]. Furthermore, evidence in PD patients has demonstrated that GPi pallidotomies improved clinical motor symptoms of bradykinesia/akinesia and gait dysfunction [27]. Therefore, according to this canonical “rate model”, hypokinetic movements and pathophysiological mechanisms in PD could be explained by altered neuronal firing rates within the basal ganglia nuclei [11,25].

1.2.4. The Rate Model Is Insufficient

More recent observations, however, indicate that the rate model is inconsistent with the range of movement disorders. According to this model of basal ganglia dysfunction, the hypokinetic and hyperkinetic movements may be explained by altered neuronal firing [25]. For example, earlier lesion studies in primates have suggested that hyperkinetic movement disorders – such as dystonia, hemiballismus, dyskinesias and chorea – originate from reduced STN activity and GPi output (Figure 1.1) [28-30]. However, in conflict with these predictions, Hutchison et al. observed similar GPi firing rates in dystonia patients and PD patients. These studies suggest that behavioural consequences are not solely predictable based on changes of discharge rates in given nuclei [31]. As another case in point, the dopamine agonist apomorphine has been shown to improve parkinsonism symptoms in PD patients while decreasing GPi activity, although without effects on STN firing [32]. Given such discrepant findings in patients, it is now well established that the classic basal ganglia rate model is not fully tenable with respect to motor behavioural implications.

The classical rate model has several limitations and leaves certain questions unanswered. For example, symptoms of bradykinesia/akinesia may be well explained by imbalanced activity in the direct and indirect pathways, but tremor and rigidity are not as easily accounted for [25]. Neither does the rate model explain why lesion treatments (e.g., GPi pallidotomy or STN lesion) are not necessarily associated with hyperkinetic movements, such as severe hemiballismus or dyskinesias [11,33]. Furthermore, how can a lesion, which obliterates tissue, and electrical stimulation (e.g., deep brain stimulation), which modulates activity, produce the same therapeutic effect of ameliorating parkinsonism symptoms [11,25]? The rate model implies that a uni-directional flow of information exists. However,

present knowledge of the basal ganglia circuitry argues against that assumption and has expanded to include numerous modulatory connections: striatal interneurons; and, connections between basal ganglia nuclei and other subcortical areas, including the raphe nuclei and pedunculopontine nuclei (PPN) [33]. On the other hand, the rate model has had a pivotal role in the defining targets, such as the STN and GPi, in stereotactic surgery for PD [22]. However, subsequent, newer models have been developed, one of which has incorporated firing *pattern* abnormalities and synchronous oscillations.

1.2.5. Oscillation Model

More recent evidence suggests that the motor symptoms in PD are caused by pathophysiological mechanisms involving aberrant neural synchrony patterns. Herein, neural synchrony refers to correlated oscillatory activity at the level of large groups of neurons, as opposed to at the level of membrane fluctuations or single cell action potentials [34]. In the oscillation model, synchronization of oscillatory rhythms supposedly underlies the parkinsonian state and motor symptoms (Figure 1.2) [11,25]. The reciprocal connections between the STN and GPe network may act as one contributing pattern generator, or "pacemaker", due to spontaneous discharge abilities of those neurons; however, the possibility of other rhythmic pattern generators, such as thalamic neurons, is not excluded [35]. On a larger scale, these synchrony patterns occur throughout a cortical-basal ganglia-thalamo-cortical network comprising the neocortex, cerebellum, striatum and STN [36]. In fact, it has been demonstrated in PD patients that the whole system has a natural tendency to resonate around at a particular frequency of around 20 Hz [37].

Several studies support the hypothesis that, in PD, abnormally exaggerated synchrony of oscillations within cortico-basal ganglia circuits exists in the beta frequency range (11-30

Hz) [11,25]. For example, dopamine depletion in mouse models is associated with akinesia, and results in a dominant power of low-frequency oscillations, including beta power, in GPe, STN, striatal and M1 neurons [38-40]. In patients in the off-medicated state, recordings of unit activity, local field potentials (LFPs) and scalp EEG – with invasive recordings made possible through the development of therapeutic functional surgical approaches, such as deep brain stimulation – have shown that prominent oscillations exist in the beta range [37,41-43] From these observations, it has been concluded that exaggerated beta synchrony as a result of dopamine depletion characterizes the parkinsonian state (Figure 1.2).

1.2.6. The Role of Beta Oscillations in Sensorimotor Processing

Due to the presence of exaggerated beta rhythms in PD patients, the role of these beta oscillations has been a subject of many recent investigations. Several studies have raised the question as to whether the high beta synchrony observed in PD is "antikinetic" and associated with poverty of movement [25]. For example, artificially driving neural rhythms at beta frequencies using brain stimulation techniques slows motor performance in PD and healthy subjects [44,45]. On the other hand, suppression of beta synchrony, or beta desynchronization, occurs prior to movement, insinuating it is involved in motor preparation and promotes movement [46]. Promoting this idea, PD therapies that restore movement deficits have been shown to suppress pathologically exaggerated beta rhythms. Following administration of L-dopa medication, the power of beta oscillations is reduced as measured by LFPs in the STN and GPi [42,47,48]. Interestingly, the degree of pathological synchrony is unrelated to the severity of motor symptoms, but rather correlates with the magnitude of the basal ganglia response to dopaminergic medication – that is, the level of motor improvement with respect to bradykinesia and rigidity [47,49]. Other therapies which

ameliorate motor symptoms, such as stereotactic lesions and high frequency (>100 Hz) electrical stimulation of the STN, undermine the rate model, yet additionally support the oscillation model [50,51]. DBS, which directly stimulates the basal ganglia circuitry, especially has been associated with attenuation of highly synchronous beta oscillations [25,52]. Therefore, the role of beta oscillations in the pathophysiology of PD has garnered growing interest.

The exact notion, however, of synchronous beta rhythms as antikinetic in motor function is highly contentious [53-55]. Based on prior work, the tight temporal coupling of synchronous neurons seen in PD within the cortical-basal ganglia-thalamo-cortical circuitry has been hypothesized to disrupt information transfer; as a result, beta synchronization has been held accountable for motor deficits and as the "bad boy" of parkinsonism [34,41,50,56]. However, more recent work demonstrates that global beta synchrony patterns are rather a vital part of normal sensorimotor processing [55]. For example, Feurra et al. showed than enhancement of beta rhythms by 20 Hz transcranial stimulation of the motor cortex enhanced motor-evoked potentials (MEPs) amplitude in healthy subjects [57]. Additionally, Leventhal et al. used normal, intact rats to demonstrate that low and high beta power are not rigidly associated with movement initiation or movement suppression, respectively; this is proven by the fact that event-related synchronization of beta oscillations follows the animals' motor output decisions to either initiate or inhibit movements after auditory cues in separate "GO" and "NO-GO" paradigms [55]. The authors suggested that elevated beta power is important in sensorimotor processing and occurs when rats use sensory cues to determine behavioural output, implicating its role in planning [55]. Therefore, beta synchronization is not necessarily antikinetic, but represents a post-decision stabilized state of cortical-basal ganglia

networks, which is hypothesized to minimize interference from other cues or competing alternative actions [55].

Therefore, the excessive beta rhythms observed in PD are not pathological *per se*, but suggested to coordinate a neural network "stuck" one set of many normal dynamic states and resonating at a particular frequency [37,55]. A general modern framework proposes that cognitive and behavioural functions are mediated by networks comprised of dynamic interactions of widely distributed, but functionally specialized cortical regions [58]. In other words, these neural networks are mediated by global synchrony patterns, which integrate neural activity and allow information transmission. However, these networks are also dynamic (i.e., metastable) with a transient existence that supposedly coincides with a given function [59,60]. For example, the strength of beta and gamma-band synchronization has been demonstrated to predict subjects' perception of integrated audiovisual information [61]. Consequently, the exaggerated beta synchrony observed in PD may characterize an overstabilized network state [54,55] – i.e., a less dynamic system. This may explain why voluntary movements are slowed when initiated during artificially enhanced beta activity [44,45]. In addition, this view explains why PD patients have difficulty switching between different cortical programs and exhibit behavioural inflexibility [62]. Based on these findings, modulation of beta oscillations is important for normal information processing and continuous reorganization of dynamic network states. This notion may hold true for PD patients with REM sleep behavioural disorder (RBD) who experience near-normal voice and movements during RBD episodes [63]. These individuals were found to display higher global theta power during wakefulness compared to patients without RBD, but no quantitative EEG differences during REM sleep were observed [64] – suggesting that it must be perhaps

network dynamics and not the exact EEG synchrony level that contributes to symptom manifestation. In summary, in PD, beta synchronization may represent an overstabilized normal network while cortical brain dynamics may be hypothetically abnormal; this proposition has not been confirmed, though. Additionally, whether there is a difference in the efficiency of the putative overstabilized network in PD compared to normal subjects has not been characterized either.

1.2.7. The Putative Role of Beta Oscillations in Cognitive Functions

In addition to sensorimotor processing, the excessive beta oscillations observed in PD may also affect the cognitive domain. In the experiments by Leventhal et al., coordinated changes in beta power during sensorimotor processing occurred throughout cortical-basal ganglia-thalamocortical circuits, including the prefrontal cortical regions [55]. The same authors also demonstrated that transient beta network synchronization is present only during successful, not failed, behavioural inhibition [55], implicating a role of beta synchronization in planning, behavioural flexibility and executive function. Given that PD patients are affected by impaired cognitive flexibility and executive dysfunction [65,66], further work is needed to understand whether aberrant beta synchrony dynamics affects other dopaminergic networks involved in executive function and goal-oriented behaviour, such as in the prefrontal cortex and ventral striatum (including the nucleus accumbens) [67].

1.2.8. Altered Parkinsonian Network Oscillations Are Not Confined to the Beta Band

Although many studies have largely focused on the exaggerated beta synchrony patterns in the Parkinsonian state, aberrant oscillatory dynamics may not be solely found in the beta band. For example, PD patients in the off-medicated state demonstrate altered directional connectivity between EEG regions within alpha (8-12 Hz), beta (13-30 Hz) and

low gamma (31-50 Hz) frequency ranges; moreover, these measures were correlated with severity of motor symptoms, further supporting a pathological role in PD [68]. In support of this, gamma oscillatory activity (35-55 Hz) recorded in STN LFPs is increased during periods of tremor and with stronger tremor [69]. However, to what extent the dynamics of gamma oscillatory rhythms may contribute to parkinsonism is not well established. Others have demonstrated that the power of gamma oscillations (~70 Hz) peak after administration of dopaminergic medication [42], suggesting that gamma synchronization may be conversely relevant towards ameliorating parkinsonism [25,54]. Nevertheless, it is apparent that other oscillatory rhythms asides from beta band activity may participate in PD pathological mechanisms.

The function of different oscillations on various temporal scales and how they interact in PD may be interesting given observations in normal cases. The phenomenon of nesting between faster and slower rhythms has been previously observed in the brain; nesting occurs when the amplitude of a faster rhythm is coupled to the phase of a slower rhythm. For example, gamma (~40 Hz) and theta (~6 Hz) oscillations underlie alternating visual percepts in a prefrontal-parietal network [70]. Nested oscillatory patterns have also been observed in the hippocampus CA1 region during maze exploration and REM sleep in rodents [71]. Since phase resetting of oscillations in the alpha (~10 Hz) range and beta range has been demonstrated to be present through basal ganglia-thalamocortical networks during normal sensorimotor processing [55], the question of interactions between beta and other rhythms in PD pathological mechanisms is not excluded. For example, it has been conjectured that slower rhythms may provide a temporal framework for cognitive moments and transient networks [58]. Further research into how other oscillatory rhythms interact across temporal

scales and whether this has any significance for sensorimotor processing in the Parkinsonian state is an open-ended question [54].

1.2.9. Current Therapies for Parkinson's Disease

Since its inception in the late 1960s, the gold standard for treating PD has been dopaminergic replacement by L-dopa medication [12]. As the precursor to dopamine, L-dopa effectively manages motor symptoms in the disease, which may be clinically quantified and monitored using the Unified Parkinson's Disease Rating Scale (UPDRS) [7,12]. However, several side effects are associated with chronic use of dopaminergic drugs: psychoses, dopamine dysregulation syndrome (an addiction to dopaminergic medication), impulse control disorders (most commonly, pathological gambling, binge eating, compulsive shopping and hypersexuality) [22,72,73]. Other notable side effects with chronic usage include dyskinesias, end-of-dose deterioration (i.e., early wearing off) and decreasing therapeutic window which reflects efficient dosage without causing side effects [22,73]. Furthermore, not all symptoms are L-dopa-responsive or are exacerbated by L-dopa, such as psychotic symptoms [73]. Therefore, although L-dopa is presently the most reliable treatment for PD, interest in non-pharmacological therapies in order to improve disease management are of valid interest.

With respect to surgical advances, deep brain stimulation (DBS) is a common mode of treatment that has largely replaced lesions and pallidotomies [51]. Common subcortical electrode targets for PD patients include the STN and GPi, and its mechanisms of action are thought to be due to disrupting pathological oscillatory dynamics in PD [51]. Asides from the individual neuronal targets, it has also been suggested that the electrical stimulation of basal ganglia nuclei may also affect neighbouring astrocytes to release neurotransmitters [51].

DBS is effective and has largely advanced our ability to measure single unit and LFP recordings in patients; however, the procedure is invasive, costly and an option usually reserved for patients at more advanced stages of the disease [51]. In lieu of DBS, non-invasive brain stimulation techniques are presently a growing avenue of research.

1.3. Non-Invasive Brain Stimulation

Since neurological and neuropsychiatric diseases, like PD, may be caused by abnormal network dynamics, much recent work has focused on the potential therapeutic application of non-invasive brain stimulation techniques for clinical intervention. Non-invasive brain stimulation methods rely on electromagnetic principles to transcranially alter brain activity [74]. Stimulation effects may be induced either focally, or spread from target regions trans-synaptically to modulate interconnected cortical and subcortical networks [74,75]. The two most common techniques are transcranial direct current stimulation (tDCS) and transcranial magnetic stimulation (TMS).

1.3.1. Transcranial Direct Current Stimulation (tDCS)

With tDCS, a weak electrical direct current is applied over the scalp to a distinct region of the scalp. The spatial distribution and direction of current flow may be manipulated using various montages and number of electrodes [76]. Anodal stimulation depolarizes neurons via decreasing GABA transmission, therefore enhancing spontaneous firing and cortical excitability; conversely, cathodal stimulation hyperpolarizes neurons via decreasing glutamatergic transmission, therefore decreasing both spontaneous firing and excitability [77,78]. Application of tDCS not only modulates neurotransmitter release, but also modulates the activation of Na^{+}- and Ca^{2+}-dependent channels and NMDA-receptor activity [77]. This ultimately has long-lasting consequences for either promoting long-term

potentiation or depression (LTP/LTD) like mechanisms [77,79]. The effects of tDCS cause local and distant plastic changes, and as well depend on numerous factors, such as size, polarity and electrode montage, applied current intensity, stimulation density and duration, and properties of the targeted tissue [77]. It is important to note that although application of currents via tDCS leads to substantial shunting in the scalp, a prior modeling study has demonstrated that sufficient current penetrates the skull in order to modulate neuronal potentials [80]. In spite of this, one particular advantage of tDCS is the recent application of other types of stimulatory signals aside from direct current, such as alternating current and random noise stimulation [81,82].

1.3.2. Transcranial Magnetic Stimulation (TMS)

TMS involves applying a transient magnetic field to the brain through a coil. This in turn induces in the cortical tissue a depolarizing, electrical current, which flows parallel to the coil and modulates neuronal excitability [74]. Depending on stimulus parameters (i.e., frequency, polarity, duration, magnetic field strength, shape of coil), reversible shifts in cortical excitability occur in focalized brain regions [83]. For example, high-frequency (5-20 Hz) repetitive TMS (rTMS) may enhance cortical excitability while low-frequency (0.2-1 Hz) may suppress excitability. An alternative paradigm involves theta-burst stimulation (TBS), which involves high-frequency (50-100 Hz) rTMS bursts given at a theta frequency (~5 Hz) [83,84]. When given intermittently (iTBS), cortical excitability is enhanced, in contrast to continuous (cTBS) stimulation which suppresses cortical excitability. In any given paradigm, effects of TMS are immediate and may last up to 30-60 minutes depending on stimulus parameters [83].

In comparison to tDCS, rTMS differs only slightly. Both rTMS and tDCS are neuromodulatory (i.e., inducing changes in neuronal excitability via influencing voltage-sensitive cation channels) while rTMS is additionally a neurostimulatory (i.e., directly inducing cell firing) tool [74-76]. Side effects using both techniques are minor, such as transient headaches or neck pain [75,76]. More focal stimulation and higher temporal resolution at millisecond-level accuracy may be achieved using rTMS [76]. On the other hand, tDCS is more portable and conducive to double-blind and sham-controlled studies. However, drawbacks of tDCS include low focality due to large electrode size [77] and low temporal resolution [76]. Furthermore, the plasticity effects of tDCS may be modulated by certain medications, including L-dopa [76,85], which is especially relevant for clinical applications in PD. For example, L-dopa has been shown to exert a dosage-dependent, inverted U-shaped effect on LTP and LTD of the primary motor cortex in normal individuals [85]. Low (25 mg) or high (200 mg) dosages of dopaminergic treatment impaired tDCS-induced plasticity as measured by MEPs; medium dosages (100 mg) were found to prolong and promote inhibitory plasticity [85].

1.3.3. Clinical Research Findings Using Non-Invasive Brain Stimulation

With the flexible capacities and overall advantages of non-invasive brain stimulation techniques, mounting evidence demonstrates their promising clinical therapeutic potential in treating a range of neurological as well as neuropsychiatric diseases. Here, we briefly discuss the beneficial implications of both tDCS and rTMS for stroke recovery, depression and cognition.

Motor recovery following chronic stroke (weeks to months after ischaemic or haemorrhagic stroke) improves as a result of the effects of non-invasive brain stimulation.

After a stroke in the motor cortex, cortical excitability of the affected side is decreased due to the lesion as well as due to increased transcallosal inhibition from the contralesional cortex [75]. Therefore, not only does facilitatory anodal stimulation and high-frequency rTMS/iTBS of the ipsilesional hemisphere increase cortical excitability in lesioned motor-related areas, but inhibitory cathodal stimulation and low-frequency rTMS/cTBS of the contralesional hemisphere also show similar improvements [75,86]. Increased cortical activation of motor-related areas has been demonstrated with anodal and cathodal tDCS of the ipsilesional and contralesional primary motor cortex respectively, which resulted in improved motor reaction time [86]. In conjunction with motor practice, the beneficial effects of non-invasive brain stimulation for chronic stroke patients are long-term, lasting up to 3 months [87]. Evidently, concurrent neurorehabilitation with non-invasive brain stimulation shows promise as a therapeutic tool to facilitate motor recovery, more so than motor therapy alone (20% gain) [88]. In the case of stroke, non-invasive brain stimulation assists with enhancing adaptive processes and inhibiting maladaptive mechanisms following cortical injury in order to reinstate balanced functional interhemispheric dynamics [75].

The effects of non-invasive brain stimulation on mood disorders and depression suggest non-invasive approaches are promising clinical therapeutic treatments options. Electroconvulsive therapy (ECT) is the most effective treatment for life-threatening or treatment-resistant depression, although it requires general anesthesia, and side effects include negative consequences on cognition [89]. Therefore, non-invasive stimulation techniques are attractive due to their ability to reduce depressive symptoms (measured by depression scales, such as the Hamilton Depression Rating Scale and Beck Depression Inventory) while focalizing effects on specific cortical regions and being better tolerated

[76,89]. Typically, TMS treatment targets the left dorsal lateral prefrontal cortex (DLPFC) whereas for tDCS, usually the left DLPFC and contralateral DLPFC/supraorbital region are stimulated by the anodal and cathodal electrodes, respectively [89]. This is particularly useful for major depressive disorder, which is associated with altered functional connectivity of specific networks, such as the DLPFC, DMPFC, dorsal medial prefrontal cortex (DMPFC), subcallosal cingulate gyrus and default mode network [90]. The left DLPFC is notably observed to be relatively hypoactive in depressed subjects, and normalized in response to treatment [74]. Much in the same way that ECT modulates functional connectivity between the default mode network and left DLPFC/DMPFC [90], TMS and tDCS are suggested to improve mood by modulating the functional connectivity of the same networks [74,91]. Overall, tDCS and TMS provide a more practical, feasible alternative to ECT for depression and mood disorders. Treatment effectiveness, however, is greatly determined by frequency, number and duration of sessions [89].

A wide range of cognitive functions may benefit from application of non-invasive brain stimulation techniques in both patient groups and normals. For example, cognitive deficits following stroke, such as hemispatial neglect and aphasia, have been suggested to benefit from targeted non-invasive stimulation of the frontoparietal and language networks, respectively [75,84]. Specifically, anodal tDCS over the ipsilesional posterior parietal cortex and cathodal tDCS over the contralesional area improved visuospatial performance in stroke patients [76,84]. One potential explanation to account for cognitive enhancement may be due to modulation of neuronal oscillations and functional networks. This is supported by the finding that working memory improved as a result of anodal tDCS of the DLPFC while also increasing power of theta and alpha EEG oscillations [79]. Interestingly, a dose-specific

response has been implicated: enhancement of working memory in PD patients off medication with 2 mA of tDCS over the DLPFC showed significant performance improvement whereas 1 mA tDCS did not [92]. In addition, decision-making has also been shown to be altered by non-invasive brain stimulation with higher risk-taking favoured by disrupting right DLFPC activity using 1 Hz low-frequency rTMS [93]. This is consistent with the observation that altered activity in DLPFC, the orbitofrontal cortex, anterior insula and anterior thalamus is characteristic of impaired decision-making in addictive behaviour – such as in heavy smokers and alcoholic individuals [94,95]. Therefore, it is not surprising that cortical modulation of DLPFC with tDCS was able to suppress stimulus-induced cravings in heavy smokers [96]. Non-invasive brain stimulation techniques additionally have been shown to numerous other cognitive functions, such as declarative memory, implicit memory and object-location memory [79]. Therefore, TMS and tDCS have a broad range of functional benefits in the domains of visuospatial processing, language, memory and decision-making. These findings open possibilities of novel therapeutics for cognitive deficits in stroke, PD, addictive behaviour and Alzheimer's disease.

Therefore, nn-invasive brain stimulation techniques are promising alternative, novel treatments to pharmacological and other therapies for neurological and neuropsychiatric conditions. In addition to stroke recovery, mood and cognitive deficits, additional conditions which are characterized by disrupted brain network dynamics may benefit from neuromodulatory approaches, such as schizophrenia, pain syndromes, focal epilepsy and dystonia [75,76]. For example, auditory hallucinations in schizophrenia may be treated by inhibitory low-frequency rTMS to the left temporo-parietal junction [74]. Overall, the

advantageous non-invasive nature, safety and tolerability of these techniques drive the currently growing interest in their application for clinical therapeutic purposes.

1.3.4. Non-Invasive Brain Stimulation in Parkinson's Disease

The application of rTMS and tDCS in PD are particularly useful given the presence of both motor and non-motor symptoms in PD. The former is well managed by L-dopa and dopaminergic medication [12]; however, it is the L-dopa-unresponsive and non-motor symptoms that are typically the most disabling aspects of the disease at advanced stages [97]. Neuromodulation, which may be achieved through DBS, is a non-pharmacological alternative, although for PD patients at more advanced stages only. The procedure is also invasive and complicated, carries certain exclusion criteria (e.g., poor dopaminergic response, unstable psychiatric disease, severe dementia), and lead placement is associated with adverse cognitive effects [51]. Non-invasive neuromodulatory approaches are highly feasible, tolerable and safe, making them more attractive approaches.

Both tDCS and rTMS have the multimodal ability to target specifically the cortical-basal ganglia circuitry by M1 stimulation as well as prefrontal loops by DLPFC stimulation [84]. Strafella et al. demonstrated that high-frequency 10 Hz rTMS of M1 and DLPFC, independently, induced ipsilateral subcortical dopamine release in the ventrolateral motor putamen and non-motor caudate nucleus, respectively [98,99]. The functional effects of M1 rTMS and anodal tDCS has both benefits for improving UPDRS motor scores in bradykinesia, rigidity and gait measures, although the functional improvement has been observed to vary according to the stimulation protocol [84]. In contrast, mood and cognitive disturbances improved as a result of DLPFC stimulation. For example, in PD patients, two weeks of rTMS treatment improved depression scores (Hamilton Rating Scale for Depression

and Beck Depression Inventory) to the same extent as a selective serotonin reuptake inhibitor, Fluoxetine [100]. Additionally, rTMS and anodal tDCS of DLPFC improved working memory disturbances in non-depressed PD patients off medication [84,92]. Therefore, motor benefits in addition to mood and cognitive improvement demonstrate that rTMS and tDCS offer potential as multimodal treatment alternatives to drugs for motor and non-motor symptoms in PD.

1.3.5. Proposed Mechanisms of Non-Invasive Brain Stimulation

The above findings of non-invasive brain stimulation treatment offered by tDCS and rTMS are presumably consequences of dysregulated subcortical-cortical networks being modulated in a beneficial manner [74]. Presently, there is growing consensus that many neurological and neuropsychiatric disorders, such as stroke, depression and schizophrenia, are network disorders – that is, involving abnormal interactions between multiple regions [74]. For example, hemiparesis in stroke is related to imbalanced interhemispheric connectivity while neglect may be due to decreased connectivity in attentional networks [74]. On the other hand, depressed subjects compared to normals display global increases in EEG functional connectivity across alpha and theta frequency bands [74]. As well, aging, and therefore age-related cognitive decline, is related with lower levels of synchronization within high-frequency beta and gamma bands [74]. Since beta oscillation dynamics are disrupted in PD, the therapeutic benefits of tDCS and rTMS for motor and non-motor symptoms likely reflect modulation of functional connections which are mediated by neuronal oscillations. In support of this, TMS and transcranial currents delivered at a particular frequency, such as alpha, are able to entrain ongoing EEG alpha oscillations in healthy individuals [101,102]. Feurra et al. further demonstrated that entraining oscillations has functional benefits, such as

enhanced MEP amplitude and motor cortical excitability following 20 Hz transcranial stimulation of motor areas [57]. The notion of enhancing functional processing by modulating EEG oscillations has also been observed: sleep-dependent consolidation of declarative memories was improved by enhancing slow oscillations (<3 Hz) during slow-wave sleep with anodal tDCS in frontal areas [79]. More clinical studies of how non-invasive brain stimulation affects oscillatory dynamics in neurological and psychiatric disorders are needed. However, these studies do suggest that non-invasive brain stimulation is able to modulate neuronal oscillations and functional networks [74], as well as demonstrates potential clinical benefits. Given that the effects of stimulation likely depend on the existing level of activity within a given network [84], the spatial and temporal features of non-invasive brain stimulation techniques permit them to act as interventions for altered functional connectivity within large-scale networks.

1.4. Galvanic Vestibular Stimulation (GVS)

Galvanic Vestibular Stimulation (GVS) is a well-established technique known to alter the firing rates of vestibular afferent nerves. Transmastoidal GVS (i.e., with cutaneous application of electrodes on the mastoid processes), at high enough levels, elicits common vestibular effects such as postural sway and ocular torsion [103-109]. This is due to the fact that the vestibular nerve runs underneath the mastoids towards brainstem nuclei (Figure 1.3) [76]. Modulation of firing activity of vestibular afferents is achieved by cathodal or anodal stimulation to increase or decrease the firing frequency, respectively [110]. Therefore, with careful placement of electrodes on the mastoid processes, firing activity of vestibular afferents will be altered according to stimulation parameters.

Unlike other vestibular stimulation techniques, such as Caloric Vestibular Stimulation (CVS), GVS has many advantages. First, CVS, which involves irrigation of the external ear canal with warm or cold water, activates horizontal semicircular canals only, whereas GVS indiscriminately bypasses the vestibular end organ and acts directly at the spike trigger zone of the afferent nerve [111,112]. Secondly, because GVS involves delivery of an applied electrical current, like tDCS, it is well suited for subliminal stimulation so that the subject is unaware of *verum* stimulation in contrast to placebo or sham stimulation. This also has the added benefit of facilitating the differentiation between effects on cognitive performance and vestibular-evoked responses, which is difficult with CVS [110]. Manipulation of the applied stimulus parameters also makes GVS much more tolerable at weaker currents in comparison to CVS. In comparison to CVS, GVS additionally is largely advantageous since it does not come with adverse side effects, such as seizures, vertigo or nausea; however, symptoms of tingling and slight itching underneath the electrodes have been reported [113].

1.4.1. The Vestibular System and Vestibular Dysfunction

Stimulation of vestibular nerves by GVS ultimately influences the activity in multiple cortical and subcortical areas (Figure 1.3). These areas are related to a vestibular network, self and visual motion and multisensory processing, including: the prefrontal cortex, premotor region, somatosensory cortex, intraparietal sulcus, inferior parietal lobule, temporo-parietal junction, middle and superior temporal gyri, posterior parietal cortex, insula, hippocampus, anterior cingulate cortex, putamen [109,114-119]. Activation of these areas may be based on manipulation of the thalamocortical vestibular system where a putative trans-synaptic pathway exists through vestibular projections to ventroanterior (VA) and ventrolateral (VL) thalamic nuclei [119-121]. Since VA and VL nuclei also receive input

from the basal ganglia and cerebellum respectively, this is notably a major vestibulomotor pathway where vestibular and motor information converge [119]. In addition to the VA-VL complex, the pulvinar and geniculate nuclei also contain vestibular-responsive neurons and higher-order properties that may allow vestibular input to affect thalamic activity and modulate cortico-cortical communication [122]. As a result, the vestibular sensory network is distributed throughout numerous brain regions.

The widespread activation of cortical and subcortical areas due to GVS illustrates the global distribution of the vestibular system, as opposed to the presence of a primary vestibular cortex [119]. This particular characteristic of the vestibular system accounts for: 1) its multimodality and integrative attributes, 2) the broad range of vestibular-related functions and 3) the ensuing cognitive dysfunctions as a result of vestibular disorders [123,124]. The vestibular system mainly functions for gaze stabilization through the vestibulo-ocular reflex, maintenance of posture and balance, and estimation of self-motion perception [123]. However, in order to do so, integration of visual, proprioceptive and somatosensory information occurs at many stages of sensory processing from the earliest thalamic stage to cortical network interactions [123]. As a result, it has a broad range of functions from reflexes (e.g., vestibulo-ocular and vestibulospinal) to higher levels of voluntary motor behaviour [123]. At higher levels, not only are voluntary motor functions such as orienting movements and steering affected by vestibular information, but the hippocampus formation has also been implicated to encode specific vestibular inputs – although, how exactly that information is utilized or integrated with extra-vestibular information during navigation and spatial memory is not yet known [123]. Lastly, the activation of extra-vestibular cortical and subcortical areas implies that vestibular processing may affect multiple cognitive and

behavioural domains. This is demonstrated by the high incidence of depression, anxiety disorders, memory loss and attention deficits in individuals with vestibular dysfunction [124]. The vestibular system is consequently an important and inherently complex sensory system.

1.4.2. Cognitive Effects of GVS

Given the high distribution of the vestibular sensory network, it is not surprising to observe that vestibular input via CVS and/or GVS has a wide range of phenomenological effects on cognition. For example, vestibular input has been demonstrated to improve neuropathic pain [125,126], tactile extinction [127] and face perception and figure copying deficits [128,129]. For stroke patients, GVS has implications for improving disorders such as prosopagnosia [128] and hemispatial neglect [130]. In contrast, for normal subjects, GVS has enhanced visual memory recall. A similar range of phenomenological effects on spatial and attentional states are also observed in caloric vestibular stimulation studies [131], suggesting that GVS has potential therapeutic utility for cognitive processing deficits, although more work is needed to elucidate this.

1.4.3. Effects of GVS in Parkinson's Disease

Recently, several studies have investigated the effects of GVS on motor symptoms in PD. For example, Pan et al. demonstrated increased wrist activity in PD patients with akinesia [132] while Yamamoto et al. demonstrated improved bradykinesia as well as motor execution through faster reaction times in a Go/NoGo performance test [133]. A slight but significant reduction in evoked postural sways was also observed in PD patients receiving GVS, suggesting that balance and posture may be additionally improved in PD [134]. In support of these studies in patients, a recent study using a 6-hydroxydopamine hemilesioned

rat model demonstrated improved balance and motor planning in the accelerating rod test [135]. It has been suggested that GVS acts by affecting activity in subcortical basal ganglia networks: in the hemiparkinsonian rat model, GVS promoted GABA release in the lesioned substantia nigra [135]. On the basis of these recent findings, GVS may possibly carry a therapeutic benefit for PD patients, although a greater repertoire of work is greatly needed to test this hypothesis.

1.4.4. Noisy GVS and Stochastic Facilitation

Interestingly, a large number of studies using GVS to improve cognitive performance and motor symptoms in PD have been based on noisy stimulation parameters (i.e., using randomly varying stimulation currents) [132,133,136] [135]. Even heart rate responses in the baroreceptor reflex were enhanced when externally applied $1/f$ noise (i.e., the power density of the stimulus is inversely proportional to the frequency) was added to the brain via GVS [137]. In this particular study, $1/f$ noise was observed to better elicit responses than white noise stimuli [137]. This suggests that $1/f$ noise was better used by the brain to optimize the baroreceptor system at a lower noise level than white noise – that is, with less power to improve responsiveness. These findings suggest that noise, in particular the $1/f$ type, enhances the neuromodulatory effects of GVS and neural processing.

Stochastic facilitation is a broad term to describe how noise facilitates the detection of weak subthreshold signals [138]. In addition to the findings above using noisy GVS, others have shown that stochastic facilitation enhances functional processing or information transfer. For example, noise addition to sensory stimuli, aside from vestibular, enhances neural responses – such as the 40 Hz synchronization response to auditory tones [60]. The benefits of noise in a given system are not surprising since the presence of noise is ubiquitous

throughout nature [139]. However, with respect to cortical and subcortical functional networks, noise in the brain is typically "coloured" as pink noise with a $1/f$ type power spectrum [139]. This phenomenon may be largely attributed to the anatomical architecture of the cortex and indicates the predominance of lower frequency components in brain rhythms [139]. Therefore, since the spatial scale at which functional networks operate is determined by the temporal scale of oscillations, slower rhythms with longer periods tend to recruit large-scale networks whereas faster rhythms are confined to local neuronal populations [139]. However, the significance of $1/f$ noise in information processing within the brain is not fully established. The above stated findings suggest that $1/f$ noise has implications for functional networks, perhaps by supporting the dynamics needed to switch between different cognitive or behavioural states [74], although a greater understanding of this is needed.

1.5. Study Aims and Hypotheses

In summary, substantial evidence as outlined in this Introduction section demonstrates that: 1) exaggerated synchronization of beta oscillations in PD may identify functional networks which are improperly modulated, thereby accounting for motor symptoms, 2) non-invasive brain stimulation techniques, such as tDCS and rTMS, are feasible and effective inventions to modulate the dynamics of functional networks not only in PD but also other neurological and psychiatric conditions, and 3) noisy GVS may ameliorate parkinsonism motor symptoms in PD by acting as a non-invasive brain stimulation method that enhances information processing within cortical and subcortical networks.

Non-invasive and non-pharmacological treatment alternatives for PD are of presently great interest. While L-dopa is effective is managing motor symptoms, not all symptoms are L-dopa-responsive, and long-term usage causes motor fluctuations and psychiatric side

effects [73]. Alternatively, DBS as well is a highly complicated and invasive procedure limited to advanced PD patients who meet certain inclusion criteria [51]. As a result, numerous minimally invasive brain stimulation techniques are currently being explored, with transcranial current stimulation and rTMS being the most common. However, novel forms of stimulation are presently emerging and being investigated, such as vagus nerve stimulation and trigeminal nerve stimulation, particularly for desynchronizing oscillatory activity in epilepsy and depression [140,141]. The exploration of these novel therapies suggest that sensory input may be a more pertinent therapeutic pathway for modulating brain networks due to its more direct effect on global thalamocortical rhythms. Since thalamocortical dysrhythmias identify diseased states and are presumably a reflection of altered global dynamics of functional networks [142,143], stimulation through the vestibular sensory stimuli may fare better in comparison to tDCS and rTMS – both of which direct effects towards a specifically targeted region and the involved network.

Since the vestibular system is widespread, multimodal and has an implicated involvement in a variety of mood, cognitive and behavioural functions, we are interested in exploring GVS as a potential therapeutic for PD, which itself is characterized by a broad and complex host of motor and non-motor symptoms. GVS is easy to manipulate, safe and, like tDCS, notably more tolerable than other non-invasive brain stimulation techniques. More importantly, vestibular input stimuli through GVS have proven effective in influencing processing of various cognitive and motor functions. Therefore, we hypothesize that noisy GVS may be a potential neuromodulatory and therapeutic tool for PD. To test our central hypothesis, we focused on two specific aims: 1) to determine the effects of noisy GVS on EEG activity in normal and PD subjects, and 2) to determine the functional significance of

noisy GVS by investigating motor behaviour in a visuomotor task. Previously, we observed through pilot investigations that there may be a motor benefit of noisy GVS in PD patients in a different visuomotor tracking task, which was coupled with various levels of ambiguous visual feedback (Figure 1.4); however, the subject pool was relatively not large enough (n=7) and the ambiguity of visual feedback may have hampered the results. Our specific aims were addressed by experiments in the following chapters of this thesis.

In Chapter 2 of this thesis, we explore the neuromodulatory effects of noisy GVS in the EEG of normal, healthy individuals (n=10). We applied stimulation while recording the online effects on the resting-state EEG with eyes open. Using linear transformation techniques, such as Independent Component Analysis and the QR decomposition, we removed the stimulus artifact from the EEG. We analyzed both transient aftereffects in the post-stimulus EEG, as well as the linear relation between EEG spectral power and stimulus intensity. According to our hypothesis, we tested whether noisy GVS was able to modulate EEG synchrony patterns.

In Chapter 3 of this thesis, we compare the effects of noisy GVS on the EEG in PD subjects off medication (n=7). In the same manner as above, we removed the stimulus artifact from the EEG using a combination of linear transformation techniques (Independent Component Analysis and the QR decomposition). We analyzed both transient aftereffects in the post-stimulus EEG, as well as the linear relation between EEG spectral power and stimulus intensity. Since noisy GVS has been implicated to have a positive effect on motor function in PD [132,144], we predicted significant effects on the spectral power of beta synchronization, which is related to sensorimotor processing [55]. In this study, we investigated ongoing EEG effects of noisy vestibular stimulation in PD subjects.

Lastly, in Chapter 4, we address the second aim by investigating the online motoric effects of noisy GVS in both normal control and PD subject groups (n=12, each). PD subjects were tested both in the off-medicated state and following administration of immediate-release levodopa. All subjects performed a visuomotor manual tracking task as previously performed for investigation in PD subjects [146]. The effects of noisy GVS on motor dynamics were assessed by Linear Dynamic System models. Given previous findings that have observed motor improvement in PD [132-135] in addition to our observed EEG results, we hypothesized that noisy GVS will affect the functional processing of motor behaviour.

CHAPTER 2: Noisy Galvanic Vestibular Stimulation Modulates the Amplitude of EEG Synchrony Patterns in Normal Subjects

2.1. Summary

Noisy galvanic vestibular stimulation has been associated with numerous cognitive and behavioural effects, such as enhancement of visual memory in healthy individuals, improvement of visual deficits in stroke patients, as well as possibly improvement of motor function in Parkinson's disease; yet, the mechanism of action is unclear. Since Parkinson's and other neuropsychiatric diseases are characterized by maladaptive dynamics of brain rhythms, we investigated whether noisy galvanic vestibular stimulation was associated with measurable changes in EEG oscillatory rhythms within theta (4-7.5 Hz), low alpha (8-10 Hz), high alpha (10.5-12 Hz), beta (13-30 Hz) and gamma (31-50 Hz) bands. We recorded the EEG while simultaneously delivering noisy bilateral, bipolar stimulation at varying intensities of imperceptible currents – at 10, 26, 42, 58, 74 and 90% of sensory threshold – to ten neurologically healthy subjects. Using standard spectral analysis, we investigated the transient aftereffects of noisy stimulation on rhythms. Subsequently, using robust artifact rejection techniques and the Least Absolute Shrinkage Selection Operator regression and cross-validation, we assessed the combinations of channels and power spectral features within each EEG frequency band that were linearly related with stimulus intensity. We show that noisy galvanic vestibular stimulation predominantly leads to a mild suppression of gamma power immediately after stimulation in lateral regions, followed by delayed increase in beta and gamma power in frontal regions approximately 20-25 s after stimulation ceased. Ongoing changes in the power of each oscillatory throughout frontal, central/parietal, occipital and bilateral electrodes predicted the intensity of galvanic vestibular stimulation in a

stimulus-dependent manner, demonstrating linear effects of stimulation on brain rhythms. We propose that modulation of neural oscillations is a potential mechanism for the previously-described cognitive and motor effects of vestibular stimulation, and noisy galvanic vestibular stimulation may provide an additional non-invasive means for neuromodulation of functional brain networks.

2.2. Introduction

The vestibular system may be considered a sixth sense [147] but thalamic and cortical processing of vestibular sensory information is especially complex, multimodal and widespread. While the parieto-insular vestibular cortex has been described as the "core" vestibular region in non-human primates [148], present views gravitate towards the notion of a highly distributed vestibular network comprising the lateral and medial frontal cortices, somatosensory cortex, premotor region, temporo-parietal junction, posterior parietal cortex, anterior and posterior insula, hippocampus and cingulate cortex [117,119]. The widespread nature of vestibular projections is mediated by multiple vestibular-responsive thalamic nuclei and corticothalamocortical communication [119,120,122,149,150]. Our understanding, however, of the vestibular influences on cortical and subcortical networks remains incomplete.

Galvanic vestibular stimulation (GVS) confers many advantages for investigating the effect of vestibular input on brain function. Transcutaneous delivery of galvanic current to the mastoid processes alters firing rates of vestibular afferents though, unlike natural or caloric stimuli, without canal or otolithic directional specificity [111,131]. Nevertheless, direct and precisely controlled perturbation of the vestibular system using GVS has facilitated the modern study of balance, dynamic movements and cognitive effects while

largely avoiding unwanted side effects of vertigo, nausea and nystagmus [113,130,136,145,151]. Therefore, due to the usefulness and tolerability of GVS, growing interest has expanded its role in neuropsychological and neurorehabilitation purposes for both normal and patient groups [76]. For example, with application of noisy (i.e., with random fluctuations) GVS, studies have demonstrated enhancement of cognitive abilities, such as visual memory, in healthy subjects [136]. Noisy GVS applications have also extended to neurological diseases, with evidence suggesting stimulation improves hemispatial neglect and prosopagnosia in stroke patients [130,152] while caloric vestibular stimulation has been shown to alleviate neuropathic pain [125,126]. Additionally, Yamamoto et al. delivered noisy GVS in the context of motor tasks to patients with central neurodegenerative disorders, including Parkinson's disease [133]. Patients improved in their motor responsiveness during periods of stimulation, an outcome that has been subsequently reproduced [132,135], although, like the previously stated cognitive findings, the mechanism remains largely unexplained.

The reported motoric benefit of noisy GVS in Parkinson's disease patients is particularly intriguing considering that the Parkinsonian state is characterized by highly synchronized beta oscillations (15-30 Hz), which propagate throughout a basal ganglia-thalamocortical network. These predominantly low-frequency oscillations (>30 Hz) have been recorded in the external globus pallidus (GPe), subthalamic nucleus (STN), striatal and M1 neurons in dopamine-depleted animal models [38-40]. Oscillatory synchronization below 30 Hz has similarly been observed in local field potential (LFP) recordings of STN, internal (GPi) and external pallidal (GPe) neurons in patients off medication [42,43,47]. In corroboration with these findings, sensorimotor EEG potentials recorded from Parkinson's

disease patients have been observed to strongly resonate at 20 Hz, and to a lesser extent at 10 Hz [37]. Partially driven by a pattern generator comprised of the STN-GPe network [35], the exaggerated entrainment of neurons in the beta band throughout a basal ganglia-thalamocortical network has been suggested to serve as a basis for bradykinesia and movement impairments [35,153]. However, the exact manner in which beta synchrony affects sensorimotor processing is currently contentious. Previous studies have suggested that the high beta synchrony observed in Parkinson's disease may be "antikinetic" or may prevent processing of novel information, thereby accounting for poverty of movement [25,53,54]. Yet, recent evidence suggests that the beta synchronization observed in the dopamine-depleted and Parkinsonian condition is indicative rather of a functional network "stuck" in one of many normal dynamic states [55].

Given the previously stated cognitive and behavioural effects of GVS, we hypothesized noisy GVS will alter neural oscillatory dynamics, particularly in the beta band. The ability of GVS to modulate slower delta and theta brain rhythms during a visual processing task has been demonstrated before in healthy subjects, although using a direct current stimulus [154]. Since variable levels of noise may optimize incoming signal detection and neural transmission [155] and in consideration of the previously stated cognitive and behavioural effects using noisy GVS [130,132,133,135,136,152], we were particularly interested in whether noisy stimulation modulates EEG rhythms. External influences via non-invasive brain stimulation techniques on the oscillatory dynamics of the brain are highly relevant since the brain uses neural synchronization as a mechanism to dynamically shift between transient functional network states [59,156]. Generally speaking, oscillatory dynamics and synchrony patterns, which have been demonstrated to temporally coincide with perceptual

cues [60,61,70], are therefore hypothetically associated with information transmission relevant for a particular behaviour or function [59]. For example, using normal, intact rats, Leventhal et al. demonstrated that beta synchronization reflects a post-decision state of motor output decision following a sensory cue [55]. Furthermore, in addition to Parkinson's disease, abnormal oscillations characterize numerous neurological and neuropsychiatric disorders such as neurogenic pain, tinnitus and depression [142]. Therefore, the effect of GVS and noisy sensory input on ongoing – normal and pathological – brain oscillatory dynamics is an unaddressed issue of further interest.

Here we investigated whether imperceptible, noisy GVS is capable of modulating standard EEG rhythms in normal, healthy subjects. We applied a noisy stimulus with $1/f$ power features, and investigated the subsequent effect on recordings within theta (4-7.5 Hz), low alpha (8-10 Hz), high alpha (10.5-12 Hz), beta (13-30 Hz) and gamma (31-50 Hz) bands. We investigated the transient aftereffects and simultaneous neural changes during eyes-open resting state as a result of transcranial noisy vestibular stimulation. Previously, large stimulus-based EEG artifacts have disrupted the ongoing measurement of microvolt-level brain oscillations, a complication presently circumvented by: 1) improved EEG amplifier design with high common-mode-rejection ratio, and 2) a combination of well-established artifact rejection and factorization analytical techniques such as Independent Component Analysis (ICA) [157] and the QR decomposition [158,159]. Using subsequent power spectral analysis and Least Absolute Shrinkage Selection Operator (LASSO) regression, we aim to demonstrate whether noisy GVS is associated with changes in the amplitude of oscillatory synchrony patterns that are due to both direct and ongoing effects. We show an immediate and brief suppression of gamma power in lateral regions after stimulation stopped;

additionally, after cessation of GVS, we observed a delayed increase (after ~20-25 s) in beta and gamma power in frontal regions, altogether indicating a global and direct effect of noisy vestibular stimulation on EEG rhythms. More importantly, using LASSO regression, we show that noisy GVS modulates the power of ongoing EEG synchrony across theta, alpha, beta and gamma bands, providing evidence of its ability to directly influence brain rhythms.

2.3. Materials and Methods

2.3.1. Subjects

Ten healthy individuals (five males, five females; aged from 20 to 63 years; mean age 37.2 ± 17.7 years; all right-handed) without any reported vestibular, auditory or neurological disorders participated in the study. Since the present study was novel and exploratory, we selected a range of young and older adults in order to preclude potential age-dependent factors that may bias our results. Data for one participant were excluded due to excessively noisy, corrupted data (<50% data yield).

2.3.2. Ethics Statement

The study was approved by the University of British Columbia Clinical Research Ethics Board. All subjects gave written, informed consent prior to participation. Research was conducted according to the principles expressed in the Declaration of Helsinki.

2.3.3. Primary Study Protocol

Subjects were comfortably seated 80 cm from a screen, and were instructed to focus their gaze on a continuously displayed fixed target to minimize distractions while the EEG was recorded (6 trials, 192 s each). In each trial, EEG was first recorded without stimulation for 60 s (pre-stimulus period), blinding subjects to the actual stimulus onset. Noisy stimulation signals were then delivered for a fixed duration of 72 s (stimulation period),

followed by a sham current for 60 s (post-stimulus period). During the stimulation period within each trial, we applied one of six imperceptible currents: 10, 26, 42, 58, 74 and 90% of the determined threshold value. For each subject, the delivery of the 6 trials and respective stimulation intensities were differently permutated in a pseudorandom order.

2.3.4. Stimulus

GVS was delivered to subjects through carbon rubber electrodes (17 cm^2) in bilateral, bipolar fashion. For bilateral stimulation, an electrode was placed over the mastoid process behind each ear (Figure 1), and coated with Tac gel (Pharmaceutical Innovations, NJ, USA) to optimize conductivity and adhesiveness. Digital signals were generated on a computer with Labview software and converted to analog signals via a NI USB-6221 BNC digital acquisition module (National Instruments, TX, USA). The analog command voltage signals were subsequently passed to a constant current stimulator (Model DS5, Digitimer, Hertfordshire, UK), which was connected to the stimulating electrodes.

Bipolar stimulation signals were zero-mean, linearly detrended, noisy currents with a 1/*f*-type power spectrum (pink noise) as has been previously applied in Parkinson's disease and healthy subjects [132,133,137]. The stimulation signal was generated between 0.1-10 Hz with a Gaussian current density, with the command signal delivered to the constant-current amplifier at 1 kHz (Figure 2). The stimulus was applied at an imperceptible level to avoid effects by general arousal and/or voluntary selective attention, with the current level individually determined according to each subject's cutaneous sensory threshold.

Since perception of GVS is inherently subjective, we utilized systematic procedures that have been previously utilized in determining subliminal current levels for both GVS and transcranial stimuli [113,136,160]. Starting from a basal current level of 20 μA, noisy test

stimuli were delivered for 20 s periods with gradual stepwise increases (20 μA) in current intensity until subjects perceived a mild, local tingling in the area of the stimulating electrodes. A threshold value was defined once subjects reported the tingling sensation as performed previously [113,136], which lasted for the duration of the test stimulus. The current level was then decreased each time by one level until sensation was no longer reported during delivery of test stimulus pulses, and increased by one step in current intensity to confirm threshold. Each delivery of a test stimulus was followed by a period of no stimulation for at least 30 s to preclude a hysteretic effect carrying over to the next test stimulus: after a 20 s of high-frequency deep brain stimulation of the STN, beta rhythms return to baseline 15 s after the stimulus finishes [52]. Subjects were blind to the onset and duration of test stimuli, as well as the threshold-testing scheme.

2.3.5. EEG Acquisition

We recorded the continuous EEG from 19 scalp electrodes using a Neuroscan Synamps^2 EEG acquisition system and standard electrode cap (Neuroscan, VA, USA). Electrode impedances were maintained below 10 kΩ using Electro-Gel (Electrode-Cap International, OH, USA). Recording electrodes were positioned according to the International 10-20 EEG System (Figure 1) with one ground electrode and linked earlobe electrodes as reference. Surface electromyographic electrodes were positioned above and below each eye for subsequent artifact removal during analysis [161]. All data were digitized at 1 kHz, and bandpass filtered between 1 and 250 Hz.

2.3.6. EEG Pre-Processing

EEG data were downsampled to 250 Hz and bandpass filtered between 1 and 50 Hz. We subsequently applied Independent Component Analysis (ICA) to remove common

artifacts from the recordings [157,162]. ICA uses linear combinations of electrodes to derive temporally independent waveforms from a mixed signal. Artifacts due to eye movements, muscle activity and heartbeats are statistically independent from ongoing brain rhythms in the time domain, making ICA ideal for artifact isolation and removal [162]. ICA was performed on concatenated EEG data from pre- and post-stimulus periods, and 15 component activations were extracted. Careful joint inspection of the scalp topography, power spectrum and activity of components allowed for deeming specific components for artifact rejection in the pre- and post-stimulus EEG periods.

We assumed that the source localization of common EEG artifact components (e.g. eye movement, muscle artifact) remained unchanged during the stimulation. We therefore utilized the unmixing matrices from ICA performed on concatenated pre- and post-stimulus periods, and applied those matrices to isolate eye, muscle and cardiac artifacts present in the stimulation periods. The use of the pre/post stimulus unmixing matrices also ensured that no bias was introduced into the intrastimulus EEG during ICA artifact removal. Common artifact components were similarly assessed and rejected by thorough joint inspection of the scalp topography, power spectrum and activity of components. EEG data were subsequently reconstructed using all other components.

Since skin has a relatively low resistivity in comparison to the skull, a fraction of the stimulating currents could potentially be directly shunted across the scalp and picked up by the recording electrodes [163]. The issues of EEG data containing stimulus artifacts or of removing too much neural information during artifact rejection pose a central concern with simultaneous electrical stimulation and recording approaches [164,165]. During the stimulation period, microvolt recordings of biological activity may be overwhelmed by

higher-voltage shunted stimuli. In order to remove stimulus-based artifacts from the EEG, we concatenated recordings of the 6 stimulation periods for each subject. To remove the direct effects of shunting, we utilized the linear-based [166,167] QR decomposition (*qr* function in Matlab). We created an augmented matrix consisting of the EEG (with artifacts removed via ICA) and the temporally-aligned stimulus signal. The QR decomposition of the real matrix *A* computes an orthogonal matrix *Q* and upper triangle matrix *R* such that $A = Q \cdot R$. In the current situation, we created the matrix *A* so the first column was the stimulus, and subsequent columns were the concatenated EEG recordings. We then performed the "economy-size" QR decomposition. The rows of *Q* corresponded to the number of time points, and the number of columns corresponded to the number of EEG channels + 1 (corresponding to the stimulus). By setting the first row of *R* to zero, to create R_0, then deriving $A_{new} = Q \cdot R_0$, we can obtain the EEG data with the stimulus regressed out. Previously, stimulus-induced artifacts have been removed from potential recordings using a least squares regression [164]. Similarly, we chose the QR decomposition due to: 1) its numerical stability and computational efficiency for a large number of EEG recording channels [158], as well as 2) its proven recognition accuracy of discriminant vectors when applied for feature extraction of high dimensional data [159]. Following rejection of stimulus-induced artifacts, the reconstructed EEG stimulation periods were then divided into non-overlapping, 1-s epochs. Each epoch was then finally inspected to ensure absence of stimulation or other artifacts.

2.3.7. Power Spectral Analysis

Aftereffects of Stimulation

In order to investigate whether the effects of GVS potentially have any direct effect on brain rhythms, we analyzed net EEG spectral changes following the highest-level stimulation condition (90% threshold). In one subject, the data was corrupted towards the end of the trial; therefore, we used the first 40 s for all subjects. For the artifact-free pre- and post-stimulus periods from the trial with current level 6, we calculated time-varying changes in power spectral density (PSD) for each electrode channel using a short-time Fourier transform (*spectrogram* function in Matlab, nFFT = 256, window = 125 points, overlap = 62 points). For each window segment, the spectral difference was taken from the post-stimulus minus the pre-stimulus periods, and we applied a one-sided t-test to see whether net spectral changes within a given frequency band were significantly different from the pre-stimulus period. Changes in spectral amplitude were analyzed for each of 5 frequency bands of interest: theta (4-7.5 Hz), low alpha (8-10 Hz), high alpha (10.5-12 Hz), beta (13-30 Hz), gamma (31-50 Hz). Spectrograms were plotted for each electrode channel and show mean spectral changes across all subjects. Since the order of the 6 stimulus levels was pseudorandom and varied for all subjects, the inherent issue of EEG non-stationarity is largely precluded. Significance was determined at $p < 0.05$.

Effects of Stimulation

In order to determine whether GVS effects were associated with ongoing EEG changes, we analyzed the PSD of activity recorded in each electrode during the stimulation period and within the same frequency bands of interest: theta, low alpha, high alpha, beta and gamma. PSD features of activity recorded were calculated for each 1-s epoch of artifact-free data using a fast Fourier transform with 1-s windows (*pwelch* function in Matlab, nFFT =

256, window = 250 points, no overlap). Specifically, we tried to predict current level given the EEG features using multivariate regression:

$$Y = X \cdot \beta + \varepsilon \qquad (1)$$

where Y was of dimensions 60 (6 current levels x 10 subjects) by 1, X was 60 by 95 (19 channels x 5 frequency bands) and ε is 95 (19 channels x 5 frequency bands) by 1 and given the EEG feature of the band-limited power over each of the six current levels was removed.

Since, in this case, the number of potential regressors (95) exceeds the number of examples (60), we utilized LASSO regression (*lasso* command in Matlab) [168]. Unlike other methods such as ridge regression or ordinary least squares, LASSO regression puts a sparsity constraint on β so that most values are zero and attempts to find the most informative electrode/band combination of EEG spectral changes to predict current level [168]. The number of regressors selected by the LASSO operator was to give the least predictive error based on a 10-fold cross-validation. Once the regressors were selected, we used robust regression (*robustfit* command in Matlab) to estimate the significance of the individual regressors.

In order to visualize possible non-linear effects of the stimulus, for the significant channels, we plotted actual changes in band-limited power level as a function of stimulus current (in effect, the appropriate column of X vs. Y in eqn 1 – Figure 2.4B).

2.4. Results

Subjects reported a cutaneous sensory threshold at mean RMS current amplitude of 160 ± 110 μA. For the highest-level stimulus condition (current level 6), mean delivered RMS voltage was recorded as 4.6 ± 2.3 V. In consistency with prior observations, subjects additionally did not report perceiving any stimulus during the stimulation periods [113,154].

Subjects also did not experience postural sway throughout the experiment trials. Some subjects reported feelings of mild dizziness or lightheadness after the experiment.

2.4.1. Noisy GVS Increased Beta and Gamma Power in the Post-Stimulus Period

In the post-stimulus period, significant net spectral effects were noted in the spectrograms for electrode channels in frontal and bilateral regions. In electrode channels F3, Fz, F4 and F8, beta power significantly increased starting 18-23 s after the stimulation had ceased (p = 0.019, 0.021, 0.018, 0.039 respectively, Figure 2.3). In a similar fashion, gamma power significantly increased starting 26-27 s later in fronto-lateral areas F3, F4 and F8 (p = 0.011, 0.037, 0.022 respectively, Figure 2.3). Overall, we conclude that the significant augmentation in power of beta and gamma rhythms in frontal areas appeared with a brief delay of approximately 20-25 s after stimulation ended, and lasted only several seconds with the strongest effects of gamma suppression in F8 lasting up to 40 s after stimulation stopped. Additionally, we note that the effects were lateralized with changes in power increases predominantly occurring in electrode channels in the right hemisphere. In T3, C3, transient and mild suppression of gamma power was observed immediately after stimulation stopped during the first 10 s of the post-stimulus period (p = 0.046, 0.023 respectively, Figure 2.3). Upon attentive inspection, we observed gamma power suppression occurred immediately after stimulation in lateral and occipital channels T4, T5, O1 and O2, lasting about 5 s (Figure 2.3); however, this suppression did not reach significance ($p > 0.05$). Lastly, since the significant p values were not greatly less than the limit (0.05), we conclude that the aftereffects of the stimulation on EEG rhythms, while visually visible across the mean of subjects, were mild and short-lived – presumably due to the weak, subsensory levels of

currents delivered (see Table 2.1 for *p* values and exact time points in the spectrograms which showed significant spectral changes).

2.4.2. Stimulation Intensity Is Linearly Related with EEG Power Features across Bands

In the theta band, the LASSO algorithm identified 6 significant electrode channels in frontal areas (Fp2, F3, Fz, F4), the posterior-midline (Pz) and right lateral side (T6). In the low alpha band, LASSO identified 7 significant electrode channels in frontal areas (Fp1, Fz, F8), the central/midline area (Cz, Pz) and right posterior area (P4, O2). In the high alpha band, LASSO identified 9 significant electrode channels in frontal channels (Fp1, Fz, F8), the central/midline area (Cz, Pz) and bilateral posterior areas (T5 P4, T6, O1). In the beta band, LASSO identified 9 significant electrode channels in frontal areas (Fp1, Fp2, F3, Fz, F8), the central area (Cz), the right lateral side (T4) and occipital areas (O1, O2). In the gamma band, LASSO identified 13 significant channels in frontal areas (Fp1, Fp2, F7, F3, F4, F8), the central/midline area (Cz, Pz) and bilaterally throughout central (T3, C4) and posterior areas (P4, T6, O1). All electrode regions selected by the LASSO operator as related linearly with band power are illustrated in Figure 2.4A. Significance was determined at $p < 0.05$ (see Table 2.2 for *p* values).

For each frequency band of interest, median spectral power measured in the above significant electrodes for all subjects were plotted as a function of stimulus intensity (Figure 2.4B). Note that this is the same as plotting the appropriate columns of *X* as a function of *Y* in eqn. 1. When the information from all columns of X (i.e., all bands) were included, plotting $X \cdot \beta$ vs *Y* resulted in a linear relation (Figure 2.4C).

2.5. Discussion

We have shown for the first time, to our knowledge, that noisy GVS influences ongoing EEG activity when applying a simultaneous galvanic vestibular current during resting state with eyes open. Transient changes in spectral features, notably in the beta and gamma bands in frontal regions, were observed after cessation of stimulation, therefore demonstrating that GVS directly modulated brain rhythms. Subsequently, upon analyzing ongoing EEG changes, we observed a dose-dependent relation between stimulation intensity and EEG power spectral features, which measure oscillatory amplitude corresponding to neural synchrony. Such dose dependency has been implicated by previous work, showing that supersensory direct current GVS applied during a visual processing task increased delta power to a greater amplitude than subsensory stimulation [154]. Furthermore, we observed spectral changes in all bands of interest (theta, alpha, beta, gamma) across predominately frontal-parietal electrodes. Therefore, our work suggests that noisy, imperceptible GVS modulates global synchronization of neural oscillatory activity across theta, alpha and – outside of the stimulus frequency – beta and gamma frequency bands with transient aftereffects.

Since we did not measure spectral changes beyond 40 s after stimulation ended, it is unknown whether power changes lasting greater than 40 s were present. However, direct stimulation of the STN for 20 s by deep brain stimulation in Parkinson's disease has resulted in beta power changes which persist for 15-25 s after stimulation cessation [52]. On this basis, due to the short duration of our weak, transcranial stimulation protocol (72 s), we infer it is unlikely novel post-stimulus spectral changes occurred beyond 40 s. Additionally, whether our observed spectral changes are long-lasting to induce synaptic plasticity is

beyond the scope of this paper. In the present study, we largely focused on simultaneous effects of GVS on EEG activity, and discuss the relevance of our results with respect to vestibular processing and neural oscillations.

Consideration must be given to the possibility that our results were influenced by imperfect artifact removal: stimulus currents might have been directly shunted along the scalp to the recording electrodes, and/or the stimulus current may have simply propagated non-specifically throughout brain tissue. However, our conclusions were likely not based on false positive results. First, we first demonstrated significant post-stimulus spectral changes immediately after cessation of stimulation, supporting our hypothesis that brain rhythms are directly influenced as a result of stimulation. Secondly, linear regression methods have been proven previously to remove stimulus-related artifacts from potential recordings in rats [164]. The applied QR decomposition method similarly relies on linear transformation with greater computational efficiency and accuracy appropriate for the high number of electrodes [158,159] to robustly isolate any EEG features that exactly resembled the stimulus. In addition, while the temporal profile of the stimulus may have been altered due to potential capacitive and inductive characteristics of scalp tissue, significant EEG changes were observed in frontal, midline and posterior regions – far from the stimulating electrodes – in both analyses of post-stimulus and ongoing effects. EEG changes were importantly observed in frequency bands greater than the stimulus range of 0.1-10 Hz (i.e., in high alpha, beta and gamma bands). Rather, our results are consistent with the notion that GVS may directly alter firing in vestibular nerve projections and ensuing thalamocortical neural connections [76].

The observed effects on EEG activity may be explained by direct modulation of vestibular processing areas and possibly indirect effects on cortico-cortical connections. GVS

is a well-established technique that delivers a weak current that bypasses hair cells and alters firing patterns of vestibular afferent nerves in the same manner as natural stimulation [111,112]. Since the vestibular nerve runs underneath the mastoids towards brainstem nuclei [76], transmastoidal stimulation has effectively and consistently been shown numerous times to activate vestibular-related subcortical and cortical regions [109,114,116-118] and elicit appropriate consequences on balance-related functions and ocular movements [106,107,169]. Direct cathodal stimulation of the vestibular end organ depolarizes the transmembrane potential predominantly at the spike trigger zone whereas anodal stimulation inhibits firing [111,112]. Therefore, depending on the existing neural connections and brain state, externally applied stimulating currents may spread from target regions trans-synaptically to modulate cortical and subcortical activity [75]. This modulation may be based on manipulation of complex thalamocortical loops receiving input from vestibular afferent projections through thalamic relay neurons, such as the pulvinar [119,150]. Unlike other non-invasive brain stimulation techniques targeting specific cortical areas, GVS therefore has a more direct influence on thalamic processing.

We delivered GVS at imperceptible levels as determined by cutaneous sensory thresholds. While objective measures such as postural sway and eye movements via activation of the vestibulo-ocular reflex would have been potentially useful to establish a definitive threshold, we relied on subjective reporting to determine each subject's individual sensory threshold to GVS for a number of reasons. Importantly, the noisy waveform of our stimulus is less apt to produce an easily quantifiable measure compared to a DC or sinusoidal stimulus [111]. Postural sway movements tend to the anodal side of stimulation [111] while the eye experiences an ipsiversive ocular torsion with respect to the anodal side of

stimulation [170]. Therefore, the noisy nature of the stimulus waveform would inherently preclude accurate measurements of sway or ocular movements. In addition, prior studies have demonstrated that low-level currents (less than 0.5 mA) are insufficient to elicit any other responses [111]. Our results are thus directly related to modulation of ongoing EEG rhythms and are not masked by postural sway, ocular movements, and perception of body rotation, auditory or pain modalities. Third, it was important that subjects were unaware of the stimulation in order to avoid confounding variables due to voluntary attention and/or general arousal via the reticular formation. Careful debriefing after the experiment revealed the subjects did not sense the stimulation at any time throughout the study, which might suggest that the determined threshold had been set inappropriately high. In contrast, if the determined threshold had been set inappropriately low, our ability to detect significant changes in brain rhythms would have been hampered. Here, we used subjective reports as a reliable approach to determine GVS sensory threshold levels as used previously [136,154], and consequently achieved significant results with the applied subthreshold current intensities. In addition, the question of whether subsensory stimulation was arguably sufficient to modulate EEG rhythms has been addressed recently [154]; the previously demonstrated changes in event-related potentials and spectral power in response to subsensory GVS – identified in the same manner according to cutaneous sensory threshold – refute the possibility of insufficient current levels [154] as do our observed post-stimulus spectral changes.

2.5.1. Modulation of Synchrony Patterns and Global Oscillatory Networks

Consistent with the view that no single vestibular cortical region exists [117,119,150], our results demonstrate that noisy GVS increased the overall amplitude of

synchrony patterns in theta, alpha, beta and gamma bands measured throughout frontal, central/parietal, bilateral and occipital electrodes. Prior studies have demonstrated that GVS induced similar broadband spectral changes in delta, theta, alpha and beta bands, throughout frontal, temporal, posterior, occipital electrodes – yet mainly over midline and lateral channels [154]. In comparison to these prior findings, we specifically observed modulation of each band power consistently at frontal sites. Specific differences may be attributed to the nature of the stimulus (direct current vs. noisy) and experimental paradigm (resting state vs. visual task-related) [154]. We conclude our results reflect global modulation of synchrony patterns across a broad range of oscillations.

The broadband changes we observed are notably interesting because synchronization of slow and fast frequency oscillations work together to mediate various cognitive and behavioural functions. Simultaneous alpha, beta and gamma oscillations integrate and cooperate in attention, working memory and perception [171]. Even theta and gamma oscillations have been shown to be "nested" (i.e., with the amplitude of the faster rhythms phase-locked to the slower oscillation), while temporally coinciding with conscious visual percepts in humans [70]. Of greater interest, integration of theta and gamma synchrony occurred throughout a large-scale prefrontal-parietal network [70]. Similarly, coherence of beta and gamma power throughout a large-scale motor-striate network has been demonstrated to dynamically change throughout a GO-NO-GO motor paradigm [58]. In the present study, we show that noisy GVS significantly increased the amplitude of theta, alpha, beta and gamma power in prefrontal and posterior (parietal and/or occipital) regions. The fact that noisy GVS modulated alpha, beta and gamma power in occipital electrodes O1 and O2, which corresponds to the striate cortex [172], is not surprising. GVS has been previously

demonstrated to enhance visual processing, such as visual memory recall in normal subjects [136] and spatial processing performance in stroke patients [110,129,130,152]. A more remarkable observation, however, is that theta, alpha and gamma power was significantly modulated throughout prefrontal and parietal (Pz/P4) electrodes, which correspond to the precuneus [172]. Strong connectivity between prefrontal cortex and precuneus is well-established [173,174], with the latter region being particularly important in gating thalamocortical activity [174] and various cognitive domains, such as episodic memory retrieval, visuo-spatial imagery and self-awareness [173]. With the functional role of large-scale synchrony patterns in mind, our results showing EEG modulation by noisy GVS may explain the previously reported phenomenological effects on cognition and behaviour.

Modulation of large-scale networks by noisy GVS may in fact reflect an influence on global information flow between cortical neurons oscillating at similar frequencies. Functional networks in the brain may demonstrate small-world properties (i.e., highly clustered nodes of locally-connected interneurons that are inter-regionally connected) [175]. In order to achieve specific behavioural goals for perception, cognition and action, communication among nodes are dynamically controlled or "gated" for optimal network configuration. Synchronization of oscillatory signals is hypothesized to serve as the dynamic gating mechanism between functional nodes [60,61,176]. The periodicity of synchrony patterns determines neuronal responsiveness. Maximal responsiveness occurs around the depolarizing or excitability peaks, thereby facilitating effective communication between neuronal groups when the timing of excitability peaks is coordinated. Conversely, information flow is minimal when oscillations are not synchronized, or excitability peaks misalign with troughs [177]. Dynamic modulation of neural synchronization patterns is

therefore suggested to be important for information processing in functional networks [58,60,178,179]. In light of this, individual activity of brain regions may not be so characteristic of networks so much as the dynamic nature of their "links", which are mediated by synchrony over multiple frequency bands [58]. Since we show that noisy GVS is linearly related with broadband synchrony changes throughout large-scale networks, our results may therefore pose noisy GVS as a relevant tool for modulating and understanding brain networks.

2.5.2. Effects of Noisy Stimulation

Stochastic facilitation (a broader term for "stochastic resonance") may be a putative mechanism through which noisy GVS modulates the amplitude of EEG synchrony. In this model, biologically relevant noise may enhance neural information processing and computational goals [155]. For example, stochastic facilitation has been suggested as the mechanism through which noisy GVS improves visual memory while constant current GVS does not [136]. If a non-linear dynamical system (e.g., a neuron) is partially depolarized by a subsensory stimulus, adding random noise to a weak stimulus may render the signal detectable via random intermittent depolarization [138,155]. Therefore, broadband sensory noise, even at high frequencies, may enhance synchronization at both intra- and inter-regional cortical levels [60]. A similar framework may apply to our results: noisy vestibular stimulation may engage synchronization of neuronal assemblies [138]. The particular 1/*f* power density of the applied stimulus may specifically recruit more global, integrative networks at slower oscillations, which perturb local, higher-frequency oscillations in rhythm-generating networks of GABA interneurons [139]. This is contrast to sinusoidal transcranial stimulation which has been shown to modulate LFPs in widespread cortical areas albeit

entraining neural oscillations instead, driving them at a particular frequency [164]. Stochastic facilitation is consequently a proposed mechanism to explain the observed effects across all EEG bands of interest, as opposed to solely within the frequency range of the stimulus (<10 Hz).

In support of this view, others have proposed stochastic facilitation as an explanation for their observations of the effects of noisy GVS. For example, noisy GVS enhanced GABA release and altered neurotransmission within the substantia nigra in both unlesioned and 6-hydroxydopamine hemilesioned Parkinsonian rats [135]. Notably, while white noise stimulation has also been shown to sensitize other systems, such as the baroreflex response, 1/*f* noisy stimulation is more optimal and effective in doing so [137]. The authors of the study suggested that 1/*f* noise "kicks" the system out of insensitive fixed states [137]; therefore, putting the brain in a more metastable (i.e., dynamic) state [59]. Accordingly, the post-stimulus changes we observed after the highest-level of current stimulation may reflect a greater dynamical state. In analyzing the weak, transient aftereffects of noisy GVS, much to our surprise, most significant were the delayed increases in beta and gamma synchronization in frontal electrodes following 20-25 s after stimulation ceased. Similar to how beta synchronization transiently rebounds after a movement or after a behavioural decision to reflect a new network state [55,180], the delayed beta and gamma synchronization may reflect greater network dynamics. One potential caveat concerning stochastic facilitation, however, is that the output performance depends upon the noise magnitude. This dependency occurs in a relation that follows an inverted U shape, indicating it is possible to overshoot optimal levels of performance [181]. Therefore, while stochastic facilitation is a strong candidate to explain our observed effects, more work is needed to elucidate whether varying

noise levels may differentially affect our results.

Lastly, despite that stochastic facilitation suggests that the neuron is a non-linear dynamical system [181], this does not invalidate the possibility of detecting linear effects between EEG spectral features and GVS current intensity. Stochastic facilitation acts at individual neurons whose firing responses are influenced in a non-linear manner. EEG oscillations, on the hand, represent a sum of added and cancelled vector signals, which may be influenced by externally applied GVS in a linear fashion.

2.5.3. Conclusions

In summary, we demonstrate clear broadband spectral changes during and after stimulation with noisy GVS. The changes we observed were widespread throughout a global assembly of frontal, central/parietal, occipital and bilateral regions. Consistent with our present observations, prior scalp EEG studies have observed broadband spectral changes in normal, healthy subjects, although during visuomotor task performance [68]. Nonetheless, we expected to see changes mainly in beta rhythms, especially based on previous accounts of noisy, imperceptible GVS ameliorating motor function in Parkinson's disease [132,133]. In Parkinson's disease, exaggerated beta synchrony propagates throughout basal ganglia-thalamocortical circuitry, accompanies motor symptoms [45,50,142], and is adjusted to a functional range of dynamics by therapies, such as deep brain stimulation of the STN and dopaminergic medication [153]. Since beta synchronization supposedly characterizes a normal dynamic state of cortical-basal ganglia networks during sensorimotor processing [55], we therefore speculate that noisy GVS will adjust maladaptive modulatory oscillatory dynamics of the same networks that may be stuck in a particular state. Our results may be

particularly relevant towards the recently reported motor improvement in a Parkinsonian rodent model [135] and patients [132,133]; yet, further work will need to confirm this.

CHAPTER 3: Neuromodulation of EEG Oscillations in Parkinson's Disease Using Subthreshold Noisy Galvanic Vestibular Stimulation

3.1. Summary

Objective: Noisy galvanic vestibular stimulation is reported to improve motor performance and postural control in both rat models and patients with Parkinson's disease. However, the fundamental mechanisms for these anectodal reports remain poorly understood. In the present study, our objectives were to modulate ongoing neural synchrony patterns in Parkinson's disease subjects *off* medication using noisy galvanic vestibular stimulation and to measure simultaneous changes in EEG oscillations.

Methods: We studied seven Parkinson's disease subjects in the off-medicated state (12-hour withdrawal from dopaminergic medication) with moderate disease severity (Hoehn & Yahr 2-3). Imperceptible, noisy stimuli with a 1/*f* power density were delivered transcutaneously and bilaterally to vestibular nerves while the resting-state EEG was recorded with eyes open. We delivered stimuli at current levels of 10, 26, 42, 58, 74 and 90% of cutaneous sensory threshold levels. To analyze post-stimulus aftereffects, we used standard spectral analysis. To measure ongoing changes in spectral band power, we used the Least Absolute Shrinkage Selection Operator regression and cross-validation to assess the combinations of channels and power spectral features within each EEG frequency band that were linearly related with stimulus intensity. Spectral features were investigated within five frequency bands of interest: theta (4-7.5 Hz), low alpha (8-10 Hz) , high alpha (10.5-12 Hz), beta (13-30 Hz) and gamma (31-50 Hz) .

Results: Noisy galvanic vestibular stimulation did not induce any significant aftereffects in spectral band power, whereas with respect to ongoing spectral changes, we observed a

linearly dependent relation between stimulus intensity and EEG band power, as determined by the LASSO regression. We note this modulation occurred in frontal, central and posterior electrode locations.

Conclusion: Ongoing spectral band power was modulated by noisy GVS. Furthermore, noisy galvanic vestibular stimulation was able to modulate oscillatory rhythms throughout a spatially distributed brain network. Given the currently growing interest in minimally invasive and alternative treatments, our results present the application of using noisy galvanic vestibular stimulation as a novel non-invasive neuromodulatory tool for Parkinson's disease.

3.2. Introduction

Parkinson's disease (PD) is a debilitating, neurodegenerative disorder of dopaminergic neurons in the substantia nigra pars compacta of the basal ganglia (BG). Loss of nigrostriatal fibres is associated with characteristic motor symptoms, such as bradykinesia, rigidity, resting tremor, postural instability and hypophonia [7]. The leading medication to treat and confirm diagnosis of PD remains to be dopaminergic replacement by levodopa [12]. However, disease symptoms become apparent once greater than half of dopaminergic fibres have already irreversibly degenerated [182,183], suggesting that, in addition to progressive loss of striatal input and dopamine depletion, other disease mechanisms may exist.

Abnormal synchrony patterns are observed in the Parkinsonian brain. In PD, the subthalamic nucleus (STN) and globus pallidus externus act as a neuronal oscillator that drives exaggerated synchrony of beta oscillations (13-30 Hz) in BG-cortical loops [35,42]. This hypothesis provides an explanation for the management of motor symptoms using Deep Brain Stimulation (DBS) targeted to the STN or globus pallidus interna [51]. In advanced disease states, DBS is an effective procedure once complications develop from long-term

intake of dopaminergic medication [51]. However, DBS is a procedure typically allowed for more advanced disease stages, and requires that patients meet certain inclusion criteria [51]. As well, with long-term usage of levodopa medication, there is an eventual decrease in the therapeutic window, which determines the efficient dosage of medication while minimizing the risk of later developing adverse side effects, such as motor fluctuations and psychiatric disorders [73]. The need for novel, minimally invasive and non-pharmacological alternative treatments is an issue of growing interest.

In the present study, we investigated the electrophysiological effects of transcutaneous noisy (i.e., with randomly varying currents) galvanic vestibular stimulation (GVS) in PD. In bilateral GVS, a small current is passed between two surface electrodes placed on each mastoid process, modulating a global, multimodal distribution of vestibular-related subcortical and cortical brain regions [76,111]. Numerous studies have observed that GVS may have beneficial effects on visual memory recall in normal subjects and damaged visuospatial processing in stroke patients [128-130,136], positing the emerging view that GVS may be a useful tool for both neuropsychology and neurorehabilitation [76,110]. In PD, similar vestibular stimuli delivered at low, imperceptible levels improved motor performance and postural control in hemiparkinsonian rodents and patients [132-135]. Despite implying that GVS – in particular, stochastic signals – may have therapeutic implications, these reports have remained fundamentally unexplained.

How can we reconcile the above reported phenomena with our knowledge of PD? We hypothesize that noisy vestibular stimuli modulates aberrant firing patterns and global synchrony networks in PD. Previously, we have already investigated that subthreshold, noisy GVS modulates beta synchrony levels in normal subjects. Here, our objective was to

investigate whether the same stimuli would modulate the dynamics of exaggerated beta synchrony in PD subjects. Since widespread slow oscillations recruit large networks [139], we applied a noisy stimulus with a $1/f$ power density as used previously [132,133,137] to modulate large-scale functional networks. To understand the effect of noisy GVS on temporal synchrony patterns and integrative frameworks, we measured the ongoing EEG response in five frequency bands of interest: theta (4-7.5 Hz), low alpha (8-10 Hz) , high alpha (10.5-12 Hz), beta (13-30 Hz) and gamma (31-50 Hz).

3.3. Materials and Methods

3.3.1. Subjects

Seven PD subjects (all male; mean age 60.0 ± 8.5 years; all right-handed) without any reported vestibular, auditory or neurological disorders participated in the study. All subjects were recruited from the Pacific Parkinson's Research Centre (Vancouver, Canada). Subjects had UPDRS motor scores at a mean of 35.4 ± 17.6 and disease severity was rated Hoehn & Yahr stages 2-3. Four PD subjects presented symptoms of dyskinesias (Table 3.1). All PD subjects were tested in the off-medicated state after a 12-hour overnight withdrawal from dopaminergic medication.

3.3.2. Ethics Statement

The study was approved by the University of British Columbia Clinical Research Ethics Board. All subjects gave written, informed consent prior to participation. Research was conducted according to the principles expressed in the Declaration of Helsinki.

3.3.3. Primary Study Protocol

Subjects were comfortably seated 80 cm from a screen, and were instructed to focus their gaze on a continuously displayed fixed target to minimize distractions while the EEG

was recorded (6 trials, 192 s each). In each trial, EEG was first recorded without stimulation for 60 s (pre-stimulus period), blinding subjects to the actual stimulus onset. Noisy stimulation signals were then delivered for a fixed duration of 72 s (stimulation period), followed by a sham current for 60 s (post-stimulus period). During the stimulation period within each trial, we applied one of six imperceptible currents: 10, 26, 42, 58, 74 and 90% of the determined threshold value. For each subject, the delivery of the 6 trials and respective stimulation intensities were differently permutated in a pseudorandom order.

3.3.4. Stimulus

GVS was delivered to subjects through carbon rubber electrodes (17 cm^2) in bilateral, bipolar fashion. For bilateral stimulation, an electrode was placed over the mastoid process behind each ear (Figure 2.1), and coated with Tac gel (Pharmaceutical Innovations, NJ, USA) to optimize conductivity and adhesiveness. Digital signals were generated on a computer with Labview software and converted to analog signals via a NI USB-6221 BNC digital acquisition module (National Instruments, TX, USA). The analog command voltage signals were subsequently passed to a constant current stimulator (Model DS5, Digitimer, Hertfordshire, UK), which was connected to the stimulating electrodes.

Bipolar stimulation signals were zero-mean, linearly detrended, noisy currents with a 1/*f*-type power spectrum (pink noise) as has been previously applied in Parkinson's disease and healthy subjects [132,133,137]. The stimulation signal was generated between 0.1-10 Hz with a Gaussian current density, with the command signal delivered to the constant-current amplifier at 1 kHz (Figure 2.2). The stimulus was applied at an imperceptible level to avoid effects by general arousal and/or voluntary selective attention, with the current level individually determined according to each subject's cutaneous sensory threshold.

Since perception of GVS is inherently subjective, we utilized systematic procedures that have been previously utilized in determining subliminal current levels for both GVS and transcranial stimuli [113,136,160]. Starting from a basal current level of 20 μA, noisy test stimuli were delivered for 20 s periods with gradual stepwise increases (20 μA) in current intensity until subjects perceived a mild, local tingling in the area of the stimulating electrodes. A threshold value was defined once subjects reported the tingling sensation as performed previously [113,136], which lasted for the duration of the test stimulus. The current level was then decreased each time by one level until sensation was no longer reported during delivery of test stimulus pulses, and increased by one step in current intensity to confirm threshold. Each delivery of a test stimulus was followed by a period of no stimulation for at least 30 s to preclude a hysteretic effect carrying over to the next test stimulus: after a 20 s of high-frequency deep brain stimulation of the STN, beta rhythms return to baseline 15 s after the stimulus finishes [52]. Subjects were blind to the onset and duration of test stimuli, as well as the threshold-testing scheme.

3.3.5. EEG Acquisition

We recorded the continuous EEG from 19 scalp electrodes using a Neuroscan Synamps^2 EEG acquisition system and standard electrode cap (Neuroscan, VA, USA). Electrode impedances were maintained below 10 kΩ using Electro-Gel (Electrode-Cap International, OH, USA). Recording electrodes were positioned according to the International 10-20 EEG System (Figure 2.1) with one ground electrode and linked earlobe electrodes as reference. Surface electromyographic electrodes were positioned above and below each eye for subsequent artifact removal during analysis [161]. All data were digitized at 1 kHz, and bandpass filtered between 1 and 250 Hz.

3.3.6. EEG Pre-Processing

EEG data were downsampled to 250 Hz and bandpass filtered between 1 and 50 Hz. We subsequently applied Independent Component Analysis (ICA) to remove common artifacts from the recordings [157,162]. ICA uses linear combinations of electrodes to derive temporally independent waveforms from a mixed signal. Artifacts due to eye movements, muscle activity and heartbeats are statistically independent from ongoing brain rhythms in the time domain, making ICA ideal for artifact isolation and removal [162]. ICA was performed on concatenated EEG data from pre- and post-stimulus periods, and 15 component activations were extracted. Careful joint inspection of the scalp topography, power spectrum and activity of components allowed for deeming specific components for artifact rejection in the pre- and post-stimulus EEG periods.

We assumed that the source localization of common EEG artifact components (e.g. eye movement, muscle artifact) remained unchanged during the stimulation. We therefore utilized the unmixing matrices from ICA performed on concatenated pre- and post-stimulus periods, and applied those matrices to isolate eye, muscle and cardiac artifacts present in the stimulation periods. The use of the pre/post stimulus unmixing matrices also ensured that no bias was introduced into the intrastimulus EEG during ICA artifact removal. Common artifact components were similarly assessed and rejected by thorough joint inspection of the scalp topography, power spectrum and activity of components. EEG data were subsequently reconstructed using all other components.

Since skin has a relatively low resistivity in comparison to the skull, a fraction of the stimulating currents could potentially be directly shunted across the scalp and picked up by the recording electrodes [163]. The issues of EEG data containing stimulus artifacts or of

removing too much neural information during artifact rejection pose a central concern with simultaneous electrical stimulation and recording approaches [164,165]. During the stimulation period, microvolt recordings of biological activity may be overwhelmed by higher-voltage shunted stimuli. In order to remove stimulus-based artifacts from the EEG, we concatenated recordings of the 6 stimulation periods for each subject. To remove the direct effects of shunting, we utilized the linear-based [166,167] QR decomposition (*qr* function in Matlab). We created an augmented matrix consisting of the EEG (with artifacts removed via ICA) and the temporally-aligned stimulus signal. The QR decomposition of the real matrix *A* computes an orthogonal matrix *Q* and upper triangle matrix *R* such that $A = Q \cdot R$. In the current situation, we created the matrix *A* so the first column was the stimulus, and subsequent columns were the concatenated EEG recordings. We then performed the "economy-size" QR decomposition. The rows of *Q* corresponded to the number of time points, and the number of columns corresponded to the number of EEG channels + 1 (corresponding to the stimulus). By setting the first row of *R* to zero, to create R_0, then deriving $A_{new} = Q \cdot R_0$, we can obtain the EEG data with the stimulus regressed out. Previously, stimulus-induced artifacts have been removed from potential recordings using a least squares regression [164]. Similarly, we chose the QR decomposition due to: 1) its numerical stability and computational efficiency for a large number of EEG recording channels [158], as well as 2) its proven recognition accuracy of discriminant vectors when applied for feature extraction of high dimensional data [159]. Following rejection of stimulus-induced artifacts, the reconstructed EEG stimulation periods were then divided into non-overlapping, 1-s epochs. Each epoch was then finally inspected to ensure absence of stimulation or other artifacts.

3.3.7. Power Spectral Analysis

Aftereffects of Stimulation

In order to investigate whether the effects of GVS potentially have any direct effect on brain rhythms, we analyzed net EEG spectral changes following the highest-level stimulation condition (90% threshold). In one subject, the data was corrupted towards the end of the trial; therefore, we used the first 40 s for all subjects. For the artifact-free pre- and post-stimulus periods from the trial with current level 6, we calculated time-varying changes in power spectral density (PSD) for each electrode channel using a short-time Fourier transform (*spectrogram* function in Matlab, nFFT = 256, window = 125 points, overlap = 62 points). For each window segment, the spectral difference was taken from the post-stimulus minus the pre-stimulus periods, and we applied a one-sided t-test to see whether net spectral changes within a given frequency band were significantly different from the pre-stimulus period. Changes in spectral amplitude were analyzed for each of 5 frequency bands of interest: theta (4-7.5 Hz), low alpha (8-10 Hz), high alpha (10.5-12 Hz), beta (13-30 Hz), gamma (31-50 Hz). Spectrograms were plotted for each electrode channel and show mean spectral changes across all subjects. Since the order of the 6 stimulus levels was pseudorandom and varied for all subjects, the inherent issue of EEG non-stationarity is largely precluded. Significance was determined at $p < 0.05$.

Effects of Stimulation

In order to determine whether GVS effects were associated with ongoing EEG changes, we analyzed the PSD of activity recorded in each electrode during the stimulation period and within the same frequency bands of interest: theta, low alpha, high alpha, beta and gamma. PSD features of activity recorded were calculated for each 1-s epoch of artifact-free

data using a fast Fourier transform with 1-s windows (*pwelch* function in Matlab, nFFT = 256, window = 250 points, no overlap). Specifically, we tried to predict current level given the EEG features using multivariate regression:

$$Y = X \cdot \beta + \varepsilon \qquad (1)$$

where Y was of dimensions 60 (6 current levels x 10 subjects) by 1, X was 60 by 95 (19 channels x 5 frequency bands) and ε is 95 (19 channels x 5 frequency bands) by 1 and given the EEG feature of the band-limited power over each of the six current levels was removed.

Since, in this case, the number of potential regressors (95) exceeds the number of examples (60), we utilized the Least Absolute Shrinkage Selection Operator (LASSO) regression (*lasso* command in Matlab) [168]. Unlike other methods such as ridge regression or ordinary least squares, LASSO regression puts a sparsity constraint on β so that most values are zero and attempts to find the most informative electrode/band combination of EEG spectral changes to predict current level [168]. The number of regressors selected by the LASSO operator was to give the least predictive error based on a 10-fold cross-validation. Once the regressors were selected, we used robust regression (*robustfit* command in Matlab) to estimate the significance of the individual regressors.

In order to visualize possible non-linear effects of the stimulus, for the significant channels, we plotted actual changes in band-limited power level as a function of stimulus current (in effect, the appropriate column of X vs. Y in eqn 1 – Figure 3.2B).

3.4. Results

Subjects reported a cutaneous sensory threshold at mean RMS current amplitude of 293 ± 155 μA. In consistency with prior observations, subjects additionally did not report perceiving any stimulus during the stimulation periods [113,154]. Subjects also did not

experience postural sway throughout the experiment trials. Some subjects reported feelings of mild dizziness or lightheadness after the experiment.

3.4.1. Post-Stimulus Aftereffects

Spectrograms show the difference in spectral power in the pre-stimulus subtracted from the post-stimulus periods, and therefore reveal any net spectral changes for the first 40 s following the cessation of stimulation. We did not note any significant transient aftereffects as a result of noisy GVS. However, while none of the spectral changes were significant, electrode regions Fp1, Fp2 and O1 demonstrate weak post-stimulus carryover effects and are of interest. In prefrontal Fp1 and Fp2, beta and gamma synchronization appeared to decrease after cessation of stimuation, while an increase in beta and gamma was observed in O1 (Figure 3.1).

3.4.2. Stimulation Intensity Is Linearly Predicted by the Overall Power of all EEG Bands

Overall, the LASSO algorithm identified a widespread distribution of significant electrode channels with modulated band power as a result of GVS (Figure 3.2A). In the theta band, the LASSO algorithm identified 7 significant electrode channels in prefrontal/frontal areas (Fp2, F3, Fz, F4), left central/parietal areas (C3, P3) and the occipital region (O2). In the low alpha band, LASSO identified 7 significant electrode channels in prefrontal/frontal areas (Fp1, F7, F3), the central/midline area (C3, Cz, Pz) and the occipital region (O2). In the high alpha band, LASSO identified 8 significant electrode channels in prefrontal/frontal channels (Fp1, Fp2, F3, Fz), the central/midline area (Cz, Pz), the left lateral side (T3) and the occipital region (O2). In the beta band, LASSO identified 5 significant electrode channels in the prefrontal cortex (Fp1), the central area (Cz), parietal cortex (P3, P4) and occipital

region (O2). In the gamma band, LASSO identified 8 significant channels in frontal areas (Fp2, F7, Fz), bilateral sites (C3, T4), midline parietal area (Pz) and central (T3, C4) and occipital cortex (O1, O2). All electrode regions selected by the LASSO operator as related linearly with band power are illustrated in Figure 3.2B. Significance was determined at $p < 0.05$ (see Table 3.2 for p values).

For each of the five frequency bands of interest, median spectral power measured in the above significant electrodes for all subjects were plotted as a function of stimulus intensity (Figure 3.2B). Note that this is the same as plotting the appropriate columns of X as a function of Y in eqn. 1. When the information from all columns of X (i.e., all bands) were included, plotting $X \cdot \beta$ vs Y resulted in a linear relation (Figure 3.2C).

3.5. Discussion

To understand how noisy GVS improved motor functions in hemiparkinsonian rats and PD subjects, it is necessary to identify the immediate and ongoing actions of GVS on brain activity. To our knowledge, this is the first study demonstrating that noisy GVS is able to modulate the synchronization of resting-state brain rhythms in PD subjects in the off-medicated state. Significant aftereffects in the post-stimulus period were not observed, although were visually noted in prefrontal regions and the occipital cortex within beta and gamma bands. More importantly, we observed a dose-dependent relation between overall combined power of all EEG bands of interest (theta, alpha, beta, gamma) and stimulus intensity. Ongoing spectral changes were observed in electrodes throughout frontal, central and posterior regions. Previously in this thesis, we have addressed how we overcame the analytical challenges of measuring ongoing EEG signals with simultaneously applied stimulus currents (refer to Chapter 2.5). Notably, changes in the high alpha band, which is

beyond the frequency range of our stimulus (0.1-10 Hz) argue against recorded potentials reflecting shunted scalp currents. Therefore, our results suggest that noisy, imperceptible GVS directly modulated network synchronization of neural rhythms in PD.

Likewise to the effects on normal subjects, noisy GVS modulated EEG oscillatory activity across distributed areas concerning frontal, central and parietal regions. Our results demonstrate an influence on network activity across temporal and spatial scales. First, we demonstrate that EEG oscillations across theta, alpha, beta and gamma band were linearly modulated with respect to stimulus intensities. Our results therefore have beneficial implications for PD symptoms since EEG connectivity across the same frequency bands, including alpha, beta and gamma, have been shown to correlate with disease severity [68]. Furthermore, the distribution of modulated regions throughout frontal, central and parietal regions is particularly intriguing given that frontal-parietal networks are relevant for large-scale integration as well as cognitive and behavioural processing [58]. For example, frontal-parietal networks have been identified using functional MRI (fMRI) during hand grasping and reaching [185]. In PD patients, de Hemptinne et al. demonstrated that the coupling between beta-phase and gamma-amplitude oscillations is exaggerated, as measured by local field potentials (LFPs) in M1 [184]. The observed beta-phase and gamma-amplitude coupling was reduced by therapeutic deep brain stimulation of the STN, suggesting that the exaggerated dynamics between beta and gamma oscillations propagating throughout BG-cortical networks interfere with large-scale information processing necessary for normal motor behavioural function [184]. In the present study, similar to normal subjects (as shown previously in Chapter 2 of this thesis), noisy GVS was able to modulate large-scale

synchrony patterns in PD, and therefore may have ramifications for modulation of motor networks.

We demonstrate that brain rhythms across temporal and spatial scales are able to be modulated by noisy GVS. This is consistent with the notion that noise with a 1/*f* power density is particularly effective at sensitizing non-linear systems to signal detection [60,137,138]. 1/*f* noise is suggested to "kick" systems out of insensitive fixed states [137]. Interestingly, PD is characterized by abnormal BG-cortical networks that are fixed in an exaggerated state. PD subjects off medication demonstrate a strong, tendency to resonate at ~20 Hz within the BG-cortical network involving the STN, suggesting that the ability of the brain to change oscillatory activity is severely hampered or limited [37]. The result of this limitation is that brain functional networks are unable to rapidly switch states as needed according to functional cognitive and behavioural demands [74]. Therefore, modulation of brain rhythms via delivery of external 1/*f* noise through vestibular stimulation is hypothetically beneficial for functional networks and therefore PD symptoms. However, further work will need to confirm this. Lastly, we note that we did not observe significant post-stimulus aftereffects in any electrodes channels (unlike in Normal subjects), indicating that perhaps the stimulus could be better optimized given that the PD brain has less dynamic functional networks.

Lastly, the linear relation and dose-dependency we observed between stimulus intensity and combined spectral power across all frequency bands is suggestive of a causal effect. This finding refutes the notion that changes in neural oscillations as a result of non-invasive and deep brain stimulation are epiphenomenal effects of behaviour [50]. Our observed causal or mechanistic effect on EEG rhythms were unlikely due to general arousal

or activation of the reticular activating system; the imperceptible nature of our stimulus avoided such a confounding variable, which has been implicated in other novel stimulatory techniques [40].

In summary, we show that noisy GVS is able to alter the EEG dynamics of brain rhythms in PD subjects in the off-medicated state. Our results suggest that noisy GVS may be a potential novel neuromodulatory tool for PD. However, since the EEG is limited in spatial resolution, the information we infer from EEG data, which is more temporally resolute, cannot fully confirm the mechanism of action for noisy GVS. Previously using fMRI, it has been demonstrated that effective connectivity is altered in PD subjects, and that dopaminergic treatment is able to partially normalize these altered connectivity patterns [186]. Although we infer frontal-parietal regions are modulated during resting-state, future studies will need to further validate the effects of GVS on functional networks at a higher spatial scale. Moreover, future work is needed to investigate how GVS may affect task-related networks in PD in order to truly determine its potential therapeutic utility.

CHAPTER 4: Noisy Galvanic Vestibular Stimulation Improved Motor Tracking Performance in Parkinson's Disease

4.1. Summary

Noisy galvanic vestibular stimulation has been shown to improve bradykinesic symptoms in hemiparkinsonian rats and Parkinson's disease (PD) patients. However, these novel applications of noisy galvanic vestibular stimulation (GVS) are not well understood, and therefore not thoroughly tested. To confirm whether noisy GVS has a therapeutic benefit for PD patients, we compared the online effects of GVS on motor performance across three subject groups: normal, PD subjects off medication (PD OFF), and PD subjects on medication (PD ON). We tested 12 healthy, age-matched normal subjects and 12 patients with mild to moderate PD (Hoehn & Yahr 1.5-2.5). All patients were withdrawn from levodopa medication at least 12 hours prior to the study, and subsequently re-tested in the on-medicated state. Subjects performed 8 trials of a sinusoidal visuomotor tracking task, which alternated between 2 task conditions depending on whether the displayed cursor position underestimated the actual error by 30% ('Better') or overestimated by 200% ('Worse'). Either sham or subthreshold, noisy GVS (0.1 – 10 Hz, 1/f-type power spectrum) was applied during each trial in a pseudorandom order. To quantify motor performance, we analyzed maximum speed and dynamics of motor performance using model parameters derived from second-order linear dynamical system models fitted to the tracking data. Noisy GVS significantly improved maximum speed in all three subject groups. Furthermore, damping ratio parameters were significantly enhanced by noisy GVS in normal and PD OFF subjects, suggesting that the dynamics of tracking performance improved, but not in combination with levodopa medication. Effects of noisy GVS on maximum speed and damping ratio measures

were independent of the task condition. In summary, we demonstrate that noisy GVS may have clinical therapeutic benefit for motor symptoms in PD.

4.2. Introduction

Motor symptoms in Parkinson's disease (PD) are mainly defined by tremor, rigidity, akinesia/bradykinesia and postural instability. While levodopa is the "gold standard" treatment for PD, chronic use eventually leads to the development of side effects, such as motor fluctuations, dyskinesias and psychiatric disorders [73]; in addition, deep brain stimulation targeted to subcortical nuclei is a complex and invasive, procedure [51]. Non-invasive brain stimulation techniques are currently a growing avenue of interest for PD and other neurological disorders due to their safety, tolerability and minimally invasive nature [75]. Since PD is characterized by abnormally exaggerated beta synchronization throughout a basal ganglia-cortical network [37], non-invasive stimulatory approaches may be used to modulate aberrant network dynamics [75]. With recent technological advances, numerous novel stimulatory techniques for PD treatment are presently being explored [40,135,187,188]

Previously, several studies have implicated that noisy galvanic vestibular stimulation (GVS) confers a motoric benefit for PD patients and rodent models [132-135]. Yamamoto et al. measured trunk dynamics as well as reaction time in a Go/NoGo paradigm [133] whereas Pan et al. measured wrist activity in akinesic PD patients [132]. Effects of noisy GVS on postural and balance responses in PD have also been measured in both humans and rats [134,135], although none of these studies have directly investigated the effect of GVS on bradykinesic symptoms relevant to motor coordination and sensorimotor processing.

Visuomotor tracking tasks are highly useful to understand mechanisms that contribute to motor coordination while maintaining accuracy and stability [189]. Corrective movements

and behaviour are required in response to varying visual error feedback, which are important for maintaining effective perception-action or sensorimotor processing [189]. In a broader sense, the ability to continually adapt one's behaviour to changing environmental or sensory stimuli is particularly relevant in PD: for example, PD patients demonstrate impaired switching between motor paradigms [54].

In the present study, we implemented a visuomotor tracking task and investigate the effect of noisy GVS on motor performance. Our visuomotor task required subjects to respond to visual error feedback that was either minimized by 30% or amplified by 200% unknowingly to the subjects in order to artificially create the appearance of 'Better' or 'Worse' motor performance, respectively. We analyzed maximum speed of tracking, as well as used second-order linear dynamical system (LDS) models to assess parameters that quantify the dynamics of motor tracking. We compared the motor tracking performance across three groups of subjects: normal, PD subjects off medication (PD OFF), PD subjects on medication (PD ON). Our results demonstrate that noisy GVS enhanced the maximum speed in all three subject groups, independent of the 'Better' or 'Worse' task conditions. Furthermore, LDS parameters, in particular damping ratio, were significantly enhanced in the normal and PD OFF subjects. These findings demonstrate that noisy GVS enhanced motor tracking performance, and imply there is a beneficial effect on the underlying task-related functional networks in both healthy individuals and PD patients. Furthermore, adjunctive application of GVS and dopaminergic medication do not appear to have a beneficial motoric effect.

4.3. Materials and Methods

4.3.1. Subjects

12 healthy age-matched control subjects (4 males, 8 females; mean age 58.3 ± 9.0 years; all right-handed) without neurological disorders participated in the study. 12 PD subjects (10 males, 2 females; mean age 61.4 ± 6.5 years; 11 right-handed, 1 left-handed). None of the participants had any reported vestibular or auditory disorders. All PD subjects were recruited from the Pacific Parkinson's Research Centre (Vancouver, Canada). PD subjects had mild to moderate disease severity (Hoehn & Yahr stages 1.5-2.5) with UPDRS motor scores at a mean of 22.3 ± 7.8 (Table 4.1). All PD subjects were first tested in the off-medicated state ('PD OFF') after a 12-hour overnight withdrawal from dopaminergic medication. Subsequently, after participating in one set of experiments, PD subjects were given immediate-release Levodopa according to their usual prescribed daily dosage. After waiting 45 minutes for the medication to take effect, PD subjects went through a repeated second set of experiments in the on-medicated state ('PD ON'). Subjects were categorized into three groups: normal, PD OFF, PD ON.

4.3.2. Ethics Statement

The study was approved by the University of British Columbia Clinical Research Ethics Board. All subjects gave written, informed consent prior to participation. Research was conducted according to the principles expressed in the Declaration of Helsinki.

4.3.3. Visuomotor Tracking Task

Subjects were comfortably seated 80 cm in front of a screen and performed a joystick tracking task as tested previously in PD [146]. On the screen, a target (blue) and cursor (yellow) connected by a black horizontal rod were displayed (Figure 4.1A). The target box

oscillated vertically up and down, while subjects controlled the cursor using a joystick with the objective of matching the horizontal position of the cursor to the target – i.e., to keep the horizontal black rod straight. The error (Δ, different between the actual positions of the target and cursor) was amplified by a scaling factor (α): $\Delta \times \alpha$ = displayed visual error feedback. In the 'Better' (B) task condition, α was set to 0.3, and in the 'Worse' (W) task condition, α was set to 2, such that it artificially appeared to subjects that they performed better or worse than expected, respectively, based on their scaled error feedback.

The target oscillated up and down at a summation of two frequencies (0.06 Hz, 0.1 Hz). The amplitude of the oscillation was additionally overlayed with an amplitude modulation feature, with minimum amplitude set at 0.4 and maximum at 0.95 of the screen.

During the experiment, subjects performed a total of 8 trials (PD subjects performed a total of 16 trials in PD OFF and PD ON states). Each trial (90 s) was comprised of three alternating blocks (30 s each) of B and W conditions – with Trial 1 ordered as B-W-B and Trial 2 ordered as W-B-W (Figure 4.1.B). During each trial, either a subthreshold current (90% of cutaneous sensory threshold) or a sham current stimulation was delivered. Four trials contained *verum* GVS delivery whereas the other four trials contained sham stimulation. Subjects were unaware of either *verum* or sham stimulation since the order in which stimuli were delivered was pseudorandom, and the *verum* stimulation was imperceptible to the subject. Each trial was followed by a break (30 s) to preclude a hysteretic effect carrying over to the next trial: after a 20 s of high-frequency deep brain stimulation of the STN, beta rhythms return to baseline 15 s after the stimulus finishes [52]. Before starting the experiment, subjects were allowed to practice tracking the target and

using the joystick as needed in at least one practice trial. Practice trials were differently structured than the 8 experiment trials described above.

4.3.4. Stimulus

GVS was delivered to subjects through carbon rubber electrodes (17 cm^2) in bilateral, bipolar fashion. For bilateral stimulation, an electrode was placed over the mastoid process behind each ear, and coated with Tac gel (Pharmaceutical Innovations, NJ, USA) to optimize conductivity and adhesiveness. Digital signals were generated on a computer using Matlab and converted to analog signals via a NI USB-6221 BNC digital acquisition module (National Instruments, TX, USA). The analog command voltage signals were subsequently passed to a constant current stimulator (Model DS5, Digitimer, Hertfordshire, UK), which was connected to the stimulating electrodes.

Bipolar stimulation signals were zero-mean, linearly detrended, noisy currents with a 1/*f*-type power spectrum (pink noise) as has been previously applied in Parkinson's disease and healthy subjects [132,133,137]. The stimulation signal was generated between 0.1-10 Hz with a Gaussian current density, with the command signal delivered to the constant-current amplifier at 60 Hz (Figure 2.2). The stimulus was applied at an imperceptible level to avoid effects by general arousal and/or voluntary selective attention, with the current level individually determined according to each subject's cutaneous sensory threshold.

Since perception of GVS is inherently subjective, we utilized systematic procedures that have been previously utilized in determining subliminal current levels for both GVS and transcranial stimuli [113,136,160]. Starting from a basal current level of 20 μA, noisy test stimuli were delivered for 20 s periods with gradual stepwise increases (20 μA) in current intensity until subjects perceived a mild, local tingling in the area of the stimulating

electrodes. A threshold value was defined once subjects reported the tingling sensation as performed previously [113,136], which lasted for the duration of the test stimulus. The current level was then decreased each time by one level until sensation was no longer reported during delivery of test stimulus pulses, and increased by one step in current intensity to confirm threshold. Each delivery of a test stimulus was followed by a period of no stimulation for at least 30 s to preclude a hysteretic effect carrying over to the next test stimulus: after a 20 s of high-frequency deep brain stimulation of the STN, beta rhythms return to baseline 15 s after the stimulus finishes [52]. Subjects were blind to the onset and duration of test stimuli, as well as the threshold-testing scheme. After completing the threshold test and throughout the experiment, stimuli were delivered at subthreshold intensities, which is achieved at 90% of the determined cutaneous sensory threshold value.

4.3.5. Behavioural Data Analysis

Three tracking position parameters were obtained from the visuomotor tracking task: desired (target/reference trajectory); displayed (desired + α (actual-desired)); actual (actual trajectory of motor movements). If the subject engaged in task performance is considered a system, the afferent component of the system was considered to be the visual error feedback (displayed – desired), while the efferent output of the system was considered to be the actual motor movements.

During pre-processing, we implemented dynamical time warping to the motor tracking data recorded from subjects. All subsequent analysis was performed using “warped” data. First, we analyzed the maximum absolute velocity (or speed) of the efferent output movements in response to visual error feedback as input (displayed – desired). We tested for

significant effects of noisy GVS (vs. sham stimulation) using a paired t-test with significance determined at $p < 0.05$.

We used System Identification techniques to assess behavioural tracking dynamics in PD. A standard discrete second-order LDS model is defined as, $x_t = Ax_{t-1} + Bu_t$ and $y_t = Cx_t + Du_t$ where u_t represents the desired sinusoidal trajectory of the target box and y_t represents the actual cursor position at time *t*. From these two sets of values, the constant matrices *A, B, C,* and *D* can be extracted. It is important to note that these matrices completely characterize all possible system responses, that is, once tracking performance is successfully modelled, then the output y_t can be predicted for any given input u_t, not just those that were chosen experimentally. Previous work, including our own, has suggested that second-order models can successfully model normal and PD subjects during a tracking task [190].

Since the system response, y_t depends on the eigenvalues of *A*, the eigenvalues can capture the essential features of each model. However, in order to make the characterizations of the models more intuitive, it is customary to transform the eigenvalues into two parameters: damping ratio (ζ) and natural frequency (ωn), such that $l_{1,2} = -z w_n \pm w_n^2\sqrt{z^2 - 1}$. A higher damping ratio is usually associated with a better performance, i.e., less oscillation and overshoot around the desired trajectory, with lower damping ratio associated with less damping (and more overshoot) in the error response. The natural frequency does not necessarily reflect that speed at which the subject was tracking, rather it reflects the responsiveness of the system: a higher natural frequency is associated with faster response; while lower natural frequency is associated with slower response. We also computed other

parameters derived non-linearly from the eigenvalues, including rise time, peak time, and settling time. We tested for significant effects of noisy GVS (vs. sham stimulation) on the LDS parameters using a paired t-test with significance set at $p < 0.05$.

4.4. Results

Cutaneous sensory thresholds were defined at a mean of 113 ± 91 μA for control subjects and 140 ± 113 μA for PD subjects. In consistency with prior observations, subjects additionally did not report perceiving any stimulus during the stimulation periods [113,154]. Subjects also did not experience postural sway throughout the experiment trials. Some subjects reported feelings of mild dizziness or lightheadness after the experiment.

4.4.1. Noisy GVS Enhanced the Speed of Tracking Behaviour

In normal subjects, there was an overall increase in the maximum speed of tracking behaviour as a result of GVS in comparison to sham stimulation ($p = 4.56E\text{-}4$, Figure 4.2). GVS also significantly increased the tracking speed in PD OFF and PD ON subjects (0.0095, 0.0022, respectively, Figure 4.2). Subsequently, we analyzed the effect of stimulation on tracking speed in Better and Worse conditions separately. For normal subjects, we observed a significant increase in tracking speed in both Better and Worse conditions ($p = 0.0270$, 0.0095, respectively). For PD OFF, motor tracking speed increased as a result of stimulation both Better and Worse conditions ($p = 0.0309$, 0.0335, respectively). Lastly, for PD ON, significant increases in tracking speed were found only in the Better condition ($p = 0.0132$).

4.4.2. Dynamics of Motor Output Responses Were Increased by Noisy GVS

In order to determine whether subjects' motor performance differed between Better and Worse task conditions, we analyzed the LDS parameters calculated from these conditions without stimulation. No significant difference between LDS parameters, or

movement dynamics, measured separately in Better and Worse task conditions was observed. We found this for both normal subjects and PD OFF, suggesting that at baseline performance, motor performance did not differentially depend on the given task condition.

Upon analyzing damping ratio, we noted that noisy GVS significantly increased the overall damping ratio measured in both Better and Worse task conditions. This increase was observed in normal subjects and PD OFF, but not PD ON (Figure 4.3).

Within the total range of LDS parameters, other values were additionally found to significantly increase as a result of noisy stimulation. In normal subjects, GVS increased damping ratio, decay rate, rise time ($p = 0.0015, 0.0575, 0.0235$, respectively) in tracking data pooled from both Better and Worse conditions. Upon analyzing solely the effects of GVS in the Better task condition, GVS increased damping ratio, natural frequency and decay rate ($p = 0.0408, 0.0316, 0.0528$, respectively), whereas in the Worse task condition, GVS increased damping ratio ($p = 0.0181$). In PD OFF subjects, noisy GVS increased overall parameters of damping ratio, decay rate and settling time (0.0011, 0.0021, 0.0347, respectively) in tracking data pooled from both Better and Worse conditions. In the Better task condition only, GVS increased damping ratio, decay rate and settling time (0.0127, 0.0344, 0.0459, respectively). In the Worse task condition, GVS increased damping ratio and decay rate (0.0165, 0.0172, respectively). In PD ON subjects, we only observed a significant effect of noisy GVS in the Worse task condition: natural frequency was found to significantly increase (0.0444).

4.5. Discussion

We show that noisy GVS enhanced the speed of tracking movements in all three subject groups (normal, PD OFF, PD ON). We note baseline performance in either Better or

Worse task condition was no different for normal and PD OFF subjects. In addition, for the normal and PD OFF subjects, GVS did not induce differential enhancement of speed dependent on task condition. In analyzing the effects of GVS on movement dynamics, we found that changes in damping ratio were the most consistent across all three subject groups. GVS increased damping ratio measures independent of the task condition. Previously, we demonstrated that noisy GVS has the ability to modulate synchrony of broadband EEG oscillations in both normal subjects and PD subjects off medication (refer to Chapters 2 and 3 in this thesis). Modulation of brain rhythms was observed at resting-state, suggesting that noisy GVS is able to modulate neural activity, although the effect on task-related brain functions and networks is not established. Here, we observed a functional effect of GVS on sensorimotor processing and motor performance in a visuomotor task, and discuss the physiological significance of our results.

Depending on the stimulus parameters (i.e., current intensity, frequency, signal shape), GVS is known to induce a broad range of effects of eye movements, postural control and movements [111]. Therefore, one potential caveat of our study may involve confounding effects of nystagmus or ocular torsion through activation of the vestibulo-ocular reflex (VOR) [170]. Since subjects rely on visual error feedback, ocular torsion would potentially hamper the perceived error feedback through a subjective tilt in the visual perceptual field [170]. However, we note that our stimulus levels were weak, subthreshold currents with the highest current delivered at around 140 ± 113 μA. Therefore, the preferred current intensities for inducing ocular torsion and subsequent perceptual tilts through GVS are around 1-3 mA [170]. Therefore, we presume that our subthreshold stimulus was not great enough to induce notable confounding effects in our experiment.

Our results showing improved motor performance are consistent with those previously reported in hemiparkinsonian rats and PD patients with application of noisy GVS with a 1/f power density [132-135]. We argue that our observed results are not the result of an attentional or general arousal effect, such as through activation of the reticular activating system. The imperceptible nature of our stimulus, which subjects were not aware of through the experiment trials, precludes this issue which is present with other forms of minimally invasive stimulation methods [40]. Rather, we speculate that our results may be explained by modulation of sensorimotor functional networks. In PD, basal ganglia-thalamocortical networks are hypothetically fixed in a resonating beta frequency [37]. The observed exaggerated beta synchronization in PD is suggested to be indicative of altered sensorimotor processing networks [55,153]. Previously, Wilkinson et al. have demonstrated that noisy GVS is able to modulate the EEG spectral power throughout delta, theta, alpha and beta bands during a face processing task [154]. Therefore, these findings suggest that noisy GVS is able to modulate oscillatory activity and task-related networks, which involve sensorimotor processing in this particular study. In consistency with this, we have demonstrated that noisy GVS is able to modulate the EEG synchrony patterns in PD patients off medication (refer to Chapter 3 of this thesis). Therefore, we conjecture that the neuromodulatory effects of noisy GVS account for the functional behavioural improvements we observe in the present study.

Interestingly, we observed an enhancement of motor performance in normal subjects. GVS induced a change in velocity and damping ratio in normal subjects that was comparable to PD OFF subjects. The observation that noisy GVS is able to cause behavioural effects in normal, healthy individuals is not entirely surprising since it has been previously

demonstrated that noisy GVS augmented visual recall memory in normal subjects [136]. This raises the question, however, of whether subject-specific stimuli may be individualized according to the state of the system – that is, whether it is healthy or diseased, and to what disease severity.

We applied second-order LDS models to characterize the nature of motor behaviour in response to stimulation. Increased damping ratios suggest that the subject performs with better tracking and a less tendency to overshoot the target's desired trajectory. We note no differential effects on motor performance by GVS upon task conditions (i.e., Better or Worse conditions). Therefore, the amount of visual feedback error the system perceives is not influenced by GVS. However, since error-related processing is dopamine-mediated [191], future work will need to identify whether error processing is affected by noisy GVS, perhaps with using a more sensitive measure.

In summary, our results suggest that noisy GVS has potential clinical benefit for PD motor symptoms. Since noisy GVS did not cause significant improvements in tracking in the PD ON group, our results suggest that noisy external sensory input via the vestibular nerves in adjunct with L-dopa therapy may be less beneficial than GVS alone.

CHAPTER 5: Conclusions

5.1. Summary of Findings

In this thesis, our results demonstrate that: 1) noisy GVS is able to modulate the large-scale, broadband EEG synchrony patterns in normal subjects, 2) noisy GVS is comparably able to modulate large-scale, broadband EEG synchrony in PD subjects in the off-medicated state, and 3) neuromodulation by noisy GVS has functional benefits for sensorimotor processing in PD. In summary, we provide evidence that GVS – in particularly noisy sensory stimuli through vestibular nerves – is a feasible method of modulating brain rhythms and functional networks in normal and PD subjects.

5.2. Study Significance

Our results are consistent with the previous motor behavioural improvements in PD patients and rats with application of GVS [132-135]. Furthermore, in consideration of the modulation we observed on EEG synchrony patterns in both normal and PD OFF subjects, our results provide a possible mechanism for the behavioural effects of GVS. This thesis supports the view that GVS may be a potential neuromodulatory tool in PD.

Neuronal oscillations and synchronization supposedly underlie large-scale functional networks interacting across temporal scales [58]. In PD, it has been recently postulated that the observed augmentation of recorded beta oscillations in basal ganglia-thalamocortical circuits reflect an overstabilized network "stuck" in a fixed state [55]. This view is particularly intriguing since emerging concepts on brain networks have implicated that functional connectivity between interconnected regions need to operate in a critical dynamic state (i.e., metastable)– one which allows them to rapidly switch cognitive states [74]. It

therefore appears then that the Parkinsonian state is characterized by not a pathological network, but aberrant dynamics.

In this thesis, we demonstrate that noisy GVS is able to modulate large-scale frontal-parietal EEG electrodes regions across a broad range of frequency bands. The applied 1/*f* noise we applied has been hypothesized to enhance signal detection in non-linear systems, such as a neuron [138]; however, on the scale of brain network, 1/*f* noise in the brain supposedly helps it operate within the critical state necessary for dynamic network modulation [139]. Given that we observed a functional improvement in motor performance as a result of stimulation, we postulate that the dynamics of sensorimotor networks may be ameliorated by noisy GVS in PD.

5.3. Study Limitations

GVS is a highly advantageous technique to stimulate the brain due to its non-invasive nature, tolerability, safety and feasibility. However, one central concern asks whether vestibular nerves are actually stimulated using GVS. GVS is a well-established technique known to alter the firing rates of vestibular afferent nerves. Transmastoidal GVS (i.e., with cutaneous application of electrodes on the mastoid processes) in humans is well known to elicit vestibular effects, such as postural sway and ocular torsion [103-109]. This is due to the fact that the vestibular nerve runs underneath the mastoids towards brainstem nuclei [76]; therefore with careful bilateral electrode placement on the mastoid processes, vestibular afferents should be stimulated. In support of this, numerous studies have consistently shown GVS activates numerous cortical and subcortical areas that are related to a vestibular network, self and visual motion, and multisensory processing – e.g., prefrontal cortex, thalamus, putamen, intraparietal sulcus, temporo-parietal junction, inferior parietal lobule,

precentral gyrus, middle temporal gyrus, superior temporal gyrus, anterior cingulate, insula, hippocampus [109,114-118]. In the experiments within this thesis and other experiments we have conducted, some subjects, when prompted, have reported common side effects consistently reported in GVS studies [113,154] – again providing evidence that vestibular nerves are efficiently stimulated by GVS. For example, during threshold testing when levels of GVS are reaching cutaneous sensory threshold, subjects have reported itchiness at electrode locations while stimulation is delivered [113,154]. The report of self-motion is highly indicate of vestibular stimulation due to activation of motion processing areas [118]. However, self-motion may also be a direct result of ocular torsion evoked by vestibulo-ocular reflex (VOR) activation, which may be possible to evoke within the range of current levels we delivered GVS [108]. Additionally, we note that, on separate occasions, we have observed in other subjects (not those included in the present study) that direct current GVS (1.5-2 mA) was able to disturb balance while standing and trajectory of gait while walking (data not shown) – demonstrating the validity of GVS as a tool for vestibular stimulation.

There is a potential concern regarding nystagmus-related eye movements via activation of the VOR. This may have had consequences for visual processing and therefore, influenced either brain rhythms and/or visual feedback in our visuomotor tracking task. However, we do not believe eye movements were a confounding variable in our experiments. First, subjects did not report an obvious tilt of the perceptual visual field, as would be induced by VOR activation [108]. Secondly, although we did not quantitatively measure the threshold for inducing nystagmus, we recognized that doing so would not be easily achieved since nystagmus movements induced by GVS are predominantly comprised of ocular torsion [108,170]. Secondly, although we did not measure quantitatively the threshold for inducing

nystagmus, we note that typical current strengths preferable for eliciting nystagmus is in the range of 1-3 mA [170]. Since our stimulus was always subthreshold (with an average of ~100-300 μA), we believe the effects of nystagmus, if any, are negligible.

Another potential caveat is that perhaps other brain regions (such as the cerebellum) asides from vestibular afferents would additionally get stimulated by GVS. However, this is likely not a substantial effect since transcranial cerebellar stimulation is performed by placing electrodes below the inion and posterior to the mastoid processes [192,193]. It is interesting to note that with subcortical stimulation through DBS, surrounding tissue in addition to the target region has been observed to get excited, as well. For example, DBS stimulates neurotransmitter release from astrocytes [51]. This makes GVS potentially advantageous in comparison to other brain stimulation techniques, such as DBS or rTMS, since GVS effects are specifically localized to vestibular nerve projections and ensuing connections.

One common critique of non-invasive brain stimulation techniques is whether the modulation of beta dynamics in PD is epiphenomenal or causal [50]. However, several studies argue against this. For example, artificially driving brain rhythms at beta frequencies results in slowed movements in both PD and healthy subjects [44,45]. If beta rhythms were an epiphenomenon in PD, adding power within the beta range would have no functional effect. Additionally, our EEG results demonstrated ongoing changes in the EEG during simultaneous stimulation (Figure 2.4, Figure 3.2), in favour of the notion of these rhythms being causal and functional. Furthermore, Hipp et al. demonstrated that large-scale oscillatory synchronization in beta and gamma bands actually predicted perception of an audiovisual stimulus [61], supporting the idea that synchrony patterns, in general, are causal and that neuromodulation by GVS has mechanistic effects on brain functional networks.

One particular area that remains unaddressed in this thesis is whether GVS has long-term plasticity effects or is simply driving the system while being applied. Whether GVS induces LTP/LTD effects is presently not well unknown [76]. Notably, during our resting-state EEG paradigm, we observed weak, yet significant, transient aftereffects in the post-stimulus spectral features in normal subjects (Figure 2.3). PD subjects, on the other hand, demonstrated no significant aftereffects in spectral features. Therefore, on this basis, the likelihood of long-term effects in the brain is poor. However, pairing of GVS with an ongoing task – such that the stimulation influences task-related vs. resting-state networks – may cause more long-term changes on the brain, although future work will need to address this.

5.4. Concluding Remarks and Future Directions

The work described in this thesis may be expanded in several other directions. For example, the possibility of optimizing the stimulus parameters is an question. As well, the effect of noisy GVS on the cognitive domain in PD is of great interest. This is based on findings demonstrating that GVS has a broad range of cognitive effects [110] and also PD patients suffer from cognitive impairment, such as executive dysfunction [7]. In order to gauge a better understanding of the therapeutic potential of GVS, analysis of other functional domains asides from motor is needed. Furthermore, an investigation of which networks, whether task-related or resting-state, are modulated by GVS will be useful. This may be achieved through EEG, and complemented by the higher spatial resolution of fMRI.

TABLES AND FIGURES

Figure 1.1. Simplified Circuitry of the Basal Ganglia

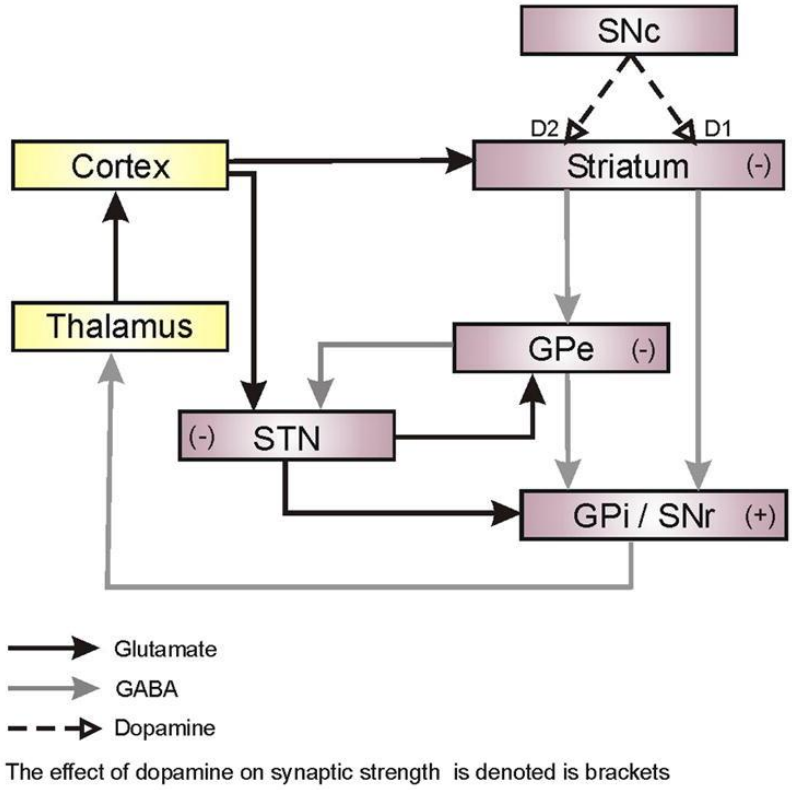

Basal ganglia circuitry outlining the subcortical and cortical connections in the direct and inhibitory pathways. From Weinberger and Dostrovsky (2011) [194]. Permission obtained.

Figure 1.2. Dopamine Levels and Beta Synchrony in Parkinson's Disease

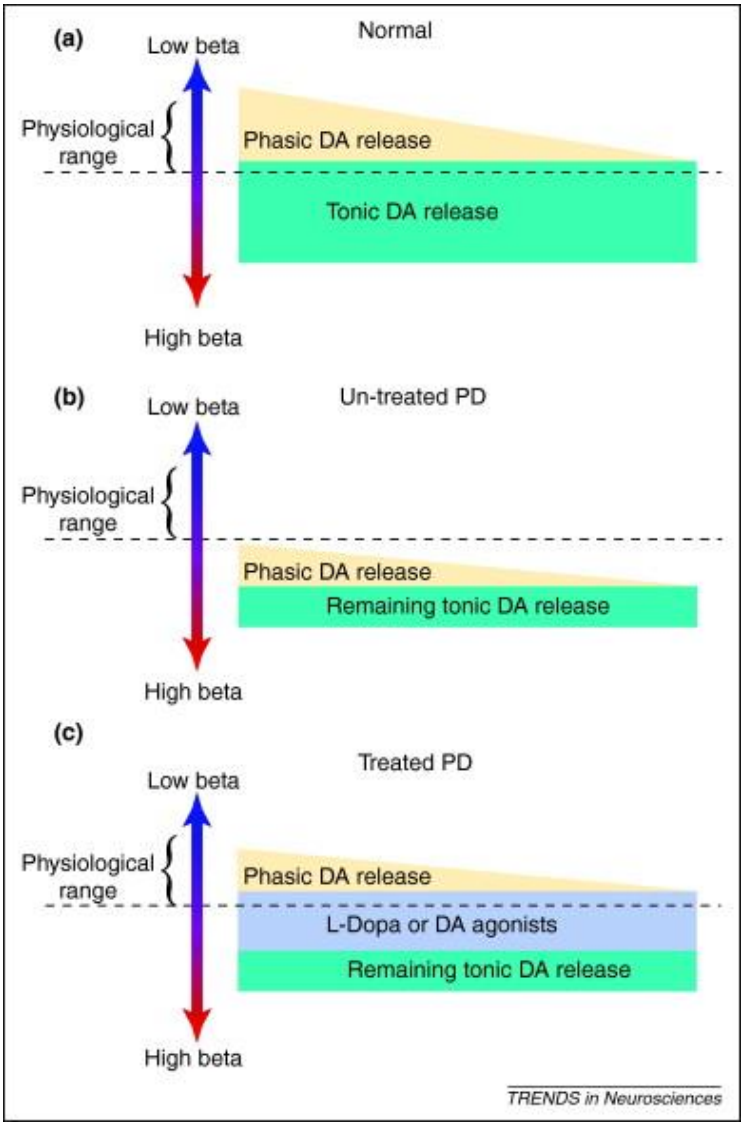

Relationship between dopamine levels, beta synchrony and physiological function of basal ganglia. Exaggerated beta synchrony levels observed in PD may be explained by dopamine depletion **(b)** in the un-treated state. Modulation of beta dynamics is therefore central to disease mechanisms. From Jenkinson and Brown (2012) [153]. Permission obtained.

Figure 1.3. Schematic of Input to Brain by Galvanic Vestibular Stimulation

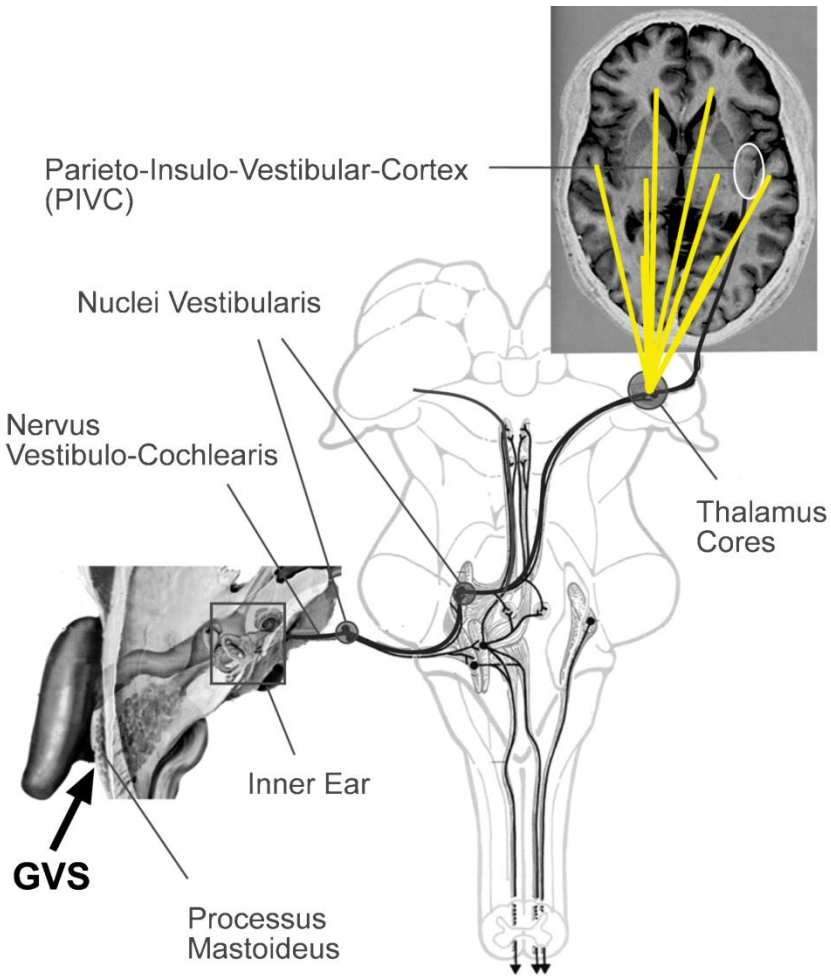

Subcortical pathways activated by transmastoidal galvanic vestibular stimulation (GVS) starting from vestibular nerve afferents to thalamic nuclei. Thalamocortical vestibular connections (yellow) from thalamic areas project to multiple cortical areas. Adapted from Utz et al. (2010) [76]. Permission obtained.

Figure 1.4. Ongoing GVS Improved Visuomotor Tracking Performance in Parkinson's Disease

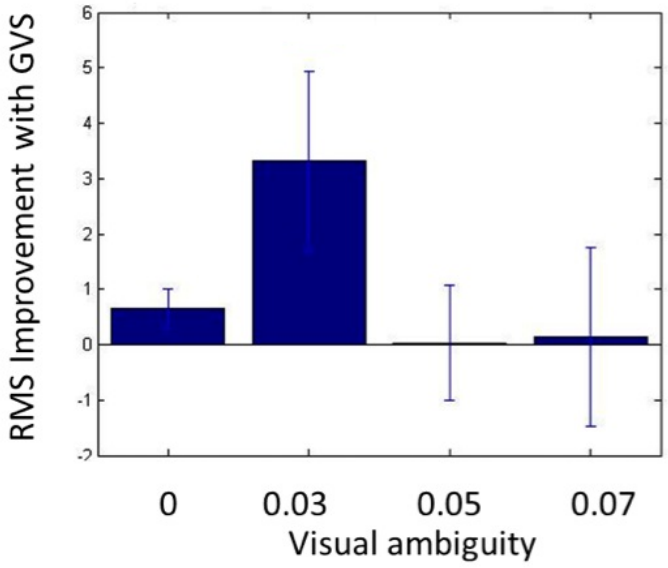

PD subjects (n=7) off medication successfully tracked a moving target (Lissajous figure trajectory) using their hand and limb in four conditions with varying levels of added noise to the target's trajectory. GVS evoked a significant improvement in RMS tracking error in the minimal visual ambiguity condition only (0.03, relative amplitude of visual ambiguity). RMS tracking error in the baseline and other ambiguous conditions (0.05 and 0.07, relative amplitude of visual ambiguity) did not show significant improvement possibly due to excessive visual feedback noise in target trajectory.

Figure 2.1. Placement of EEG and Stimulating Electrodes

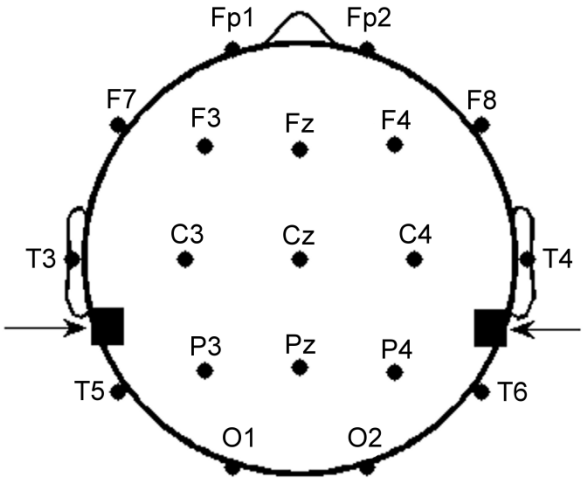

19 recording electrodes were placed on the scalp according to the International 10-20 System. Galvanic vestibular stimulation (GVS) electrodes were placed with one electrode on the mastoid process behind each ear (denoted by arrows) for bilateral configuration and transmastoidal stimulation.

Figure 2.2. Characteristics of the Stimulus

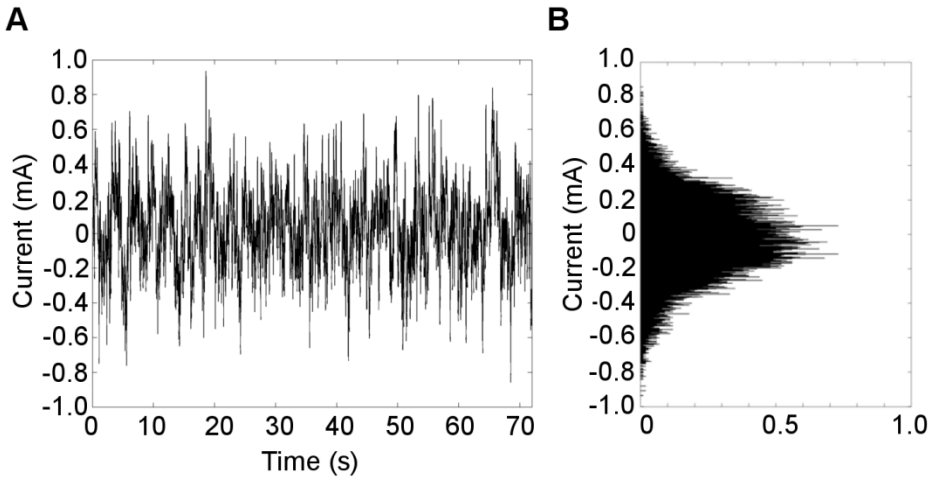

A. Typical recording from a subject receiving a noisy stimulus applied for 72 s duration. The stimulus presented is at the highest current intensity (current level 6), which is set to 90% of the subject's individual sensory threshold (RMS current value of 242 μA). **B.** Probability density function of the stimulus current follows a Gaussian distribution.

Figure 2.3. Post-Stimulus Spectral Effects of Noisy GVS in Normal Subjects

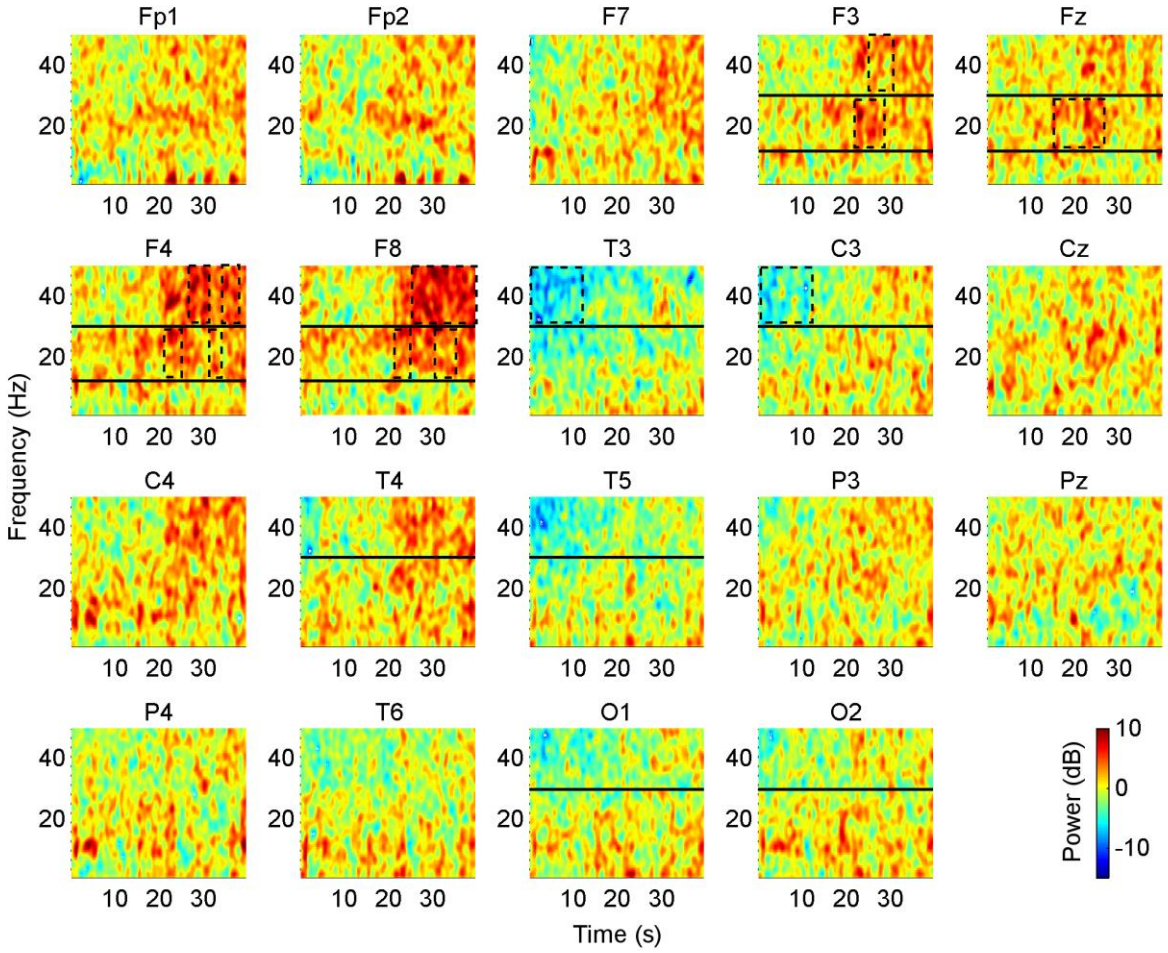

Spectrograms of the effects of noisy GVS after stimulation in Normals. Spectrograms plot the difference in spectral power in the pre-stimulus subtracted from the post-stimulus periods, thus showing net spectral changes for the first 40 s following the cessation of stimulation. Beta and gamma changes occurred after a marked delay following the end of stimulation. In frontal regions (F3, Fz, F4 and F8), beta power increased significantly starting 18-23 s after stimulation ended, while gamma power in F3, F4 and F8 increased significantly starting 26-27 s after stimulation ended. In lateral electrodes T3 and C3, gamma power was suppressed significantly within the first 10 s immediately following stimulation. For spectrograms of electrodes F3, Fz, F4 and F8, beta and gamma frequency bands are delineated by an upper horizontal black line at 30 Hz and a lower horizontal black line at 12 Hz. For electrodes T3, C3, T4, T5, O1 and O2, the gamma band is delineated by the horizontal black line at 30 Hz. Rectangles outlined in dotted black lines enclose significant spectral changes. Spectral power is reported in dB, as indicated by the colour legend. Significance was determined at $p < 0.05$ (see Table 2.1 for adjusted p values).

Figure 2.4. Combined Band Power in Significant Channels Predicted Stimulus Intensity in a Linear Manner in Normal Subjects

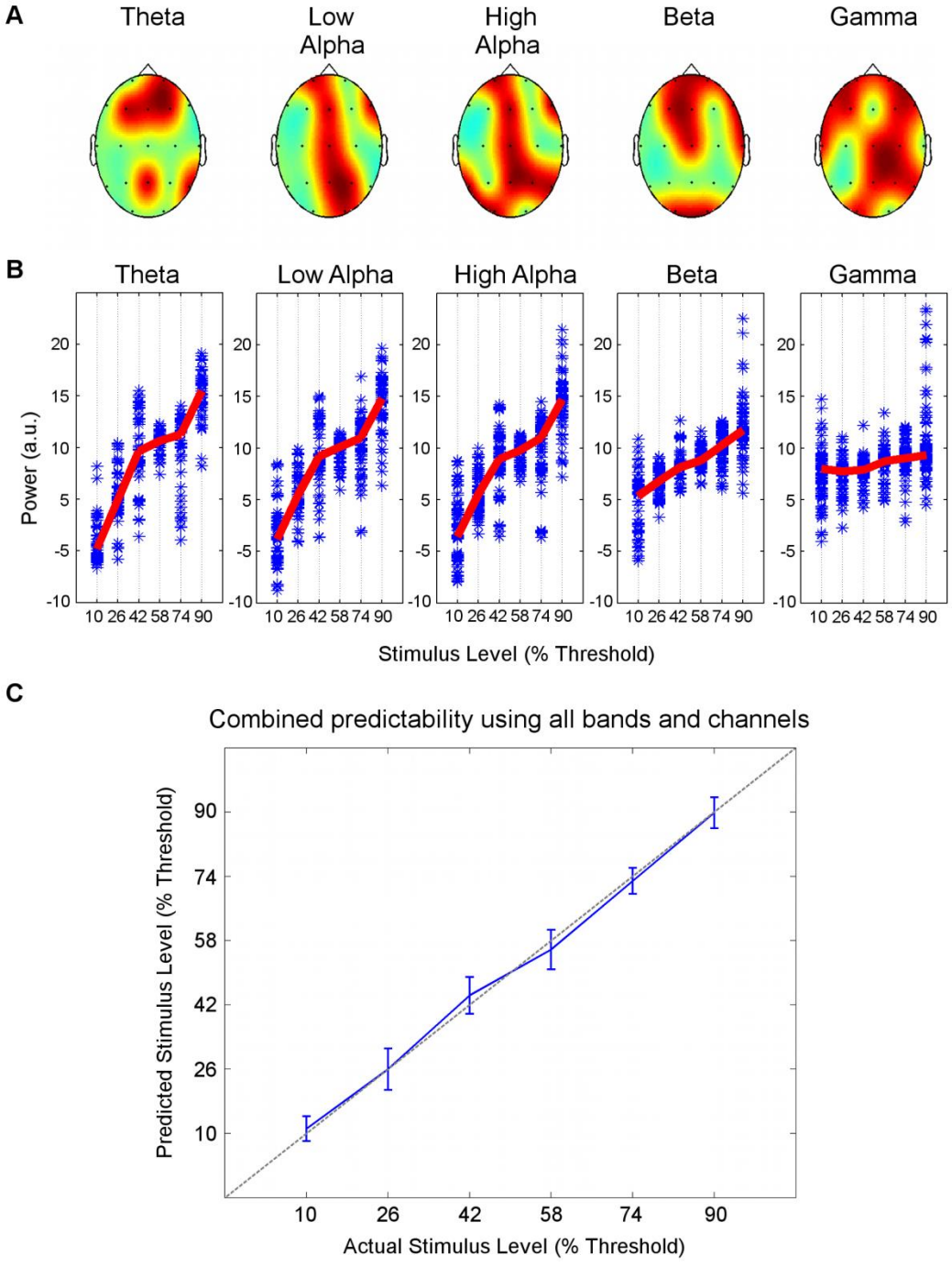

A. LASSO regularization identified significant channel/band combinations whose spectral features predicted the stimulus intensity in a linear manner. Significant channels selected from each band LASSO are shown on scalp maps in red. Theta band power was significant in channels Fp2, F3, Fz, F4, Pz, T6, low alpha band power in Fp1, Fz, F8, Cz, Pz, P4, O2, high alpha band power in Fp1, Fz, F8, Cz, Pz, T5 P4, T6, O1, beta band power in Fp1, Fp2, F3, Fz, F8, Cz, T4, O1, O2, and gamma band power was significant in Fp1, Fp2, F7, F3, F4, F8, Cz, Pz, T3, C4, P4, T6, O1. **B.** Spectral power in significant channels are plotted as function of stimulus intensity. The mean spectral power for each subject has been removed. Line plots (red) represent the median spectral values for all significant channels across all subjects. **C.** The ability of EEG features to linearly estimate stimulus intensity when all bands are included were confirmed by plotting predicted estimates against actual values of stimulus intensity. Blue line indicates the stimulus intensity predicted by LASSO-selected EEG estimates whereas the dotted gray line represents an ideal linear relation. Error bars are estimated from leave-one-out cross validation.

Figure 3.1. Post-Stimulus Spectral Effects of Noisy GVS in PD OFF Subjects

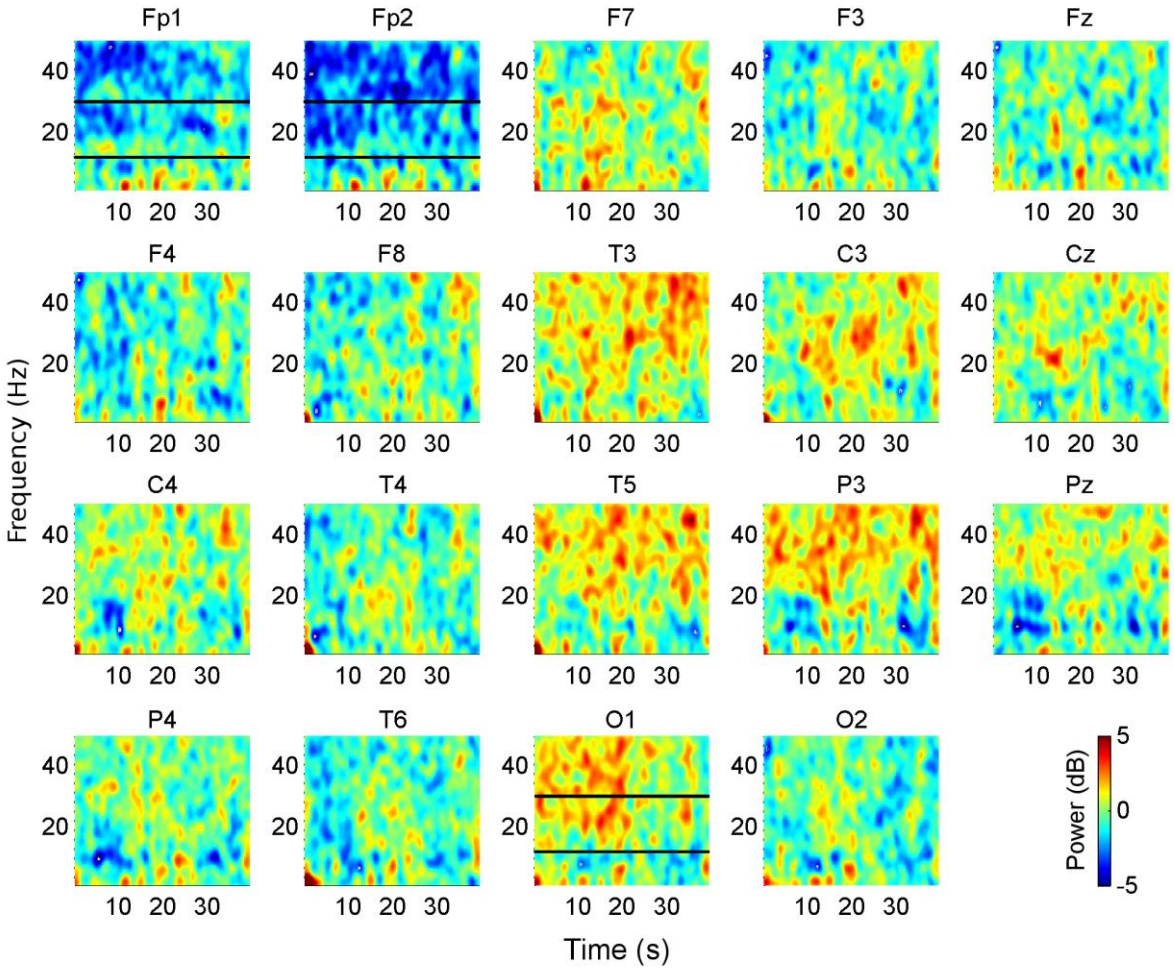

Spectrograms of the effects of noisy GVS after stimulation in PD OFF subjects. Spectrograms plot the difference in spectral power in the pre-stimulus subtracted from the post-stimulus periods, thus showing net spectral changes for the first 40 s following the cessation of stimulation. While none of the changes were significant, electrode regions Fp1, Fp2 and O1 show obvious post-stimulus carryover effects. In prefrontal Fp1 and Fp2, beta and gamma synchronization appeared to decrease, while an increase was observed in O1. Black lines represent 12 Hz and 30 Hz to delineate low and high frequencies, respectively.

Figure 3.2. Combined Band Power in Significant Channels Predicted Stimulus Intensity in a Linear Manner in PD OFF Subjects

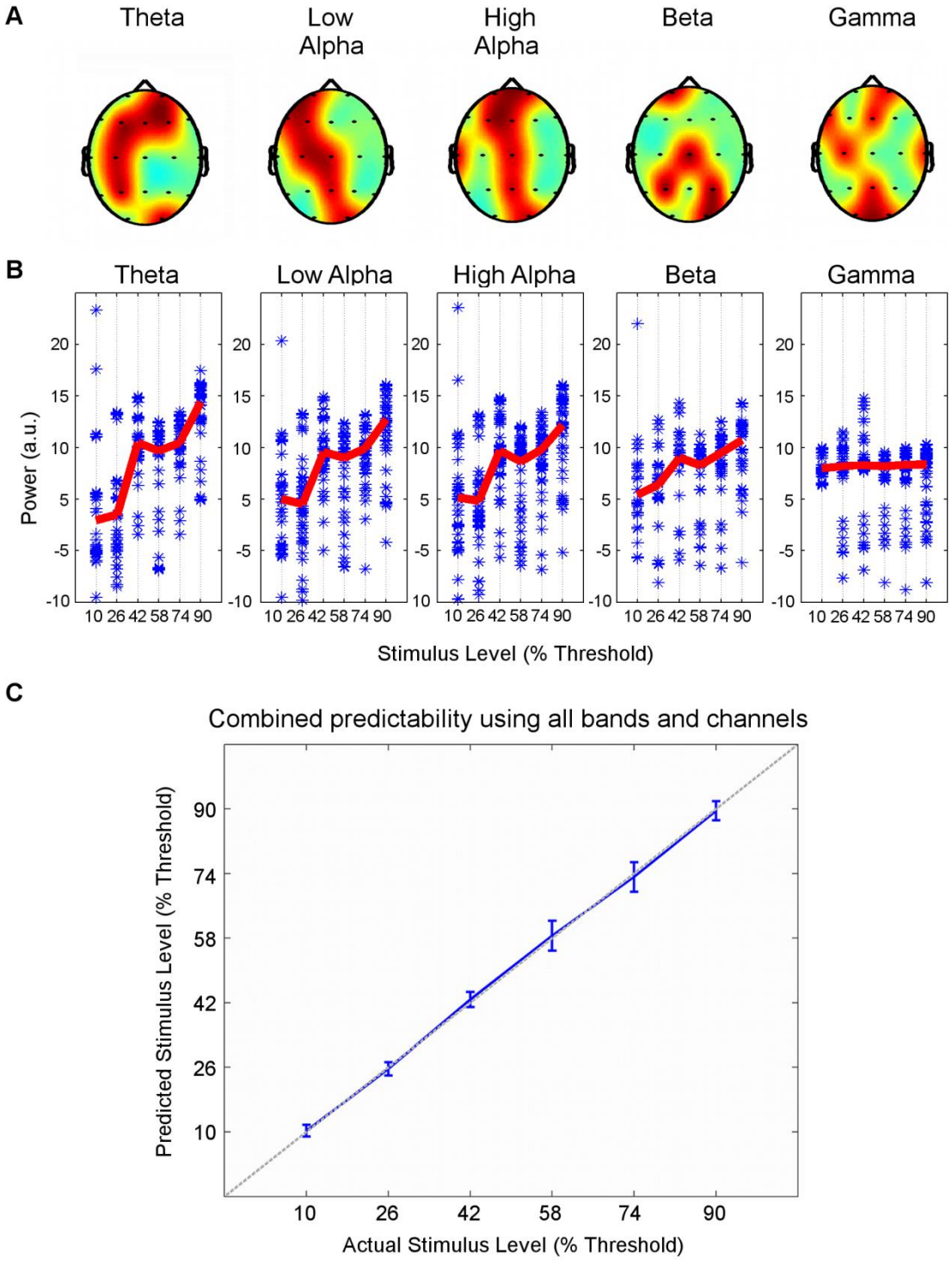

A. LASSO regularization identified significant channel/band combinations whose spectral features predicted the stimulus intensity in a linear manner in PD OFF subjects. Significant channels selected from each band LASSO are shown on scalp maps in red for each frequency band of interest. **B.** Spectral power in significant channels are plotted as function of stimulus intensity. The mean spectral power for each subject has been removed. Line plots (red) represent the median spectral values for all significant channels across all subjects. **C.** The ability of EEG features to linearly estimate stimulus intensity when all bands are included were confirmed by plotting predicted estimates against actual values of stimulus intensity. Blue line indicates the stimulus intensity predicted by LASSO-selected EEG estimates whereas the dotted gray line represents an ideal linear relation. Error bars are estimated from leave-one-out cross validation.

Figure 4.1. Behavioural Task

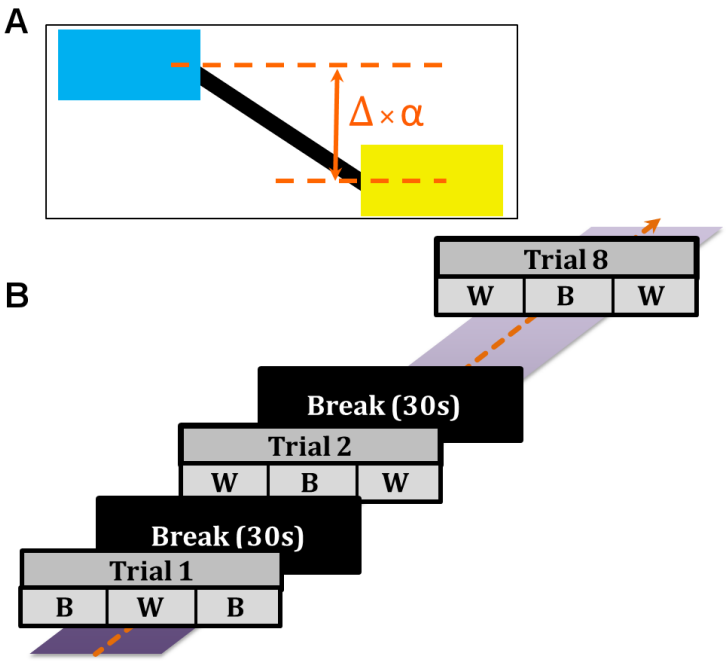

A. Subjects faced a screen with a target (blue) that moved vertically up and down, and controlled a cursor (yellow) using a joystick. The error difference (Δ) between the actual positions of the target and cursor was amplified by a scaling factor (α): Δ × α = displayed visual error feedback. In the 'Better' (B) condition, α was set to 0.3, and in the 'Worse' (W) condition, α was set to 2, such that it appeared that subjects performed better or worse respectively based on their visual error feedback. **B.** Trials (90 s) alternated between B and W conditions (each condition 30 s). Each trial was followed by a break of 30 s until a culmination of 8 trials total were completed for the experiment.

Figure 4.2. GVS Enhanced the Speed of Movements

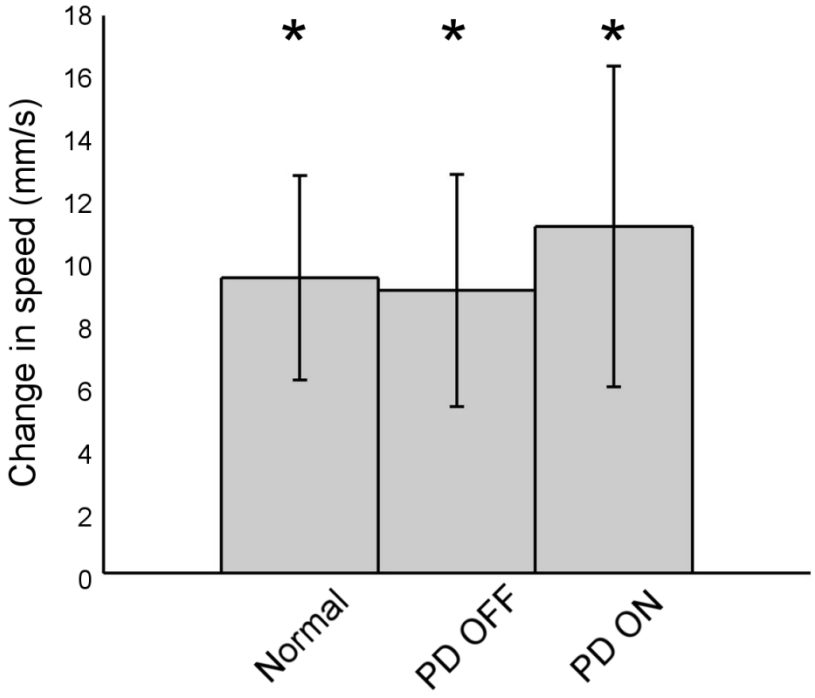

Plotted are the changes in velocity between stimulation trials and sham trials. GVS significantly increased the speed of movements in a visuomotor tracking task for all three groups: normal, PD OFF, PD ON. Asterisks mark significant effects ($p<0.05$).

Figure 4.3. Effects of GVS on Damping Ratio in Visuomotor Task

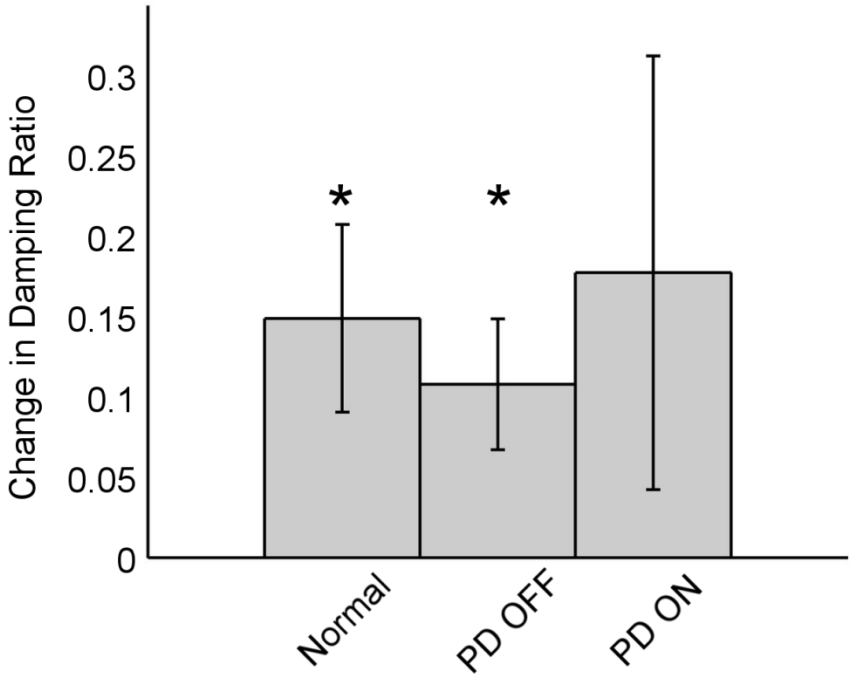

Plotted are the changes in damping ratio dynamics between trials with GVS minus trials with sham stimulation. GVS significantly increased the damping ratio of movements in normal and PD OFF. Asterisks mark significant effects ($p<0.05$).

Table 2.1. Significant *p* Values of Post-Stimulus Changes in Normal Subjects

Electrode Channel	Frequency Band	Time (s)	*p* Value *†
F3	Beta	23-27	0.019
Fz	Beta	18-26	0.021
F4	Beta	22-23, 34-36	0.018, 0.026
F8	Beta	22-25, 31-34	0.039, 0.017
F3	Gamma	26-28	0.011
F4	Gamma	27-31, 36-37	0.037, 0.030
F8	Gamma	26-40	0.022
T3	Gamma	<10	0.046
C3	Gamma	<10	0.023

* Only significant *p* values (<0.05) are reported, indicating whether the power of a given band in the post-stimulus EEG was different from the pre-stimulus EEG.
† A one-sided t-test was performed on the power difference between post- and pre-stimulus EEG data at each Fourier transform window. Reported *p* values are an average of those found significant within the identified time span by multiple one-sided t-tests. Only significant values spanning a time period of at least 2 s were considered.

Table 2.2. Significant Electrode Channels and Band Power in Normal Subjects

Electrode Channel	Theta (4-7.5 Hz)	Low Alpha (8-10 Hz)	High Alpha (10.5-12 Hz)	Beta (13-30 Hz)	Gamma (31-50 Hz)
Fp1	–	4.49E-09	3.16E-06	3.80E-14	9.68E-09
Fp2	7.84E-07	–	–	1.37E-05	3.31E-12
F7	–	–	–	–	4.56E-16
F3	5.06E-16	–	–	2.99E-17	2.05E-17
Fz	2.19E-15	4.82E-14	7.46E-13	8.66E-17	–
F4	5.64E-14	–	–	–	2.94E-13
F8	–	1.77E-05	2.74E-14	4.78E-12	3.50E-11
T3	–	–	–	–	3.70E-09
C3	–	–	–	–	–
Cz	–	2.97E-11	1.44E-8	4.46E-13	3.54E-13
C4	–	–	–	–	4.64E-11
T4	–	–	–	2.40E-07	–
T5	–	–	6.22E-07	–	–
P3	–	–	–	–	–
Pz	5.46E-14	5.71E-10	2.75E-09	–	4.24E-16
P4	–	1.61E-04	6.13E-11	–	1.01E-10
T6	4.03E-09	–	1.56E-03	–	1.02E-13
O1	–	–	2.20E-12	5.80E-09	3.48E-11
O2	–	9.43E-07	–	1.77E-08	–

Electrode channels and recorded band power determined by LASSO to predict a linear relation between EEG features and stimulus intensity in normal subjects. Only significant *p* values ($p<0.05$) are reported. All other *p* values were not significant and are denoted by −.

Table 3.1. PD Subjects' Characteristics for EEG Experiments

Patient number	Age (yr)	Sex	Duration since diagnosis (yr)	UPDRS motor score	Hoehn & Yahr stage	Clinical Dyskinesia Rating	
						Hyperkinesia	Dystonia
1	45	M	4.5	11	2	—	—
2	65	M	16	57	3	5	9
3	66	M	5	45	3	2	0
4	64	M	4.5	22	2	8	0
5	63	M	10	54	2.5	—	—
6	51	M	8	37	2.5	3	3
7	66	M	7	22	2	—	—

UPDRS = Unified Parkinson's Disease Rating Scale. — = Not Applicable

Table 3.2. Significant Electrode Channels and Band Power in PD OFF Subjects

Electrode Channel	Theta (4-7.5 Hz)	Low Alpha (8-10 Hz)	High Alpha (10.5-12 Hz)	Beta (13-30 Hz)	Gamma (31-50 Hz)
Fp1	−	2.73E-48	5.08E-47	1.12E-48	−
Fp2	2.62E-47	−	6.54E-38	1.37E-05	2.94E-44
F7	−	4.26E-47	−	−	8.10E-52
F3	6.94E-52	3.83E-48	4.00E-49	−	−
Fz	9.35E-40	−	2.05E-38	−	6.56E-49
F4	1.33E-45	−	−	−	−
T3	−	−	7.46E-43	4.78E-12	3.50E-11
C3	1.04E-51	4.65E-51	−	−	1.05E-42
Cz	−	4.06E-36	3.95E-45	2.25E-46	−
T4	−	−	−	−	3.65E-53
P3	1.62E-51	−	−	4.16E-44	−
Pz	−	2.26E-44	2.63E-46	−	5.65E-45
P4	−	−	−	3.90E-50	−
O1	−	−	−	−	2.26E-51
O2	1.91E-50	3.60E-48	2.69E-48	3.90E-50	1.60E-44

Electrode channels and recorded band power determined by LASSO to predict a linear relation between EEG features and stimulus intensity in normal subjects. Only significant *p* values ($p<0.05$) are reported. All other *p* values were not significant and are denoted by −.

Table 4.1. PD Subjects' Characteristics for Behavioural Task

Patient number	Age (yr)	Sex	Duration since diagnosis (yr)	UPDRS motor score	Hoehn & Yahr stage	Handedness
1	58	M	4	18	2	R
2	64	F	4	12	1.5	R
3	67	M	4	16	2	R
4	56	M	2.5	21	2	L
5	53	M	3	32	2.5	R
6	49	M	7.5	35	2	R
7	65	F	5	32	2	R
8	68	M	1.5	22	2	R
9	66	M	1	24	2	R
10	70	M	1	21	2	R
11	59	M	1.5	10	2	R
12	62	M	3.5	24	2	R

UPDRS = Unified Parkinson's Disease Rating Scale

BIBLIOGRAPHY

1. de Lau LM, Breteler MM (2006) Epidemiology of Parkinson's disease. Lancet Neurol 5: 525-535.

2. Van Den Eeden SK, Tanner CM, Bernstein AL, Fross RD, Leimpeter A, et al. (2003) Incidence of Parkinson's disease: variation by age, gender, and race/ethnicity. Am J Epidemiol 157: 1015-1022.

3. Fritsch T, Smyth KA, Wallendal MS, Hyde T, Leo G, et al. (2012) Parkinson disease: research update and clinical management. South Med J 105: 650-656.

4. Shulman JM, De Jager PL, Feany MB (2011) Parkinson's disease: genetics and pathogenesis. Annu Rev Pathol 6: 193-222.

5. Meissner WG, Frasier M, Gasser T, Goetz CG, Lozano A, et al. (2011) Priorities in Parkinson's disease research. Nat Rev Drug Discov 10: 377-393.

6. Langston JW (2006) The Parkinson's complex: parkinsonism is just the tip of the iceberg. Ann Neurol 59: 591-596.

7. Jankovic J (2008) Parkinson's disease: clinical features and diagnosis. J Neurol Neurosurg Psychiatry 79: 368-376.

8. Nussbaum RL, Ellis CE (2003) Alzheimer's disease and Parkinson's disease. N Engl J Med 348: 1356-1364.

9. Wichmann T, DeLong MR (2006) Basal ganglia discharge abnormalities in Parkinson's disease. J Neural Transm Suppl: 21-25.

10. Kravitz AV, Freeze BS, Parker PR, Kay K, Thwin MT, et al. (2010) Regulation of parkinsonian motor behaviours by optogenetic control of basal ganglia circuitry. Nature 466: 622-626.

11. Wichmann T, DeLong MR, Guridi J, Obeso JA (2011) Milestones in research on the pathophysiology of Parkinson's disease. Mov Disord 26: 1032-1041.

12. Poewe W, Antonini A, Zijlmans JC, Burkhard PR, Vingerhoets F (2010) Levodopa in the treatment of Parkinson's disease: an old drug still going strong. Clin Interv Aging 5: 229-238.

13. Braak H, Del Tredici K, Bratzke H, Hamm-Clement J, Sandmann-Keil D, et al. (2002) Staging of the intracerebral inclusion body pathology associated with idiopathic Parkinson's disease (preclinical and clinical stages). J Neurol 249 Suppl 3: III/1-5.

14. Ross CA, Poirier MA (2004) Protein aggregation and neurodegenerative disease. Nat Med 10 Suppl: S10-17.

15. Luk KC, Kehm V, Carroll J, Zhang B, O'Brien P, et al. (2012) Pathological alpha-synuclein transmission initiates Parkinson-like neurodegeneration in nontransgenic mice. Science 338: 949-953.

16. Langston JW, Forno LS, Tetrud J, Reeves AG, Kaplan JA, et al. (1999) Evidence of active nerve cell degeneration in the substantia nigra of humans years after 1-methyl-4-phenyl-1,2,3,6-tetrahydropyridine exposure. Ann Neurol 46: 598-605.

17. Gaig C, Marti MJ, Ezquerra M, Rey MJ, Cardozo A, et al. (2007) G2019S LRRK2 mutation causing Parkinson's disease without Lewy bodies. Journal of Neurology Neurosurgery and Psychiatry 78: 626-628.

18. Exner N, Lutz AK, Haass C, Winklhofer KF (2012) Mitochondrial dysfunction in Parkinson's disease: molecular mechanisms and pathophysiological consequences. EMBO J 31: 3038-3062.

19. Dexter DT, Jenner P (2013) Parkinson disease: from pathology to molecular disease mechanisms. Free Radic Biol Med.

20. Klein C, Westenberger A (2012) Genetics of Parkinson's disease. Cold Spring Harb Perspect Med 2: a008888.

21. Chaudhuri KR, Schapira AH (2009) Non-motor symptoms of Parkinson's disease: dopaminergic pathophysiology and treatment. Lancet Neurol 8: 464-474.

22. Obeso JA, Marin C, Rodriguez-Oroz C, Blesa J, Benitez-Temino B, et al. (2008) The basal ganglia in Parkinson's disease: current concepts and unexplained observations. Ann Neurol 64 Suppl 2: S30-46.

23. Yin HH, Knowlton BJ (2006) The role of the basal ganglia in habit formation. Nat Rev Neurosci 7: 464-476.

24. Jellinger KA (2012) Neuropathology of sporadic Parkinson's disease: evaluation and changes of concepts. Mov Disord 27: 8-30.

25. Hutchison WD, Dostrovsky JO, Walters JR, Courtemanche R, Boraud T, et al. (2004) Neuronal oscillations in the basal ganglia and movement disorders: evidence from whole animal and human recordings. J Neurosci 24: 9240-9243.

26. Bergman H, Wichmann T, Delong MR (1990) Reversal of Experimental Parkinsonism by Lesions of the Subthalamic Nucleus. Science 249: 1436-1438.

27. Baron MS, Vitek JL, Bakay RA, Green J, Kaneoke Y, et al. (1996) Treatment of advanced Parkinson's disease by posterior GPi pallidotomy: 1-year results of a pilot study. Ann Neurol 40: 355-366.

28. Hamada I, Delong MR (1992) Excitotoxic Acid Lesions of the Primate Subthalamic Nucleus Result in Reduced Pallidal Neuronal-Activity during Active Holding. Journal of Neurophysiology 68: 1859-1866.

29. Hamada I, Delong MR (1992) Excitotoxic Acid Lesions of the Primate Subthalamic Nucleus Result in Transient Dyskinesias of the Contralateral Limbs. Journal of Neurophysiology 68: 1850-1858.

30. Crossman AR, Mitchell IJ, Sambrook MA, Jackson A (1988) Chorea and Myoclonus in the Monkey Induced by Gamma-Aminobutyric Acid Antagonism in the Lentiform Complex - the Site of Drug-Action and a Hypothesis for the Neural Mechanisms of Chorea. Brain 111: 1211-1233.

31. Hutchison WD, Lang AE, Dostrovsky JO, Lozano AM (2003) Pallidal neuronal activity: implications for models of dystonia. Ann Neurol 53: 480-488.

32. Levy R, Dostrovsky JO, Lang AE, Sime E, Hutchison WD, et al. (2001) Effects of apomorphine on subthalamic nucleus and globus pallidus internus neurons in patients with Parkinson's disease. Journal of Neurophysiology 86: 249-260.

33. Obeso JA, Lanciego JL (2011) Past, present, and future of the pathophysiological model of the basal ganglia. Frontiers in Neuroanatomy 5.

34. Gatev P, Darbin O, Wichmann T (2006) Oscillations in the basal ganglia under normal conditions and in movement disorders. Mov Disord 21: 1566-1577.

35. Bevan MD, Magill PJ, Terman D, Bolam JP, Wilson CJ (2002) Move to the rhythm: oscillations in the subthalamic nucleus-external globus pallidus network. Trends Neurosci 25: 525-531.

36. Uhlhaas PJ, Singer W (2006) Neural synchrony in brain disorders: relevance for cognitive dysfunctions and pathophysiology. Neuron 52: 155-168.

37. Eusebio A, Pogosyan A, Wang S, Averbeck B, Gaynor LD, et al. (2009) Resonance in subthalamo-cortical circuits in Parkinson's disease. Brain 132: 2139-2150.

38. Mallet N, Pogosyan A, Marton LF, Bolam JP, Brown P, et al. (2008) Parkinsonian beta oscillations in the external globus pallidus and their relationship with subthalamic nucleus activity. J Neurosci 28: 14245-14258.

39. Mallet N, Pogosyan A, Sharott A, Csicsvari J, Bolam JP, et al. (2008) Disrupted dopamine transmission and the emergence of exaggerated beta oscillations in subthalamic nucleus and cerebral cortex. J Neurosci 28: 4795-4806.

40. Fuentes R, Petersson P, Siesser WB, Caron MG, Nicolelis MA (2009) Spinal cord stimulation restores locomotion in animal models of Parkinson's disease. Science 323: 1578-1582.

41. Weinberger M, Hutchison WD, Dostrovsky JO (2009) Pathological subthalamic nucleus oscillations in PD: can they be the cause of bradykinesia and akinesia? Exp Neurol 219: 58-61.

42. Brown P, Oliviero A, Mazzone P, Insola A, Tonali P, et al. (2001) Dopamine dependency of oscillations between subthalamic nucleus and pallidum in Parkinson's disease. J Neurosci 21: 1033-1038.

43. Levy R, Hutchison WD, Lozano AM, Dostrovsky JO (2002) Synchronized neuronal discharge in the basal ganglia of parkinsonian patients is limited to oscillatory activity. J Neurosci 22: 2855-2861.

44. Chen CC, Litvak V, Gilbertson T, Kuhn A, Lu CS, et al. (2007) Excessive synchronization of basal ganglia neurons at 20 Hz slows movement in Parkinson's disease. Exp Neurol 205: 214-221.

45. Pogosyan A, Gaynor LD, Eusebio A, Brown P (2009) Boosting cortical activity at Beta-band frequencies slows movement in humans. Curr Biol 19: 1637-1641.

46. Zhang Y, Chen Y, Bressler SL, Ding M (2008) Response preparation and inhibition: the role of the cortical sensorimotor beta rhythm. Neuroscience 156: 238-246.

47. Kuhn AA, Tsui A, Aziz T, Ray N, Brucke C, et al. (2009) Pathological synchronisation in the subthalamic nucleus of patients with Parkinson's disease relates to both bradykinesia and rigidity. Exp Neurol 215: 380-387.

48. Levy R, Ashby P, Hutchison WD, Lang AE, Lozano AM, et al. (2002) Dependence of subthalamic nucleus oscillations on movement and dopamine in Parkinson's disease. Brain 125: 1196-1209.

49. Weinberger M, Mahant N, Hutchison WD, Lozano AM, Moro E, et al. (2006) Beta oscillatory activity in the subthalamic nucleus and its relation to dopaminergic response in Parkinson's disease. J Neurophysiol 96: 3248-3256.

50. Eusebio A, Brown P (2009) Synchronisation in the beta frequency-band--the bad boy of parkinsonism or an innocent bystander? Exp Neurol 217: 1-3.

51. Okun MS (2012) Deep-brain stimulation for Parkinson's disease. N Engl J Med 367: 1529-1538.

52. Wingeier B, Tcheng T, Koop MM, Hill BC, Heit G, et al. (2006) Intra-operative STN DBS attenuates the prominent beta rhythm in the STN in Parkinson's disease. Exp Neurol 197: 244-251.

53. Dostrovsky J, Bergman H (2004) Oscillatory activity in the basal ganglia--relationship to normal physiology and pathophysiology. Brain 127: 721-722.

54. Engel AK, Fries P (2010) Beta-band oscillations--signalling the status quo? Curr Opin Neurobiol 20: 156-165.

55. Leventhal DK, Gage GJ, Schmidt R, Pettibone JR, Case AC, et al. (2012) Basal ganglia beta oscillations accompany cue utilization. Neuron 73: 523-536.

56. Brown P (2006) Bad oscillations in Parkinson's disease. J Neural Transm Suppl: 27-30.

57. Feurra M, Bianco G, Santarnecchi E, Del Testa M, Rossi A, et al. (2011) Frequency-dependent tuning of the human motor system induced by transcranial oscillatory potentials. J Neurosci 31: 12165-12170.

58. Varela F, Lachaux JP, Rodriguez E, Martinerie J (2001) The brainweb: phase synchronization and large-scale integration. Nat Rev Neurosci 2: 229-239.

59. Buzsáki G (2006) Rhythms of the brain. Oxford ; New York: Oxford University Press. xiv, 448 p. p.

60. Ward LM, MacLean SE, Kirschner A (2010) Stochastic resonance modulates neural synchronization within and between cortical sources. PLoS One 5: e14371.

61. Hipp JF, Engel AK, Siegel M (2011) Oscillatory Synchronization in Large-Scale Cortical Networks Predicts Perception. Neuron 69: 387-396.

62. Stoffers D, Berendse HW, Deijen JB, Wolters EC (2001) Motor perseveration is an early sign of Parkinson's disease. Neurology 57: 2111-2113.

63. De Cock VC, Vidailhet M, Leu S, Texeira A, Apartis E, et al. (2007) Restoration of normal motor control in Parkinson's disease during REM sleep. Brain 130: 450-456.

64. Gagnon JF, Fantini ML, Bedard MA, Petit D, Carrier J, et al. (2004) Association between waking EEG slowing and REM sleep behavior disorder in PD without dementia. Neurology 62: 401-406.

65. Cools R, Barker RA, Sahakian BJ, Robbins TW (2001) Mechanisms of cognitive set flexibility in Parkinson's disease. Brain 124: 2503-2512.

66. Svenningsson P, Westman E, Ballard C, Aarsland D (2012) Cognitive impairment in patients with Parkinson's disease: diagnosis, biomarkers, and treatment. Lancet Neurol 11: 697-707.

67. Floresco SB, Ghods-Sharifi S, Vexelman C, Magyar O (2006) Dissociable roles for the nucleus accumbens core and shell in regulating set shifting. J Neurosci 26: 2449-2457.

68. Tropini G, Chiang J, Wang ZJ, Ty E, McKeown MJ (2011) Altered directional connectivity in Parkinson's disease during performance of a visually guided task. Neuroimage 56: 2144-2156.

69. Weinberger M, Hutchison WD, Lozano AM, Hodaie M, Dostrovsky JO (2009) Increased gamma oscillatory activity in the subthalamic nucleus during tremor in Parkinson's disease patients. J Neurophysiol 101: 789-802.

70. Doesburg SM, Green JJ, McDonald JJ, Ward LM (2009) Rhythms of consciousness: binocular rivalry reveals large-scale oscillatory network dynamics mediating visual perception. PLoS One 4: e6142.

71. Belluscio MA, Mizuseki K, Schmidt R, Kempter R, Buzsaki G (2012) Cross-frequency phase-phase coupling between theta and gamma oscillations in the hippocampus. J Neurosci 32: 423-435.

72. Voon V, Mehta AR, Hallett M (2011) Impulse control disorders in Parkinson's disease: recent advances. Curr Opin Neurol 24: 324-330.

73. Shaw KM, Lees AJ, Stern GM (1980) The impact of treatment with levodopa on Parkinson's disease. Q J Med 49: 283-293.

74. Shafi MM, Westover MB, Fox MD, Pascual-Leone A (2012) Exploration and modulation of brain network interactions with noninvasive brain stimulation in combination with neuroimaging. Eur J Neurosci 35: 805-825.

75. Fregni F, Pascual-Leone A (2007) Technology insight: noninvasive brain stimulation in neurology-perspectives on the therapeutic potential of rTMS and tDCS. Nat Clin Pract Neurol 3: 383-393.

76. Utz KS, Dimova V, Oppenlander K, Kerkhoff G (2010) Electrified minds: transcranial direct current stimulation (tDCS) and galvanic vestibular stimulation (GVS) as methods of non-invasive brain stimulation in neuropsychology--a review of current data and future implications. Neuropsychologia 48: 2789-2810.

77. Medeiros LF, de Souza IC, Vidor LP, de Souza A, Deitos A, et al. (2012) Neurobiological effects of transcranial direct current stimulation: a review. Front Psychiatry 3: 110.

78. Stagg CJ, Best JG, Stephenson MC, O'Shea J, Wylezinska M, et al. (2009) Polarity-sensitive modulation of cortical neurotransmitters by transcranial stimulation. J Neurosci 29: 5202-5206.

79. Hansen N (2012) Action mechanisms of transcranial direct current stimulation in Alzheimer's disease and memory loss. Front Psychiatry 3: 48.

80. Miranda PC, Lomarev M, Hallett M (2006) Modeling the current distribution during transcranial direct current stimulation. Clin Neurophysiol 117: 1623-1629.

81. Antal A, Boros K, Poreisz C, Chaieb L, Terney D, et al. (2008) Comparatively weak after-effects of transcranial alternating current stimulation (tACS) on cortical excitability in humans. Brain Stimul 1: 97-105.

82. Terney D, Chaieb L, Moliadze V, Antal A, Paulus W (2008) Increasing human brain excitability by transcranial high-frequency random noise stimulation. J Neurosci 28: 14147-14155.

83. Ridding MC, Rothwell JC (2007) Perspectives - Opinion - Is there a future for therapeutic use of transcranial magnetic stimulation? Nature Reviews Neuroscience 8: 559-567.

84. Schulz R, Gerloff C, Hummel FC (2013) Non-invasive brain stimulation in neurological diseases. Neuropharmacology 64: 579-587.

85. Monte-Silva K, Liebetanz D, Grundey J, Paulus W, Nitsche MA (2010) Dosage-dependent non-linear effect of L-dopa on human motor cortex plasticity. J Physiol 588: 3415-3424.

86. Stagg CJ, Bachtiar V, O'Shea J, Allman C, Bosnell RA, et al. (2012) Cortical activation changes underlying stimulation-induced behavioural gains in chronic stroke. Brain 135: 276-284.

87. Chang WH, Kim YH, Bang OY, Kim ST, Park YH, et al. (2010) Long-term effects of rTMS on motor recovery in patients after subacute stroke. J Rehabil Med 42: 758-764.

88. Lindenberg R, Renga V, Zhu LL, Nair D, Schlaug G (2010) Bihemispheric brain stimulation facilitates motor recovery in chronic stroke patients. Neurology 75: 2176-2184.

89. Allan C, Kalu UG, Sexton CE, Ebmeier KP (2012) Transcranial stimulation in depression. Br J Psychiatry 200: 10-11.

90. Abbott CC, Lemke NT, Gopal S, Thoma RJ, Bustillo J, et al. (2013) Electroconvulsive therapy response in major depressive disorder: a pilot functional network connectivity resting state FMRI investigation. Front Psychiatry 4: 10.

91. Keeser D, Meindl T, Bor J, Palm U, Pogarell O, et al. (2011) Prefrontal transcranial direct current stimulation changes connectivity of resting-state networks during fMRI. J Neurosci 31: 15284-15293.

92. Boggio PS, Ferrucci R, Rigonatti SP, Covre P, Nitsche M, et al. (2006) Effects of transcranial direct current stimulation on working memory in patients with Parkinson's disease. J Neurol Sci 249: 31-38.

93. Fecteau S, Fregni F, Boggio PS, Camprodon JA, Pascual-Leone A (2010) Neuromodulation of decision-making in the addictive brain. Subst Use Misuse 45: 1766-1786.

94. Brody AL, Mandelkern MA, London ED, Childress AR, Lee GS, et al. (2002) Brain metabolic changes during cigarette craving. Arch Gen Psychiatry 59: 1162-1172.

95. George MS, Anton RF, Bloomer C, Teneback C, Drobes DJ, et al. (2001) Activation of prefrontal cortex and anterior thalamus in alcoholic subjects on exposure to alcohol-specific cues. Arch Gen Psychiatry 58: 345-352.

96. Boggio PS, Liguori P, Sultani N, Rezende L, Fecteau S, et al. (2009) Cumulative priming effects of cortical stimulation on smoking cue-induced craving. Neurosci Lett 463: 82-86.

97. Hely MA, Morris JG, Reid WG, Trafficante R (2005) Sydney Multicenter Study of Parkinson's disease: non-L-dopa-responsive problems dominate at 15 years. Mov Disord 20: 190-199.

98. Strafella AP, Paus T, Fraraccio M, Dagher A (2003) Striatal dopamine release induced by repetitive transcranial magnetic stimulation of the human motor cortex. Brain 126: 2609-2615.

99. Strafella AP, Paus T, Barrett J, Dagher A (2001) Repetitive transcranial magnetic stimulation of the human prefrontal cortex induces dopamine release in the caudate nucleus. J Neurosci 21: RC157.

100. Fregni F, Santos CM, Myczkowski ML, Rigolino R, Gallucci-Neto J, et al. (2004) Repetitive transcranial magnetic stimulation is as effective as fluoxetine in the treatment of depression in patients with Parkinson's disease. J Neurol Neurosurg Psychiatry 75: 1171-1174.

101. Thut G, Veniero D, Romei V, Miniussi C, Schyns P, et al. (2011) Rhythmic TMS causes local entrainment of natural oscillatory signatures. Curr Biol 21: 1176-1185.

102. Zaehle T, Rach S, Herrmann CS (2010) Transcranial alternating current stimulation enhances individual alpha activity in human EEG. PLoS One 5: e13766.

103. Wardman DL, Day BL, Fitzpatrick RC (2003) Position and velocity responses to galvanic vestibular stimulation in human subjects during standing. J Physiol 547: 293-299.

104. Day BL, Severac Cauquil A, Bartolomei L, Pastor MA, Lyon IN (1997) Human body-segment tilts induced by galvanic stimulation: a vestibularly driven balance protection mechanism. J Physiol 500 (Pt 3): 661-672.

105. Cauquil AS, Day BL (1998) Galvanic vestibular stimulation modulates voluntary movement of the human upper body. J Physiol 513 (Pt 2): 611-619.

106. Zink R, Steddin S, Weiss A, Brandt T, Dieterich M (1997) Galvanic vestibular stimulation in humans: effects on otolith function in roll. Neurosci Lett 232: 171-174.

107. Severac Cauquil A, Faldon M, Popov K, Day BL, Bronstein AM (2003) Short-latency eye movements evoked by near-threshold galvanic vestibular stimulation. Exp Brain Res 148: 414-418.

108. Schneider E, Glasauer S, Dieterich M (2002) Comparison of human ocular torsion patterns during natural and galvanic vestibular stimulation. J Neurophysiol 87: 2064-2073.

109. Stephan T, Deutschlander A, Nolte A, Schneider E, Wiesmann M, et al. (2005) Functional MRI of galvanic vestibular stimulation with alternating currents at different frequencies. Neuroimage 26: 721-732.

110. Smith PF, Geddes LH, Baek JH, Darlington CL, Zheng Y (2010) Modulation of memory by vestibular lesions and galvanic vestibular stimulation. Front Neurol 1: 141.

111. Fitzpatrick RC, Day BL (2004) Probing the human vestibular system with galvanic stimulation. J Appl Physiol 96: 2301-2316.

112. Goldberg JM, Smith CE, Fernandez C (1984) Relation between discharge regularity and responses to externally applied galvanic currents in vestibular nerve afferents of the squirrel monkey. J Neurophysiol 51: 1236-1256.

113. Utz KS, Korluss K, Schmidt L, Rosenthal A, Oppenlander K, et al. (2011) Minor adverse effects of galvanic vestibular stimulation in persons with stroke and healthy individuals. Brain Inj 25: 1058-1069.

114. Bense S, Stephan T, Yousry TA, Brandt T, Dieterich M (2001) Multisensory cortical signal increases and decreases during vestibular galvanic stimulation (fMRI). J Neurophysiol 85: 886-899.

115. Bucher SF, Dieterich M, Wiesmann M, Weiss A, Zink R, et al. (1998) Cerebral functional magnetic resonance imaging of vestibular, auditory, and nociceptive areas during galvanic stimulation. Ann Neurol 44: 120-125.

116. Lobel E, Kleine JF, Bihan DL, Leroy-Willig A, Berthoz A (1998) Functional MRI of galvanic vestibular stimulation. J Neurophysiol 80: 2699-2709.

117. Lobel E, Kleine JF, Leroy-Willig A, Van de Moortele PF, Le Bihan D, et al. (1999) Cortical areas activated by bilateral galvanic vestibular stimulation. Ann N Y Acad Sci 871: 313-323.

118. Smith AT, Wall MB, Thilo KV (2012) Vestibular inputs to human motion-sensitive visual cortex. Cereb Cortex 22: 1068-1077.

119. Lopez C, Blanke O (2011) The thalamocortical vestibular system in animals and humans. Brain Res Rev 67: 119-146.

120. Meng H, May PJ, Dickman JD, Angelaki DE (2007) Vestibular signals in primate thalamus: properties and origins. J Neurosci 27: 13590-13602.

121. Percheron G, Francois C, Talbi B, Yelnik J, Fenelon G (1996) The primate motor thalamus. Brain Res Brain Res Rev 22: 93-181.

122. Sherman SM (2005) Thalamic relays and cortical functioning. Prog Brain Res 149: 107-126.

123. Cullen KE (2012) The vestibular system: multimodal integration and encoding of self-motion for motor control. Trends Neurosci 35: 185-196.

124. Smith PF, Zheng YW, Horii A, Darlington CL (2005) Does vestibular damage cause cognitive dysfunction in humans? Journal of Vestibular Research-Equilibrium & Orientation 15: 1-9.

125. McGeoch PD, Williams LE, Lee RR, Ramachandran VS (2008) Behavioural evidence for vestibular stimulation as a treatment for central post-stroke pain. J Neurol Neurosurg Psychiatry 79: 1298-1301.

126. McGeoch PD, Ramachandran VS (2008) Vestibular stimulation can relieve central pain of spinal origin. Spinal Cord 46: 756-757.

127. Schmidt L, Utz KS, Depper L, Adams M, Schaadt AK, et al. (2013) Now You Feel both: Galvanic Vestibular Stimulation Induces Lasting Improvements in the Rehabilitation of Chronic Tactile Extinction. Front Hum Neurosci 7: 90.

128. Wilkinson D, Ko P, Kilduff P, McGlinchey R, Milberg W (2005) Improvement of a face perception deficit via subsensory galvanic vestibular stimulation. Journal of the International Neuropsychological Society 11: 925-929.

129. Wilkinson D, Zubko O, Degutis J, Milberg W, Potter J (2010) Improvement of a figure copying deficit during subsensory galvanic vestibular stimulation. J Neuropsychol 4: 107-118.

130. Rorsman I, Magnusson M, Johansson BB (1999) Reduction of visuo-spatial neglect with vestibular galvanic stimulation. Scand J Rehabil Med 31: 117-124.

131. Miller SM, Ngo TT (2007) Studies of caloric vestibular stimulation: implications for the cognitive neurosciences, the clinical neurosciences and neurophilosophy. Acta Neuropsychiatrica 19: 183-203.

132. Pan W, Soma R, Kwak S, Yamamoto Y (2008) Improvement of motor functions by noisy vestibular stimulation in central neurodegenerative disorders. J Neurol 255: 1657-1661.

133. Yamamoto Y, Struzik ZR, Soma R, Ohashi K, Kwak S (2005) Noisy vestibular stimulation improves autonomic and motor responsiveness in central neurodegenerative disorders. Ann Neurol 58: 175-181.

134. Pal S, Rosengren SM, Colebatch JG (2009) Stochastic galvanic vestibular stimulation produces a small reduction in sway in Parkinson's disease. J Vestib Res 19: 137-142.

135. Samoudi G, Nissbrandt H, Dutia MB, Bergquist F (2012) Noisy galvanic vestibular stimulation promotes GABA release in the substantia nigra and improves locomotion in hemiparkinsonian rats. PLoS One 7: e29308.

136. Wilkinson D, Nicholls S, Pattenden C, Kilduff P, Milberg W (2008) Galvanic vestibular stimulation speeds visual memory recall. Exp Brain Res 189: 243-248.

137. Soma R, Kwak S, Yamamoto Y (2003) Functional stochastic resonance in human baroreflex induced by 1/f-type noisy galvanic vestibular stimulation. Fluctuations and Noise in Biological, Biophysical, and Biomedical Systems 5110: 69-76.

138. Moss F, Ward LM, Sannita WG (2004) Stochastic resonance and sensory information processing: a tutorial and review of application. Clin Neurophysiol 115: 267-281.

139. Buzsaki G, Draguhn A (2004) Neuronal oscillations in cortical networks. Science 304: 1926-1929.

140. Degiorgio CM, Soss J, Cook IA, Markovic D, Gornbein J, et al. (2013) Randomized controlled trial of trigeminal nerve stimulation for drug-resistant epilepsy. Neurology 80: 786-791.

141. De Ferrari GM, Schwartz PJ (2011) Vagus nerve stimulation: from pre-clinical to clinical application: challenges and future directions. Heart Fail Rev 16: 195-203.

142. Llinas RR, Ribary U, Jeanmonod D, Kronberg E, Mitra PP (1999) Thalamocortical dysrhythmia: A neurological and neuropsychiatric syndrome characterized by magnetoencephalography. Proc Natl Acad Sci U S A 96: 15222-15227.

143. Schulman JJ, Cancro R, Lowe S, Lu F, Walton KD, et al. (2011) Imaging of thalamocortical dysrhythmia in neuropsychiatry. Front Hum Neurosci 5: 69.

144. Yamamoto M, Okuma Y, Maeda T, Kimura K (2012) Pramipexole-induced camptocormia in Parkinson's disease: 8 reversible cases. Movement Disorders 27: S523-S523.

145. Wilkinson D, Zubko O, Sakel M (2009) Safety of repeated sessions of galvanic vestibular stimulation following stroke: a single-case study. Brain Inj 23: 841-845.

146. Au WL, Lei N, Oishi MM, McKeown MJ (2010) L-dopa induces under-damped visually guided motor responses in Parkinson's disease. Exp Brain Res 202: 553-559.

147. Angelaki DE, Cullen KE (2008) Vestibular system: the many facets of a multimodal sense. Annu Rev Neurosci 31: 125-150.

148. Guldin WO, Grusser OJ (1998) Is there a vestibular cortex? Trends Neurosci 21: 254-259.

149. Guillery RW (1995) Anatomical evidence concerning the role of the thalamus in corticocortical communication: a brief review. J Anat 187 (Pt 3): 583-592.

150. Lopez C, Blanke O, Mast FW (2012) The human vestibular cortex revealed by coordinate-based activation likelihood estimation meta-analysis. Neuroscience 212: 159-179.

151. Day BL (1999) Galvanic vestibular stimulation: new uses for an old tool. J Physiol 517 (Pt 3): 631.

152. Wilkinson D, Ko P, Kilduff P, McGlinchey R, Milberg W (2005) Improvement of a face perception deficit via subsensory galvanic vestibular stimulation. J Int Neuropsychol Soc 11: 925-929.

153. Jenkinson N, Brown P (2011) New insights into the relationship between dopamine, beta oscillations and motor function. Trends Neurosci 34: 611-618.

154. Wilkinson D, Ferguson HJ, Worley A (2012) Galvanic vestibular stimulation modulates the electrophysiological response during face processing. Vis Neurosci 29: 255-262.

155. McDonnell MD, Ward LM (2011) The benefits of noise in neural systems: bridging theory and experiment. Nat Rev Neurosci 12: 415-426.

156. Deco G, Jirsa VK, McIntosh AR (2011) Emerging concepts for the dynamical organization of resting-state activity in the brain. Nat Rev Neurosci 12: 43-56.

157. Jung TP, Makeig S, Humphries C, Lee TW, McKeown MJ, et al. (2000) Removing electroencephalographic artifacts by blind source separation. Psychophysiology 37: 163-178.

158. Aqil M, Hong KS, Jeong MY, Ge SS (2012) Online Brain imaging by QR Factorization of Normalized Regressor Functions. IEEE International Conference on Mechatronics and Automation 2012, Proceedings: 1370-1374.

159. Zheng N, Qi L, Gao L, Guan L (2012) Generalized Mmsd Feature Extraction Using Qr Decomposition. 2012 Ieee Visual Communications and Image Processing (Vcip).

160. Hummel F, Celnik P, Giraux P, Floel A, Wu WH, et al. (2005) Effects of non-invasive cortical stimulation on skilled motor function in chronic stroke. Brain 128: 490-499.

161. Nuwer MR, Comi G, Emerson R, Fuglsang-Frederiksen A, Guerit JM, et al. (1999) IFCN standards for digital recording of clinical EEG. The International Federation of Clinical Neurophysiology. Electroencephalogr Clin Neurophysiol Suppl 52: 11-14.

162. Makeig S, Bell AJ, Jung TP, Sejnowski TJ (1996) Independent component analysis of electroencephalographic data. Advances in Neural Information Processing Systems 8 8: 145-151.

163. Rush S, Driscoll DA (1968) Current distribution in the brain from surface electrodes. Anesth Analg 47: 717-723.

164. Ozen S, Sirota A, Belluscio MA, Anastassiou CA, Stark E, et al. (2010) Transcranial electric stimulation entrains cortical neuronal populations in rats. J Neurosci 30: 11476-11485.

165. Hernandez-Pavon JC, Metsomaa J, Mutanen T, Stenroos M, Maki H, et al. (2012) Uncovering neural independent components from highly artifactual TMS-evoked EEG data. J Neurosci Methods 209: 144-157.

166. Abdelnour AF, Huppert T (2009) Real-time imaging of human brain function by near-infrared spectroscopy using an adaptive general linear model. Neuroimage 46: 133-143.

167. Parra LC, Spence CD, Gerson AD, Sajda P (2005) Recipes for the linear analysis of EEG. Neuroimage 28: 326-341.

168. Tibshirani R (1996) Regression shrinkage and selection via the Lasso. Journal of the Royal Statistical Society Series B-Methodological 58: 267-288.

169. Bent LR, McFadyen BJ, Merkley VF, Kennedy PM, Inglis JT (2000) Magnitude effects of galvanic vestibular stimulation on the trajectory of human gait. Neurosci Lett 279: 157-160.

170. Zink R, Bucher SF, Weiss A, Brandt T, Dieterich M (1998) Effects of galvanic vestibular stimulation on otolithic and semicircular canal eye movements and perceived vertical. Electroencephalogr Clin Neurophysiol 107: 200-205.

171. Palva S, Palva JM (2007) New vistas for alpha-frequency band oscillations. Trends Neurosci 30: 150-158.

172. Homan RW, Herman J, Purdy P (1987) Cerebral location of international 10-20 system electrode placement. Electroencephalogr Clin Neurophysiol 66: 376-382.

173. Cavanna AE, Trimble MR (2006) The precuneus: a review of its functional anatomy and behavioural correlates. Brain 129: 564-583.

174. Vaudano AE, Laufs H, Kiebel SJ, Carmichael DW, Hamandi K, et al. (2009) Causal Hierarchy within the Thalamo-Cortical Network in Spike and Wave Discharges. Plos One 4.

175. Bullmore E, Sporns O (2009) Complex brain networks: graph theoretical analysis of structural and functional systems. Nat Rev Neurosci 10: 186-198.

176. Singer W (2011) Dynamic formation of functional networks by synchronization. Neuron 69: 191-193.

177. Fries P (2005) A mechanism for cognitive dynamics: neuronal communication through neuronal coherence. Trends in Cognitive Sciences 9: 474-480.

178. Gross J, Schnitzler A, Timmermann L, Ploner M (2007) Gamma oscillations in human primary somatosensory cortex reflect pain perception. PLoS Biol 5: e133.

179. Fell J, Axmacher N (2011) The role of phase synchronization in memory processes. Nat Rev Neurosci 12: 105-118.

180. Keinrath C, Wriessnegger S, Muller-Putz GR, Pfurtscheller G (2006) Post-movement beta synchronization after kinesthetic illusion, active and passive movements. Int J Psychophysiol 62: 321-327.

181. McDonnell MD, Abbott D (2009) What Is Stochastic Resonance? Definitions, Misconceptions, Debates, and Its Relevance to Biology. Plos Computational Biology 5.

182. Fearnley JM, Lees AJ (1991) Ageing and Parkinson's disease: substantia nigra regional selectivity. Brain 114 (Pt 5): 2283-2301.

183. Marsden CD (1990) Parkinson's disease. Lancet 335: 948-952.

184. de Hemptinne C, Ryapolova-Webb ES, Air EL, Garcia PA, Miller KJ, et al. (2013) Exaggerated phase-amplitude coupling in the primary motor cortex in Parkinson disease. Proc Natl Acad Sci U S A 110: 4780-4785.

185. Molinari E, Baraldi P, Campanella M, Duzzi D, Nocetti L, et al. (2013) Human Parietofrontal Networks Related to Action Observation Detected at Rest. Cerebral Cortex 23: 178-186.

186. Palmer SJ, Eigenraam L, Hoque T, Mccaig RG, Troiano A, et al. (2009) Levodopa-Sensitive, Dynamic Changes in Effective Connectivity during Simultaneous Movements in Parkinson's Disease. Neuroscience 158: 693-704.

187. Faught E, Tatum W (2013) Trigeminal stimulation: A superhighway to the brain? Neurology 80: 780-781.

188. Nicolelis MA, Fuentes R, Petersson P, Thevathasan W, Brown P (2010) Spinal cord stimulation failed to relieve akinesia or restore locomotion in Parkinson disease. Neurology 75: 1484; author reply 1484-1485.

189. Ryu YU, Buchanan JJ (2012) Accuracy, stability, and corrective behavior in a visuomotor tracking task: a preliminary study. PLoS One 7: e38537.

190. Oishi MM, TalebiFard P, McKeown MJ (2011) Assessing manual pursuit tracking in Parkinson's disease via linear dynamical systems. Ann Biomed Eng 39: 2263-2273.

191. Frank MJ, Seeberger LC, O'Reilly R C (2004) By carrot or by stick: cognitive reinforcement learning in parkinsonism. Science 306: 1940-1943.

192. Boehringer A, Macher K, Dukart J, Villringer A, Pleger B (2012) Cerebellar transcranial direct current stimulation modulates verbal working memory. Brain Stimul.

193. Ferrucci R, Brunoni AR, Parazzini M, Vergari M, Rossi E, et al. (2013) Modulating Human Procedural Learning by Cerebellar Transcranial Direct Current Stimulation. Cerebellum.

194. Weinberger M, Dostrovsky JO (2011) A basis for the pathological oscillations in basal ganglia: the crucial role of dopamine. Neuroreport 22: 151-156.